Distribution Agreement

In presenting this thesis or dissertation as a partial fulfillment of the requirements for an advanced degree from Emory University, I hereby grant to Emory University and its agents the non-exclusive license to archive, make accessible, and display my thesis or dissertation in whole or in part in all forms of media, now or hereafter known, including display on the world wide web. I understand that I may select some access restrictions as part of the online submission of this thesis or dissertation. I retain all ownership rights to the copyright of the thesis or dissertation. I also retain the right to use in future works (such as articles or books) all or part of this thesis or dissertation.

Signature:

_____ _____

Brenda Huang Date

The Role of Oligodendrocyte Dysfunction in Huntington's Disease

By

Brenda Huang
Doctor of Philosophy

Graduate Division of Biological and Biomedical Sciences
Genetics and Molecular Biology

Xiao-Jiang Li, M.D, Ph.D
Advisor

Gary Bassell, Ph.D
Committee Member

Joe Cubells, M.D, Ph.D
Committee Member

Yue Feng, M.D, Ph.D
Committee Member

Ken Moberg, Ph.D
Committee Member

Accepted:

Lisa A. Tedesco, Ph.D
Dean of the James T. Laney School of Graduate Studies

Date

The Role of Oligodendrocyte Dysfunction in Huntington's Disease

By

Brenda Huang
B.S. Georgetown University, 2007

Advisor: Xiao-Jiang Li, M.D, Ph.D

An abstract of
A dissertation submitted to the Faculty of the
James T. Laney School of Graduate Studies of Emory University
in partial fulfillment of the requirements for a degree of
Doctor of Philosophy
in Graduate Division of Biological and Biomedical Sciences
Genetics and Molecular Biology
2015

Abstract

The Role of Oligodendrocyte Dysfunction in Huntington's Disease

By Brenda Huang

Huntington's disease (HD) is a neurodegenerative disorder that is caused by an expanded polyglutamine tract in the N-terminal region of huntingtin. It is characterized by cognitive and behavioral deficits, as well as movement disorders. While mutant huntingtin is expressed ubiquitously, there is preferential degeneration of the medium spiny neurons of the striatum, followed by widespread degeneration in later stages of the disease. It is well known that mutant huntingtin can affect neuronal function by interfering with a number of processes such as gene expression and trafficking. However, the effects of mutant huntingtin on the function of glial cells, in particular oligodendrocytes, remain to be fully investigated. There is increasing evidence of white matter abnormalities in both HD patients and HD mouse models, suggesting that mutant huntingtin might affect oligodendrocyte function. We hypothesize that mutant huntingtin causes oligodendrocyte dysfunction, which contributes to the pathogenesis of the disease. To this end, we generated transgenic mice (PLP-htt) that express an N-terminal fragment of mutant huntingtin exclusively in oligodendrocytes. These mice develop a tremor by 2 months of age and have locomotor and behavioral deficits, including body weight loss, reduced lifespan, and increased seizure susceptibility compared to control mice. Reduced myelin sheath thickness in the striatum, as well as reduced mRNA and protein expression of essential myelin genes, suggest that oligodendrocyte-specfic expression of mutant huntingtin causes an age-dependent dysregulation of myelin gene expression. Additionally, we found that mutant huntingtin binds to a transcription factor, MYRF, which is essential for myelin gene expression and maintenance of myelin. As mutant huntingtin accumulates in the cell, it binds to MYRF so that MYRF is unable to activate the transcription of myelin genes, such as myelin basic protein. We did not observe abnormalities in oligodendrocyte differentiation or proliferation, and myelination and myelin gene expression were normal in young mice. Thus, our findings suggest that mutant huntingtin impairs oligodendrocyte function in adult mice, which results in demyelination and likely contributes to the neuronal degeneration that is observed in Huntington's disease.

The Role of Oligodendrocyte Dysfunction in Huntington's Disease

By

Brenda Huang
B.S. Georgetown University, 2007

Advisor: Xiao-Jiang Li, M.D, Ph.D

A dissertation submitted to the Faculty of the
James T. Laney School of Graduate Studies of Emory University
in partial fulfillment of the requirements for a degree of
Doctor of Philosophy
in the Graduate Division of Biological and Biomedical Sciences
Genetics and Molecular Biology
2015

ACKNOWLEDGEMENTS

I would like to thank my advisor, Xiao-Jiang Li, for his support and guidance during my years at Emory. He gave me the opportunity to start and finish a very interesting project, one that I am extremely proud of. He was always pushing me to be a better scientist, which I am extremely grateful for. I would also like to thank Shihua Li, who has been a constant source of knowledge in the lab. She always had an answer for all of my questions, and I am still amazed by her ability to remember everything. I would also like to thank my committee members, Gary Bassell, Joe Cubells, Yue Feng, and Ken Moberg, who have been extremely encouraging and helpful. They have been great resources, and always had great suggestions and ideas. They were crucial for the success of my work, and it was a pleasure to work with them. I am also grateful to past and present members of the Li lab for their friendship and willingness to help whenever I had a question. I would like to thank my friends, both at Emory and beyond. Of course, I would like to thank my family, in particular my mother and twin sister Amanda, for their support and encouragement. They were almost 900 miles away, but they were always available when I needed them. Last, but not least, I would like to thank Kevin Van Bortle, who has been with me in every step of this process. He always believes in me and gives me confidence when I need it. He is an amazing person and scientist, and he inspires me to be my best.

Table of Contents

List of Figures and Tables

CHAPTER 1: INTRODUCTION

CHAPTER 3: SELECTIVE EXPRESSION OF MUTANT HUNTINGTIN IN OLIGODENDROCYTES CAUSES BEHAVIORAL ABNORMALITIES AND DEMYELINATION

CHAPTER 1:

INTRODUCTION

1.1 Polyglutamine Disease Family

Polyglutamine diseases comprise a family of neurodegenerative conditions that are caused by an in-frame CAG repeat expansion within the protein-coding region of a specific gene. They represent the most common form on inherited neurodegenerative disease. The CAG repeat expansion mutation produces pathogenic proteins that contain an elongated polyglutamine tract and are prone to misfolding. To date, there are nine known polyglutamine diseases, which include Huntington's disease (HD), spinobulbar muscular atrophy (SBMA), dentatorubral-pallidoluysia atrophy (DRPLA), and spinocerebellar ataxia (SCA) 1, 2, 3, 6, 7, and 17. All of these diseases are dominantly inherited, with the exception of SBMA, which is inherited in an X-linked, recessive manner (Lim et al., 2008).

For each of the polyglutamine diseases, the affected gene as well as the normal range of CAG repeats in the gene are different. However, in all of these diseases, once the number of repeats exceeds a certain threshold, the mutated allele produces a pathogenic protein with an expanded polyglutamine tract, with longer tracts resulting in more severe diseases and earlier onset. The expansion is believed to increase the probability of the polyglutamine region adopting an abnormal conformation (Paulson et al., 2000). This conformation change confers a gain of function to the protein by allowing it to misfold, aggregate, and interact abnormally with other proteins. For example, mutant Ataxin 2 (ATXN2), which causes SCA2, binds to a poly(A)-binding protein, PABPC1, and sequesters it into aggregates. PABPC1 mediates the circularization of mRNA, which precedes translation initiation, and is also involved in poly(A) tail shortening and nonsense mediated decay. Therefore, binding of mutant ATX2 to PABPC1 may affect

RNA processing (Damrath et al., 2012). In Huntington's disease, the polyglutamine expansion enhances the interaction between huntingtin and a transcription factor, Sp1, which prevents Sp1 from binding to the promoter of target genes to activate gene transcription (Li et al., 2002). Similarly, mutant TBP, which causes SCA17, has an enhanced interaction with the general transcription factor IIB (TFIIB), resulting in the reduced expression of proteins such as heat shock protein HSPB1 (Friedman et al., 2007). In SBMA, mutant androgen receptor (AR) binds to Retinoblastoma protein (Rb), impairing the ability of Rb to repress the transcriptional activity of E2F transcription factors (Suzuki et al., 2009). Mutant AR also interacts with Pax Transactivation-domain Interacting Protein (PTIP), which functions in DNA damage and repair pathways, suggesting that the mutant protein promotes cell death by making cells more vulnerable to DNA damage and compromising their DNA repair response (Xiao et al., 2012).

In addition to a gain of function, the polyglutamine expansion can also result in a loss of function by reducing the interaction between the protein and its interacting partners. Lim et al. found that ATXN1, which is the causative protein in SCA1, forms a complex with transcriptional repressor, capicua, in order to repress capicua target genes. The polyglutamine expansion attenuates the interaction between ATXN1 and capicua, which diminishes the ability of capicua to repress transcription ((Lam et al., 2006; Lim et al., 2008). Kalchman et al. found that htt interacts with Huntingtin Interacting Protein 1 (HIP1), and increased polyglutamine tract length diminishes this interaction. The interaction between normal htt and HIP1 may be necessary for cytoskeletal function, and a polyglutamine expansion results in a loss of normal htt function that compromises the integrity of the cytoskeleton (Kalchman et al., 1997)

Polyglutamine diseases are caused by the same mutation and share features such as aggregate formation, neuronal degeneration, and late-onset of symptoms. However, these diseases affect very specific brain regions and cell types. For example, the spinocerebellar ataxia-causing proteins (Ataxin 1, 2, 3, 7, CACNA1A, and TBP), mostly affect purkinje cells of the cerebellum, while mutant huntingtin primarily affects the medium spiny neurons of the striatum (Zoghbi and Orr, 2000). These differences suggest that, while the polyglutamine expansion is necessary for disease, "protein context" is important for the selective nature of the disease.

1.2 Huntington's Disease

Huntington's disease is caused by a CAG repeat expansion in the huntingtin gene (HTT), which encodes the huntingtin protein (htt) with a polyglutamine expansion in the N-terminus. It is the most common polyglutamine disease, with a prevalence of 4-10 per 100,000 (Ross and Tabrizi, 2011). The average age of onset is 40 years, and death usually occurs 15-20 years after the onset of symptoms. Unaffected individuals have 6 to 34 CAG repeats, while affected individuals have more than 36 repeats. The age of onset is inversely correlated with repeat length, and the presence of more than 60 CAG repeats results in juvenile HD, in which symptoms occur before the age of 20 (Duyao et al., 1993). Clinical features include motor dysfunction, such as chorea, dystonia, and rigidity, as well as psychiatric and cognitive changes, which are caused by progressive neuronal dysfunction and loss in the central nervous system (Li and Li, 2006). However, other, non-neurological features such as muscle atrophy, cardiac failure, and glucose intolerance

strongly indicate that the mutant huntingtin also has a toxic effect on peripheral tissues (van der Burg et al., 2009).

The huntingtin protein consists of 3144 amino acids, with a polyglutamine tract in exon 1. Huntingtin is expressed ubiquitously, with highest expression levels in the testes and brain (DiFiglia et al., 1995). It is composed predominantly of HEAT (**H**untingtin, elongation factor 3 (**E**F3), a subunit of protein phosphatase 2**A**, and the yeast kinase **T**OR1) repeats, which vary in length between 37 and 43 amino acids and occur as consecutive units (Andrade and Bork, 1995; Takano and Gusella, 2002). HEAT repeats are found in several cytoplasmic proteins that are involved in cytoplasmic-nuclear transport, suggesting that huntingtin may also shuttle between the nucleus and cytoplasm. This idea is also supported by the fact that the first 17 amino acids (N17) of huntingtin function as a cytoplasmic retention and/or nuclear export signal, as well as by the presence of a nuclear localization signal at amino acids 1182-1190 and recently-identified nuclear localization signal between amino acids 174-207 (Bessert et al., 1995; Cornett et al., 2005; Desmond et al., 2012). HEAT repeats also form α-helices that are believed to be important for protein-protein interactions, suggesting that huntingtin may act as a scaffold protein and facilitate the formation of protein complexes.

Although huntingtin is capable of shuttling between the cytoplasm and nucleus, it is mostly cytoplasmic. However, one of the pathological hallmarks of HD is the presence of intranuclear aggregates. Huntingtin is normally cleaved by a number of caspases, calpains, and matrix metalloproteases to generate N-terminal htt fragments (Landles et al., 2010; Miller et al., 2010). Additionally, it has recently been shown that aberrant splicing of HTT occurs in HD mouse models and human patients, which results in a short

mRNA that is translated into an exon 1 mutant htt protein (Sathasivam et al., 2013). The polyglutamine expansion causes these N-terminal fragments to misfold, accumulate in the nucleus and form aggregates. Additionally, phosphorylation of serine 16 in the N17 region of htt, can prevent nuclear N-terminal fragments from interacting with nuclear pore protein Tpr, promoting nuclear accumulation of htt (Havel et al., 2011). This accumulation of mutant htt leads to neuronal dysfunction and eventually neuronal death. Another pathological hallmark of HD is the selective degeneration of the medium spiny neurons (MSNs) of the striatum. These neurons, which comprise 95% of neurons in the striatum, receive inputs from the cerebral cortex and thalamus (Matamales et al., 2009). Output from the striatum is organized into direct and indirect pathways, which act in opposing ways to affect movement (Wall et al., 2013). Thus, MSNs are essential for motor control, and in HD, loss of MSNs reduces inhibitory control of unwanted movements and results in chorea (Kreitzer and Malenka, 2008). The striatum is also important for higher cognitive functions such as learning and memory, which become impaired in HD (Barnes et al., 2005; Scimeca and Badre, 2012). While the striatum is selectively degenerated, in later stages of the disease, neurodegeneration becomes more widespread and extends into other regions such as the cerebral cortex and thalamus (Eidelberg and Surmeier, 2011; Vonsattel and DiFiglia, 1998). Therefore, due to the significant neuronal loss in the striatum as well as other areas in the brain, it is essential to understand how mutant huntingtin affects neuronal function and survival.

1.3 Neuronal Dysfunction and Death in Huntington's Disease

Due to the neurodegenerative nature of HD, the effects of mutant huntingtin on neuronal function and survival have been extensively studied. Several proteins have been identified that interact with the N-terminal region of htt (Li and Li, 2004). As previously mentioned, htt is believed to be a scaffold protein and interacts with proteins that are involved in a number of cellular processes that occur in both the cytoplasm and nucleus. The polyglutamine expansion causes aberrant interactions between mutant huntingtin and its partners. For example, huntingtin normally binds to cytoplasmic protein Hap1 (Huntingtin-Associated Protein 1). Hap1 forms a complex with huntingtin and P150, a subunit of dynactin. P150 mediates the binding of dynactin to microtubules and to the microtubule motor protein dynein, and the interaction between dynactin, dynein, and microtubules is required for the intracellular transport of vesicles and organelles (Eidelberg and Surmeier, 2011; Li et al., 1998). The huntingtin/Hap1/P150 complex is required for the transport of vesicles containing brain-derived neurotrophic factor (BDNF), which is produced by cortical neurons and transported to striatum to promote neuronal survival (Gauthier et al., 2004). Mutant htt interacts more strongly with Hap1 and P150, and this increased interaction prevents the htt/Hap1/P150 complex from associating with microtubules, leading to decreased transport of BDNF-containing vesicles and loss of neutrophic support.

Mutant htt has also been shown to interfere with mitochondrial function to impair energy metabolism in the brain. Impaired trafficking can affect the transport and distribution of mitochondria in neuronal processes (Orr et al., 2008). Mutant htt can also induce the fragmentation of mitochondria, which affects mitochondrial transport and

leads to cell death (Song et al., 2011). Additionally, the mutant protein associates with the TIM23 complex in the inner membrane of the mitochondria to inhibit mitochondrial protein import to trigger neuronal death (Yano et al., 2014).

In the cytoplasm, mutant huntingtin can also interact with components of the ubiquitin-proteasome system and autophagy to impair protein degradation. For example, mutant htt binds to p62, a cargo-recognition protein, and reduces the ability of autophagosomes to recognize cargo (Martinez-Vicente et al., 2010). This leads to the accumulation of mutant htt as well as other misfolded or damaged proteins and cellular debris. Mutant htt can also sequester components of the ubiquitin-proteasome system (UPS) to impair its function, and both soluble and aggregated mutant htt have been shown to interact directly with proteasome to physically block substrates from entering the proteasome for degradation (Bence et al., 2001; Bennett et al., 2005; Davies et al., 2007; Diaz-Hernandez et al., 2006). Godin et al. found that htt associates with the β-catenin and the β-catenin destruction complex, which targets β-catenin for degradation by the UPS. The polyglutamine expansion decreases the association between htt, β-catenin, and the destruction complex, such that β-catenin is unable to be directed to the core of the destruction complex, leading to the accumulation of β-catenin, which is toxic for striatal neurons (Godin et al., 2010). Therefore, impairment of autophagy and the UPS by mutant htt leads to the toxic accumulation of proteins in the neuron.

In addition to cytoplasmic processes, mutant htt also affects nuclear functions such as gene expression. N-terminal fragments of mutant htt can enter the nucleus and interact with transcription factors. For example, compared to normal htt, mutant htt binds more strongly to transcription factor, Sp1, which inhibits the binding of Sp1 to the

promoter of its target genes and suppresses the transcriptional activity of genes that are required for neuronal functioning (Chen-Plotkin et al., 2006; Li et al., 2002). Mutant htt also binds to CREB-binding protein (CBP), which is a transcriptional co-activator and is required for the expression of pro-growth and pro-survival genes ((Lonze and Ginty, 2002; Sugars and Rubinsztein, 2003). Therefore, mutant htt can interfere with gene expression to impair neuronal function and survival.

1.4 Glial Dysfunction in Huntington's Disease

While the effects of mutant huntingtin on neuronal function have been extensively studied, less is known about how mutant huntingtin affects glial cell function. Glial cells significantly outnumber neurons in most regions of the brain, and they are essential to the function and survival of neurons (Herculano-Houzel, 2009). Hence, understanding the impact of mutant htt on glia could reveal important aspects of the disease process underlying HD. In the central nervous system, there are three types of glial cells: astrocytes, microglia, and oligodendrocytes.

Astrocytes are the most numerous glial cell type in the CNS and are involved in synapse formation and maintenance (Chen and Swanson, 2003). They also maintain a proper extracellular environment for the neuron by regulating the levels of potassium and other ions, transport trophic factors to neurons, and are responsible for glutamate uptake at synaptic clefts (Lobsiger and Cleveland, 2007). Astrocytes increase in number and size, and undergo changes in morphology (a process known as reactive gliosis) in response to damage or injury in the brain in order to protect neurons from further damage (Pekny and Nilsson, 2005). Through the use of human patient samples and various

animal models, studies have shown that astrocytes are impaired in HD. Faideau et al. found that mhtt aggregates are present in astrocytes of brains from HD subjects in both early and late stages of the disease, and that the number of aggregates corresponds to disease severity (Faideau et al., 2010). They also observed reactive astrocytes in Grade 0 HD subjects in the absence of significant neuronal dysfunction or loss, suggesting that mutant htt causes astrocytes to undergo reactive gliosis, which can cause neuronal dysfunction and death. Additionally, Faideau et al. found that the expression level of a protein, GLT-1, was reduced in human samples in an HD grade-dependent manner. GLT-1 is a glutamate transporter that is expressed by astrocytes and is essential for the removal of glutamate from the synapse. Reduced GLT-1 levels can cause a significant reduction in glutamate uptake and subsequent excitotoxicity and neuron death. Bradford et al. generated a mouse model that expresses mutant htt specifically in astrocytes (Bradford et al., 2009). They found that mutant htt binds to Sp1 and reduces its association with the GLT-1 promoter, thereby reducing GLT-1 expression in astrocytes and leading to impaired glutamate uptake and increased neuronal excitotoxicity.

The second type of glial cell in the CNS is microglia, which are the macrophages of the CNS and support neuronal survival by removing cellular debris. As a key component of the inflammatory response, microglia are highly response to almost any injury or disease of the CNS, and like astrocytes, they undergo reactive gliosis. Multiple studies have shown the presence of reactive microglia in human HD brains as well as HD mouse models, and that microglia activation correlates with disease severity (Franciosi et al., 2012; Pavese et al., 2006; Sapp et al., 2001). Interestingly, reactive microglia are also present in the brains of presymptomatic HD gene carriers, suggesting that microglia

activation is an event that occurs early in the disease process and might contribute to neuronal dysfunction and loss (Tai et al., 2007). Crotti et al. found that the expression of mutant htt in microglia promotes pro-inflammatory gene expression in both mouse models of HD and human HD tissue. As a result, mutant htt-expressing microglia have an exaggerated response to inflammatory stimuli, which induces neuronal degeneration (Crotti et al., 2014). These studies suggest that mutant htt can impair glial function to affect neuronal survival in a non-cell-autonomous manner.

Oligodendrocytes, the third type of glial cell, form myelin, a lipid-rich membrane that wraps around the axons of neurons to provide protection as well as electrical insulation to allow rapid transmission of electrical signals between neurons (Temburni and Jacob, 2001). Myelinated axons comprise the white matter of the brain. Ghosh et al. found that targeted ablation of oligodendrocytes in mouse and *Drosophila* induces demyelination and axonal damage followed by neuronal apoptosis (Ghosh et al., 2011). Recently, oligodendrocytes have been shown to metabolically support axons by providing them with lactate via monocarboxylate transporter 1 (MCT1), which is highly enriched in oligodendrocytes (Lee et al., 2012). Disruption of MCT1 leads to axon degeneration and neuron death, indicating that this metabolic support function of oligodendocytes is essential for axon function and neuronal survival. Additionally, oligodendrocytes also produce insulin-like growth factor (IGF-1), brain-derived neurotrophic factor (BDNF), glial-derived neurotrophic factor (GDNF), nerve growth factor (NGF), and neurotrophin-3 (NT-3) to support the function and survival of neurons (Dai et al., 2003; Wilkins et al., 2001; Wilkins et al., 2003). *Shiverer* mice, which lack myelin basic protein, the major protein component of myelin, are a commonly used as a

model of dysmyelinating disorders. Pitt et al. found that dysmyelination axons in *shiverer* mice are vulnerable to AMPA-receptor mediated axonal toxicity, suggesting that defective myelination may cause axonal degeneration and subsequent neuronal degeneration (Pitt et al., 2010). Together, these studies clearly demonstrate the importance of the trophic and myelination functions of oligodendrocytes, and that proper oligodendrocyte function is crucial for neuron survival.

These studies, which demonstrate the essential role of oligodendrocytes in neuronal function and survival, suggest that oligodendrocyte dysfunction may play a causative role in neurodegeneration. In fact, defects in myelination have been associated with neurodegenerative disorders such as multiple sclerosis (MS), amyotrophic lateral sclerosis (ALS), and Alzheimer's disease (Desai et al., 2010; Dutta and Trapp, 2011; Philips et al., 2013; Stadelmann et al., 2011). It is believed that, in MS, inflammatory demyelination renders axons vulnerable to insults and can result in the transection and degeneration of axons, which can lead to neuronal degeneration. Therefore, it is likely that oligodendrocyte dysfunction plays a role in HD.

Certain features of HD indicate that oligodendrocytes may be involved in neurodegeneration. Degeneration of myelinated axons have been observed in human tissue, as well as in mouse and monkey models of HD (Li et al., 2001; Sapp et al., 1999; Wade et al., 2008; Wang et al., 2008). However, it is unknown whether axon degeneration is caused by the presence of mutant htt in axonal processes, or if mutant htt within oligodendrocytes affects myelination to make axons more susceptible to degeneration. Myelination defects, in particular, reduced myelin sheath thickness, have been observed in mouse models of HD (Xiang et al., 2011). However, it is well

established that oligodendrocyte proliferation, differentiation, myelination, and survival require growth factors and cytokines that are produced by neurons, astrocytes, and microglia (Pang et al., 2013; Simons and Trajkovic, 2006). Therefore, the myelination defects observed in HD mouse models might be a secondary effect of impaired neuronal, astrocyte, or microglia function, or they may be a result of mutant htt expression in oligodendrocytes. White matter defects are also present in HD patients. The longitudinal TRACK-HD study observed pre-symptomatic HD gene carriers and patients in the early stages of HD, and found reduced white matter volume in the brains of HD gene carriers prior to the onset of symptoms (Tabrizi et al., 2009). While these studies suggest that oligodendrocyte dysfunction may play a role in neuronal death in HD, the precise manner in which mutant htt affects oligodendrocyte function, and how the impact of mutant htt on oligodendrocytes might contribute to HD pathogenesis, have yet to be determined.

1.5 Mouse models

Mouse models are the most popular animal models for studying the mechanisms of Huntington's disease (**Table 1.1)**. These models can be divided into two broad categories: gene knock-in and transgenic. Most knock-in mice are generated by knocking a human HTT exon 1 with an expanded CAG tract into the endogenous mouse Htt gene locus. These mice express full-length htt protein with a chimeric human/mouse exon 1, at the endogenous level and in a spatially and temporally appropriate manner, allowing us to study mutant htt in a context that is similar to that in HD. Knock-in mouse models differ in the length of their CAG tract, ranging from 50-200 repeats, and the degree to which they recapitulate the features of HD (Lin et al., 2001; Menalled et al., 2003; Menalled et

al., 2002; White et al., 1997). Models without large CAG repeat expansion (<80 CAGs) tend to lack noticeable abnormal behavior or neuropathology until very late in life (Menalled and Chesselet, 2002). The CAG140Q (HD140Q KI) mice, however, successfully model the age-dependent aggregation of mutant htt, locomotor and behavioral abnormalities, selective striatal degeneration, and progressive nature of HD, providing insight into the different stages of HD pathogenesis (Hickey et al., 2008; Lerner et al., 2012; Menalled et al., 2003).

In addition to knock-in models, there are also transgenic mouse models that express full-length mutant htt. These models are generated with a yeast artificial chromosome (YAC) or bacterial artificial chromosome (BAC) that contains the entire human *HTT* locus with mixed CAA-CAG repeats (Gray et al., 2008; Hodgson et al., 1999; Slow et al., 2003). Similar to the HD140Q KI mouse, YACHD and BACHD mice exhibit progressive motor dysfunction, behavioral abnormalities, and late-onset, selective striatal degeneration. While mouse models that express full-length mutant htt replicate many of the key features of HD, they also express mutant htt ubiquitously, making it difficult to study the effects of mutant htt on specific cell types in the brain.

As previously mentioned, proteolysis of huntingtin is a critical step in HD pathogenesis (Graham et al., 2006; Wellington et al., 2002). N-terminal mutant htt fragments have been observed in human HD brains, and Landles et al. identified 14 prominent N-terminal fragments in the CAG140Q knock-in model (Kim et al., 2001; Landles et al., 2010; Wang et al., 2008). Transgenic mouse models have been created that express different N-terminal fragments. These models show early accumulation of mutant htt into aggregates as well as rapid progression of symptoms. Models that express shorter

N-terminal fragments, such as the R6/2 mouse, which expresses mutant htt-exon 1, and N171-82Q, which expresses the first 171 amino acids of htt, display abnormal behavior at a very young age and have a dramatically reduced life span (Mangiarini et al., 1996; Yu et al., 2003). Therefore, N-terminal models have a more robust phenotype and accelerated progression of disease compared to full-length models, making it possible to study the effects of mutant htt in a shorter period of time. In order to determine how mutant htt affects specific cell types, the expression of N-terminal htt can be driven by cell-specific promoters. For example, the N171-82Q mouse expresses mutant htt under the mouse prion promoter, which is highly expressed in neurons of the CNS. The GFAP-htt mouse expresses the first 208 amino acids of htt under the glial fibrillary acid protein (GFAP) promoter to drive expression specifically in astrocytes (Bradford et al., 2009). Crotti et al. created a double transgenic mouse in which the expression of mutant htt-exon 1 can be induced in microglia using the microglia-specific promoter CX3CR1. Such models have made it possible to determine how mutant htt affects neuronal, astrocyte, and microglia function. However, there currently is no model that expresses mutant htt selectively in oligodendrocytes, and therefore the effects of mutant htt on oligodendrocyte function are still unknown.

1.6 Dissertation Goals

In order to fully understand Huntington's disease, it is necessary to understand how mutant htt affects the functions of different cell types to lead to neuronal degeneration. Previous studies have shown that mutant htt causes astrocyte and microglia dysfunction, which leads to neuronal degeneration. However, it is unknown if and how

oligodendrocyte dysfunction contributes to HD (**Figure 1.1**). Given the importance of oligodendrocytes to the function and survival of neurons, the current dissertation project seeks to determine if mutant htt affects oligodendrocyte function, and if so, whether htt-induced oligodendrocyte dysfunction leads to neuronal degeneration in Huntington's disease. In this study, I have generated a novel transgenic mouse model that expresses an N-terminal fragment of mutant htt under the proteolipid protein (PLP) promoter, an oligodendrocyte-specific promoter. Characterization of this model will allow us to understand how oligodendrocytes contribute to HD, and provide greater insight into potential therapeutic targets as well as mechanisms that may also play a role in other neurodegenerative diseases.

Table 1.1 Mouse Models of Huntington's Disease

Model	Type	Transgene Product	Repeat Length	Promoter/ cell type	Neuropathology	Behavioral phenotype
BACHD	Transgenic	Full-length human Htt, floxed exon 1	97 (mixed CAA-CAG)	HTT/ ubiquitous	12m: brain atrophy, reduced cortical and striatal volume	2m: rotarod impairment
YAC72	Transgenic	Full-length human Htt	72	HTT/ ubiquitous	12m: selective striatal neurodegeneration	7m: hyperactivity
YAC128	Transgenic	Full-length human Htt	100, 126 (mixed CAA-CAG)	HTT/ ubiquitous	Striatal and cortical degeneration	3m: gait abnormalities 4m: rotarod impairment
R6/2	Transgenic	Human Htt exon 1	145	HTT/ ubiquitous	Reduced brain weight, neuronal atrophy, gliosis	5-6 weeks: motor deficits
GFAP-160Q	Transgenic	Human Htt, 208aa	160	GFAP/ astrocytes	18m: reactive astrocytes, no neuronal degeneration	12m: rotarod impairment 16m: body weight loss, clasping
N171-82Q	Transgenic	Human Htt, 171aa	82	mouse Prion/ neuron	Gross brain atrophy, striatal neuron atrophy	16 weeks: htt aggregates
HdhQ72-80	Knock-in	Full-length chimeric human/mouse exon 1	72-80	Hdh/ ubiquitous	No neuronal loss or gliosis, intranuclear inclusions by 96 weeks	Rotarod impairment
Hdh94	Knock-in	Full-length chimeric human/mouse exon 1	94	Hdh/ ubiquitous	6m: microaggregates, 18m: intranuclear inclusions	2m: hyperactivity 4m: hypoactivity 24m: gait abnormalities
HdhQ111	Knock-in	Full-length chimeric human/mouse exon 1	109	Hdh/ ubiquitous	2.5m: nuclear staining 5m: microaggregates	Gait impairment by 96 weeks
CAG140Q	Knock-in	Full-length chimeric human/mouse exon 1	140	Hdh/ ubiquitous	4m: nuclear staining, intranuclear inclusions, neuropil aggregates	1m: hyperactivity 4m: hypoactivity 12m: gait abnormalities
Hdh150Q	Knock-in	Endogenous mouse htt	150	Hdh/ ubiquitous	14m: intranuclear aggregates, gliosis, axonal degeneration	4-10m: gait and locomotor deficits, clasping
zQ175	Knock-in	Full-length chimeric human/mouse exon 1	198	Hdh/ ubiquitous	4m: reduced striatal and cortical volume, reduced neuronal density	8 weeks: hypoactivity 30 weeks: rotarod impairment

Figure 1.1

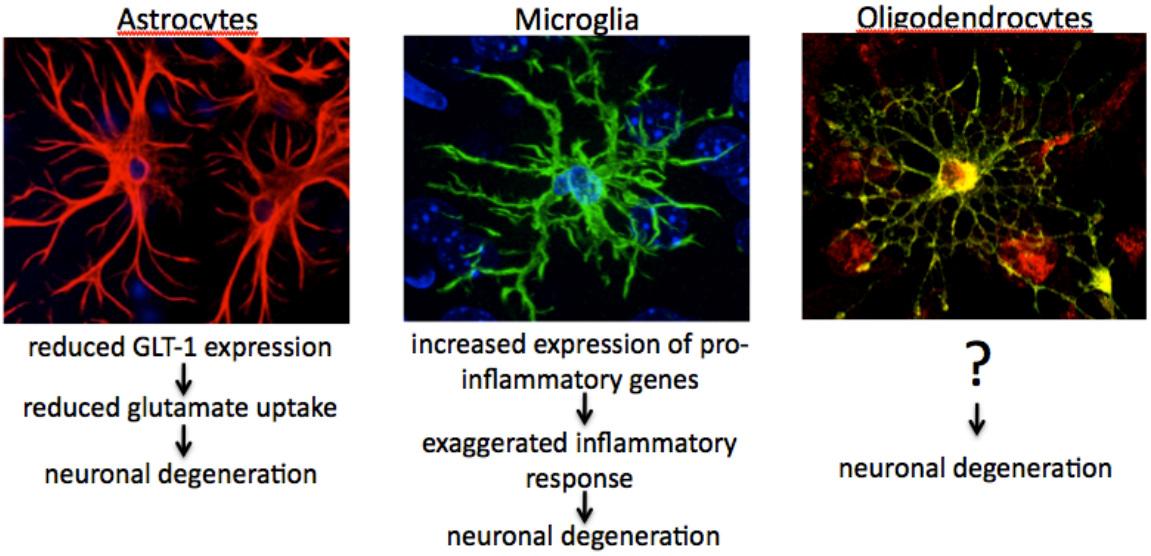
Astrocytes
Microglia
Oligodendrocytes
reduced GLT-1 expression
reduced glutamate uptake
neuronal degeneration
increased expression of pro-inflammatory genes
exaggerated inflammatory response
neuronal degeneration
?
neuronal degeneration

Figure 1.1

Glial dysfunction in Huntington's disease. Mutant htt can cause astrocyte and microglia dysfunction, which results in neuronal degeneration. However, it is not known if mutant htt causes oligodendrocyte dysfunction. The goals of this dissertation are to determine if and how mutant huntingtin affects oligodendrocyte function, and if mutant huntingtin-induced dysfunction of oligodendrocytes can cause neuronal degeneration in Huntington's disease.

CHAPTER 2:

MATERIALS AND METHODS

This chapter was submitted in part as: Brenda Huang, Wenjie Wei, Guohao Wang, Marta A. Gaertig, Yue Feng, Wei Wang, Xiao-Jiang Li, and Shihua Li. Mutant huntingtin downregulates myelin regulatory factor-mediated myelin gene expression and affects mature oligodendrocytes. *Neuron*. In Press. 2015. Xiao-Jiang Li and Shihua Li helped with the experimental design. Xiao-Jiang Li, Shihua Li, and Wenjie Wei participated in writing and editing of the manuscript.

2.1 Animals

To generate PLP-htt transgenic mice, cDNA encoding N-terminal human htt (amino acids 1-212) containing 23Q or 150Q was subcloned into the pNEB193 vector using BamHI and XbaI. The plasmid was then digested with PmeI and AscI, and the htt-containing fragment was inserted into the PLP promoter cassette. The pNEB193 vector and PLP promoter cassette were generated previously (Fuss et al., 2000). Pronuclear injection of the linearized construct was performed by the Transgenic Mouse and Gene Targeting Core at Emory University. Founder mice were obtained and maintained at the Emory mouse facility. Genomic DNA was isolated from mouse tails, and PCR genotyping with primers that flank the polyQ region was used to screen for transgenic mice. The sequences of the primers are as follows: forward: 5′-ATGAAGGCCTTCGAGTCCCTCAAGTCCTTC-3′, and reverse, 5′-AAACTCACGGTCGGTGCAGCGGCTCCTCAG-3′. We identified 9 positive PLP-150Q founders and 7 positive PLP-23Q founders. Transgene expression was determined via western blotting. PLP-GFP mice were obtained from Dr. Wendy Macklin (University of Colorado Denver) and bred with PLP-htt mice to generate double-transgenic mice. Full-length mutant htt CAG140Q (HD140Q KI, or HD KI) mice were provided by Dr. Michael Levine (University of California, Los Angeles, CA). GFAP-htt mice were generated previously (Bradford et al., 2009).

2.2 Reagents

Commercial antibodies used in this study include: 1C2 (Millipore, MAB1574), BrdU (AbD Serotec, OBT0030G), CNP (Abcam, ab6319), Flag (Cell Signaling, 2044S),

GAPDH (Millipore, MAB374), GFAP (Cell Signaling, 3670), MBP (Millipore, MAB386), MCT1 (Biorybt, orb11030), MOBP (Santa Cruz, sc-14520), MOG (Millipore, MAB5680), MYRF (Sigma, HAP018310), MYC (Cell Signaling, 2276S), MYC (Santa Cuz Biotechnology, sc-40), NeuN (Millipore, ABN78), Olig2 (Millipore, AB9610) and PLP (Millipore, MAB388). Rabbit polyclonal antibody (EM48) and mouse monoclonal antibody (mEM48) against the N-terminal region (amino acids 1-256) were generated as described in our previous study (Li et al., 2002).

PRK plasmids expressing HA-tagged N-terminal huntingtin (amino acids 1-212) (PRK-htt-23Q or PRK-htt-150Q) and NLS-tagged N-terminal huntingtin (NLS-htt-23Q or NLS-htt-150Q) were generated as described previously (Havel et al., 2011). MYRF was amplified from mouse cDNA. The following primers were used to produce full-length MYRF with an N-terminal myc tag and C-terminal flag tag, and the product was inserted into the PRK5 vector using ClaI and Xba1 restriction sites. Forward: 5'-ACATCGATACCATGGAACAAAAGCTCATTAGCGAGGAAGACCTTATGGAGGTGGTGGACGAGAC-3', Reverse: 5'-ACTCTAGATCATTTGTCATCGTCATCCTTGTAGTCGTCACACAGGCGGTAGAAGTGGAAGTAG-3'.

To generate N-terminal MYRF (nMYRF) containing a myc tag, the following primer pairs were used, and the product was inserted into the PRK5 vector using ClaI and SalI restriction sites. Forward: 5'- ACATCGATACCATGGAACAAAAGCTCATTAGCGAGGAAGACCTTATGGAGGTGGTGGACGAGAC-3', Reverse: 5'-5'-TCTTGTCGACCTAGGTGGTGTCCACCTCCTGCACGTGCTC-3'.

To generate nMYRF (1-251), the following primers were used:
Forward: 5'-ACATCGATACCATGGAACAAAAGCTCATTAGCGAGGAAGACCTT

ATGGAGGTGGTGGACGAGAC-3', Reverse: 5'-AGTCTAGACTACTTCATGTAGA GGTCC-3'.

To generate nMYRF (215-635), the following primers were used: Forward: 5'-ACATCGATACCATGGAACAAAAGCTCATTAGCGAGGAAGACCTT ATAACCCCGGAGACTCTATGC-3', Reverse: 5'-TCTTGTCGACCTAGGTGGTGTC CACCTCCTGCACGTGCTC-3'.

To generate nMYRF (281-635), the following primers were used: Forward: 5'-ACATCGATACCATGGAACAAAAGCTCATTAGCGAGGAAGACCTT CTACACCAGC-3', Reverse: 5'-TCTTGTCGACCTAGGTGGTGTCCACCTCCTGCA CGTGCTC-3'.

To generate nMYRF (215-275), the following primers were used: Forward: 5'-ACATCGATACCATGGAACAAAAGCTCATTAGCGAGGAAGACCTT TGCCACGTGGGAGTTTCTTCC-3', Reverse: 5'-ACTCTAGACTACTGGGTGTGAT GGAGCTC-3'.

To generate C-terminal MYRF (cMYRF) containing a flag tag, the following primers were used, and the PCR product was inserted into the PRK5 vector using BamHI and XbaI restriction sites: Forward: 5'-ATGGATCCTTGGTCGTCCACGGCAACG-3' Reverse: ACTCTAGATCATTTGTCATCGTCATCCTTGTAGTCGTCACACAGGCG GTAGAAGTGGAAGTAG-3'.

To generate GST-tagged nMYRF, the following primers were used, and the PCR product was inserted into the PGEX4T-1 vector using EcoR1 and Sal1 restriction sites. Forward: 5'-AGAATTCGCCATGGAGGTGGTGGACGAGACCGAAGCGCTGCAG-3', Reverse: 5'-TCTTGTCGACCTAGGTGGTGTCCACCTCCTGCACGTGCTC-3'.

For the luciferase reporter assay, the MBP promoter was amplified from mouse genomic DNA using the following primers: Forward: 5'-ATGGTACCCTGTGTGAGCATGTGA CA-3', Reverse: 5'-TTTAAGCTTGAACAGTCCCCGTGAGG-3'. The promoter was inserted into the luciferase reporter vector pGL4.14 (Promega) using KpnI and HindIII restriction sites.

2.3 Mouse Behavior Analysis

Mouse body weight was measured once every month, and survival was monitored regularly. The motor function of the mice was assessed with the rotarod test (Rotamex, Columbus Instruments). Mice were trained on the rotarod at 5 RPM for 5 min for 3 consecutive days. After training, the mice were tested for 3 consecutive days, 3 trials per day. The rotarod gradually accelerated to 40 RPM over a 5-min period. Latency to fall was recorded for each trial. At least 15 mice were analyzed per group when comparing PLP-150Q, PLP-23Q and WT. When comparing all PLP-150Q lines, at least 5 animals were analyzed per group.

The flurothyl-induced seizure experiment was performed as previously described (Makinson et al., 2014). Mice were placed in a clear Plexiglas chamber and exposed to flurothyl (2,2,2-trifluroethylether) (Sigma, 287571) at a rate of 20 μl/min. Latency to generalized seizure was recorded. Mice were at least 3 months old, and at least 10 animals were analyzed for each group. Locomotor activity was assessed using an automated system (PAS, San Diego Instruments) that records all photobeam interruptions. Each mouse was housed in a separate chamber with food and water.

Activity was recorded once every 30 min for 30 h. The first 6 h were excluded from analysis. At least 8 animals were analyzed per group.

2.4 Immunofluorescence, Immunohistochemistry and Electron Microscopy

Mice were anaesthetized with 5% chloral hydrate and perfused with 0.9% NaCl followed by 4% PFA. The brains were removed and post-fixed in 4% PFA overnight at 4°C. The brains were transferred to 30% sucrose for 48 h, then cut to 20- or 40-μm sections with the cryostat (Leica 1920) at -20°C. Sections were blocked in 4% donkey serum with 0.2% Triton X-100 and 3% BSA in PBS for 1 h. For immunofluorescent staining, 20-μm sections were incubated with primary antibodies in the same buffer at 4°C overnight. After washing, the sections were incubated in fluorescent secondary antibodies and Hoechst stain. Fluorescent images were acquired with a Zeiss microscope (Carl Zeiss Imaging, Axiovert 200 MOT) and either a 40x or 63x lens (LD-Achroplan 40x/0.6 or 63x/0.75) with a digital camera (Hamamatsu, Orca-100) and Openlab software (Improvision). For immunohistochemistry with DAB staining, after blocking, 40-μm sections were incubated with mEM48 for at least 48 h at 4°C. A biotin/avidin immunoassay (Vector Laboratories) and DAB kit (Invitrogen, 00-2020) were used. Images were acquired with a Zeiss microscope (Carl Zeiss Imaging, Imager A.2) and either a 40x or 63x lens (Plan-Apochromat 40x/0.95 or 63x/1.4) with a digital camera (Carl Zeiss Imaging, AxioCam HRc) and AxioVision software.

For immunofluorescent staining of transfected HEK293 cells, cells were transfected with full-length MYRF alone or full-length MYRF with htt-150Q. After transfection, the cells were fixed with cold 4% PFA for 15 min, then blocked with 5%

donkey serum, 0.3% Triton X-100, and 3% BSA in 1x PBS. The cells were incubated overnight at 4°C with myc or flag antibody. Cells that were co-transfected with full-length MYRF and PRK-htt-150Q were incubated overnight with anti-myc and EM48.

For EM, mice were perfused with 0.9% NaCl followed by 4% PFA containing 2.5% glutaraldehyde. After post-fixation, the brain was cut to 50-μm sections using the vibratome (CM1850, Leica). The sections were processed as previously described[45]. Axon and myelin fiber diameters were measured using ImageJ (NIH). More than 300 axons were examined for each genotype.

2.5 Analysis of Oligodendrocyte Morphology

To examine oligodendrocyte morphology, PLP-htt and HD KI mice were crossed with PLP-GFP. After perfusion with 4% PFA, mouse brains were cut into 18 μm sections on the cryostat. Images were acquired with a Zeiss microscope (Carl Zeiss Imaging, Imager A.2), digital camera (Carl Zeiss Imaging, AxioCam HRc), and 40x lens (LD-Achroplan 40x/0.6). Using the Simple Neurite Tracer plugin for ImageJ (Longair et al., 2011), lengths of GFP positive processes in the striatum and cortex were measured from the cell body to the tip of the process. Lengths were reported in arbitrary units (AU), which are defined as the pixel values from 8-bit luminance images used for quantification. For PLP-htt mice, 3 three-month old animals were examined for each genotype, and at least 148 cells per genotype were analyzed. For analysis of HD KI mice, 3 one-year old mice were analyzed for each genotype, and at least 165 cells per genotype were analyzed.

For oligodendrocyte quantification. PLP-htt mice were bred with PLP-GFP mice. After perfusion, brains were cut into 20 μm sections. Images were acquired with a Zeiss microscope (Carl Zeiss Imaging, Imager A.2), digital camera (Carl Zeiss Imaging, AxioCam HRc), and 10x lens (EC Plan-Neufluar 10x/0.3). The Cell Counter plugin for ImageJ was used to count the number of GFP+ oligodendrocytes per 10x field. 3 one-month old mice were analyzed for each genotype.

2.6 BrdU Incorporation Assay

3 week-old mice were given intraperitoneal administrations of BrdU (50 mg/kg body weight) (Sigma, B5002) for 4 consecutive days. The animals were then sacrificed 24 h after final BrdU injection. After fixation and sectioning, the sections were subjected to BrdU and neuronal cell staining. As antigen retrieval is required for BrdU staining, sections were first treated with 2 N HCl for 30 min at 37°C and then neutralized with 0.1 M sodium borate (pH 8.5) for 15 min at room temperature. Images were acquired with a Zeiss microscope (Carl Zeiss Imaging, Imager A.2), digital camera (Carl Zeiss Imaging, AxioCam HRc), 3 mice were analyzed for each genotype

2.7 Cell Culture

Human embryonic kidney (HEK) 293 cells were cultured in DMEM/F12 containing 10% fetal bovine serum, 100 U/ml penicillin, 100 μg/ml streptomycin (Invitrogen) and 0.25 μg Fungizone (Amphotericin B).

2.8 Western Blotting and Co-Immunoprecipitation.

To examine myelin protein levels, brain tissues were dissected out and sonicated 3 times for 10 s in 1x SDS sample buffer and 0.5% Triton-X 100 in 1x PBS containing protease inhibitor mixture (Roche) and 100 μM PMSF. The samples were incubated at 100°C for 10 min and centrifuged at 4°C for 10 min at 16,000 x *g*. Samples were resolved in a 4-20% Tris-glycine SDS-polyacrylamide gel (Invitrogen) and transferred onto a nitrocellulose membrane. Blots were developed with ECL Prime (GE Healthcare, RPN2232). ImageJ was used for western blot quantification.

For *in vivo* co-immunoprecipitation, 50 μg of mouse brainstem were homogenized in 1 ml 1% NP40 in a glass Douncer with 50 strokes, then sonicated on ice for 10 s. The lysate was spun at 500 x *g* for 2 min. Samples were precleared with 30 μl of Protein A agarose beads (Sigma, P1406) for 2 h, then incubated overnight with mEM48 on a rocker at 4°C. The samples were incubated with 30 μl Protein A beads for 2 h at 4°C on a rocker, then spun at 1000 x *g* for 2 min. The beads were washed three times with cold 1% NP40, then resuspended in 1x SDS sample buffer. For *in vitro* co-IP, HEK293 cells were transfected with MYRF and either PRK-htt or NLS-htt. 48 h following transfection, cells were harvested and lysed in cold 1% NP40. Samples were precleared and incubated overnight with either flag or myc antibody at 4°C.

2.9 Fluorescence-Activated Cell Sorting of Oligodendrocytes

Double transgenic mice obtained by crossing PLP-GFP mice and PLP-htt mice were used for sorting of GFP positive oligodendrocytes. Brains of 1.5-month old mice were dissected and minced. Following homogenization of the brain tissue, accutase was

added for further dissociation. Samples were mixed for 30 min at 4°C, then centrifuged at 425 × *g* for 2 min, The pellet was resuspended in ice-cold Hibernate A. To remove large debris and cell clusters, the cell suspension was subjected to serial filtration through pre-wetted 70 μm then 40 μm cell strainers into 50 ml Corning tubes on ice. Cells were then pelleted by centrifugation at 550 × *g* for 5 min and resuspended in sorting buffer. A FACS Aria (BD Biosciences) instrument was used for both cell sorting and analysis, which was performed by the Flow Cytometry Facility Core at Emory University.

2.10 Microarray and qRT-PCR

For the microarray, total RNA was isolated from the mouse spinal cord with the RNeasy Lipid Tissue Mini Kit (Qiagen) from 2 WT and 4 PLP-150Q mice. The Mouse Gene 1.0 ST Array was used (Affymetrix). Raw data were subjected to background adjustment and normalization as previously described (Friedman et al., 2007). Probe sets with at least 1.5 fold-change and ANOVA p-value <0.05 were considered significant. Data were subsequently subjected to Ingenuity Pathway Analysis (Ingenuity Systems). For qRT-PCR, total striatal RNA was isolated from 3 1-month-old mice of each genotype and 3 3-month-old mice from each genotype. For human samples, total RNA was isolated from cortex of 3 HD samples and 3 control samples. Reverse transcription reactions were performed with 1.5 μg of total RNA using the Superscript III First-Strand Synthesis System (Invitrogen, 18080-051). 1 μl of cDNA was combined with 10 μl SYBR Select Master Mix (Applied Biosystems, 4472908) and 1 μl of each primer in a 20-μl reaction. The reaction was performed in a thermal cycler (Eppendorf, Realplex Mastercycler). The sequences of the primers are as follows:

Stard4: forward: 5’- TGTCCGTGGCTATAACCATCC-3’

Stard4: reverse: 5’-TGCTGTATCTACGGCAGACTGAG-3’

SREBF2: forward: 5’-AGCGAGCTACTGCCATCCTGC-3’

SREBF2: reverse: 5’-AGCAGCTTCAGCCAGCAGCAC-3’

PGC1a: forward: 5’-AAGCCAAACCAACAACTTTATCTC-3’

PGC1: reverse: 5’-AGTTCGCTCAATAGTCTTGTTCTC-3’

MBP: forward: 5’-AGTACCTGGCCACAGCAAGT-3’

MBP: reverse: 5’-AGGATGCCCGTGTCTCTGT-3’

HTT: forward: 5′-ATGGCGACCCTGGAAAAGCT-3′

HTT: reverse: 5′-TGCTGCTGGAAGGACTTGAG-3′

GAPDH: forward: 5’-AACTTTGTCAAGCTCATTTCCTGGT-3’

GAPDH: reverse: 5’-GGTTTCTTACTCCTTGGAGGCCATG-3’

MBP primer sequences have been previously described (Mack et al., 2007). GAPDH served as an internal control. Relative expression levels were calculated using 2^-deltaCT, with WT set at 1.

2.11 Luciferase Reporter Assay

HEK293 cells were transfected with MYRF, PRK-htt-23Q or PRK-htt-150Q and MBP promoter-luciferase. After two days, cells were harvested. Each sample was divided into two. One half was lysed in 1% NP40, and protein levels were determined via western blotting. The remaining half was used for the Luciferase Assay System (Promega, E1483), and reporter activity was detected with a plate reader (BioTek, Synergy H4). For the rescue experiment, HEK293 cells were transfected with different combinations of the

following plasmids: MBP-promoter luciferase, PRK-htt-23Q or PRK-htt-150Q, MYRF, and nMYRF or cMYRF.

2.12 Chromatin Immunoprecipitation (ChIP)

The method for ChIP was adapted from our recent publication (Yang et al., 2014). Briefly, HEK293 cells were transfected with MYRF, PRK-htt-23Q or PRK-htt-150Q, and the MBP-promoter luciferase reporter. Cells were harvested two days later, fixed with 1% formaldehyde for 10 minutes at 37 °C, and transferred to SDS lysis buffer. Sonication was performed to shear DNA to lengths between 200 and 1000 base pairs. ChIP assay kit (Millipore, 17-295) was then used to obtain nMYRF immunoprecipitated DNAs. Anti-Myc antibody (Santa Cuz Biotechnology, sc-40) was used to pull down nMYRF. For the control, anti-Myc was omitted in the ChIP assay. The precipitated DNAs were subjected to qRT-PCR for quantification of the MBP promoter DNAs associated with nMYRF. The sequences of the primers are as follows:

MBP1: forward: 5'- TCTAGTCGTCTCCTAGGTGACTGCAC-3',

MBP1: reverse: 5'-TCACTCTGAACAGTCCCCGTGAG-3';

MBP2: forward: 5'- ACGTCCTTCTGTGTGAGCATGTG-3',

MBP2: reverse: 5'-TAGTGTGCACTCACAGTGGTAGACAG-3'

2.13 GST-Pulldown Assay

nMYRF was inserted into the PGEX4T-1 GST Expression Vector (GE Healthcare, 28-9645-49). GST-nMYRF was transformed into BL21(DE3) cells. Cells were induced with 1 μM IPTG at OD 0.6 and shaken overnight at 30°C. The cells were

harvested in GST binding buffer (1% Triton-X 100 in 1x PBS) and sonicated on ice for 20 min, then spun at 12,000 rpm for 10 min at 4°C. The supernatant was incubated with 1-ml GST beads (Sigma, G4510) overnight on a rocker at 4°C. The beads were spun at 1000 x *g* and washed 3 times with binding buffer, then resuspended in 1x PBS containing protease inhibitor mixture and PMSF. N-terminal huntingtin (aa1-212) was generated by *in vitro* translation (Promega, L2081) using PRK-htt as a template. For the *in vitro* binding assay, beads bound by GST-MYRF fusion protein were added to *in vitro* synthesized N-terminal huntingtin and gently rocked overnight at 4°C. The beads were spun at 1000 x *g*, washed 3 times with binding buffer and resuspended in 1x PBS.

2.14 Statistical Analysis

Results are expressed as mean ± SEM. Prism6 (GraphPad Software) was used for statistical analysis. When only two experimental groups were compared, the Student's t-test was used to calculate statistical significance. For all other experiments, statistical significance was calculated using one-way ANOVA or two-way ANOVA, followed by Tukey's multiple comparisons test. A p-value <0.05 was considered significant.

CHAPTER 3:

SELECTIVE EXPRESSION OF MUTANT HUNTINGTIN IN OLIGODENDROCYTES CAUSES BEHAVIORAL ABNORMALITIES AND DEMYELINATION

This chapter was submitted in part as: Brenda Huang, Wenjie Wei, Guohao Wang, Marta A. Gaertig, Yue Feng, Wei Wang, Xiao-Jiang Li, and Shihua Li. Mutant huntingtin downregulates myelin regulatory factor-mediated myelin gene expression and affects mature oligodendrocytes. Neuron. In Press. 2015. Brenda Huang performed all of the experiments described in this chapter with the exception of those described in Figures 3.11, 3.12A, and 3.16, which were performed by Wenjie Wei. Xiao-Jiang Li, Shihua Li, and Wenjie Wei helped in writing and editing the manuscript.

3.1 Abstract

Growing evidence indicates that non-neuronal mutant huntingtin toxicity plays an important role in Huntington's disease (HD). However, whether and how mutant huntingtin affects oligodendrocytes, which are essential for neuronal function and axonal integrity, remain unclear. We first verified the presence of mutant huntingtin in oligodendrocytes of HD140Q knock-in mice. We then established transgenic mice (PLP-150Q) that selectively express mutant huntingtin in oligodendrocytes. PLP-150Q mice show progressive neurological symptoms such as locomotor impairment, reduced body weight, and early death, as well as age-dependent demyelination and reduction of myelin gene expression. We demonstrate that mutant htt specifically affects the myelinating function of oligodendrocytes, which strongly suggests that mutant htt can impair oligodendrocyte function and contribute to neuronal toxicity.

3.2 Introduction

Huntington's disease (HD) is caused by polyglutamine expansion in the N-terminal region of huntingtin, a large protein that consists of 3144 amino acids. Despite the ubiquitous expression of mutant htt in the brain and peripheral tissues, the major pathological feature of HD is selective neurodegeneration (Munoz-Sanjuan and Bates, 2011; Vonsattel and DiFiglia, 1998). Similarly, selective neurodegeneration is also seen in many other neurodegenerative diseases, among them Alzheimer's and Parkinson's diseases, which suggests multiple factors may contribute to selective neurodegeneration. Given the known genetic mutation in HD and its well-characterized neuropathology, HD

makes an ideal model for investigating how selective neuropathology can be caused by a disease protein that is widely expressed.

Most previous studies focused on the effect of mutant htt on neuronal cells and revealed that N-terminal fragments of mutant htt are pathogenic and cause cell-autonomous or non-cell-autonomous disease processes in a variety of animal models (Heng et al., 2008; Lee et al., 2013). In the brain, the majority of cells are glial cells, which are non-neuronal cells that are essential for the survival and function of neuronal cells. There are three types of glial cells: astrocytes, microglial cells and oligodendrocytes. Glial dysfunction has been well documented to contribute to a variety of neurodegenerative diseases. For example, oligodendrocyte dysfunction plays an important role in ALS (Funfschilling et al., 2012; Kang et al., 2013; Philips et al., 2013). In HD patient brains, glial degeneration and pathology have also been documented (Bartzokis et al., 2007; Fennema-Notestine et al., 2004; Rosas et al., 2003). Recent studies show that mutant htt is expressed in glial cells and affects the function of astrocytes (Bradford et al., 2009; Shin et al., 2005; Tong et al., 2014) and microglial cells (Crotti et al., 2014). For example, as in neuronal cells, mutant htt in astrocytes can impact multiple targets, including GLT-1 to affect glutamate uptake (Bradford et al., 2009; Shin et al., 2005) and K channel function (Tong et al., 2014) to increase striatal neuronal excitability and vulnerability. Moreover, deficient myelination is seen in HD mouse models (Wade et al., 2008; Xiang et al., 2011). Nonetheless, since deficient myelination can be caused by multiple factors including neuronal and non-neuronal toxicity, whether and how mutant htt affects the function of oligodendrocytes remain to be investigated.

The importance of investigating htt's effects in oligodendrocytes is supported by

the critical role of oligodendrocytes in maintaining axonal function, and by observations of early pathological changes in HD (Bankston et al., 2013; Li et al., 2001; Wang et al., 2008). Oligodendrocytes produce myelin, which electrically insulates axons, allowing rapid and efficient propagation of nerve signals. Evidence also suggests that oligodendrocytes provide metabolic support to axons, which is critical for their function and survivial. Defective oligodendrocyte function and deficient myelination are found in numerous neurodegenerative diseases (Bankston et al., 2013). In HD knock-in mice that do not show obvious neuronal loss, axonal degeneration is an early pathologic event (Li et al., 2001). In transgenic HD monkey brain, axonal degeneration is also seen in the absence of cell body degeneration (Wang et al., 2008). Such axonal degeneration could be caused by mutant htt in axons, as well as htt-induced defective oligodendrocyte function. Investigating the effect of mutant htt in oligodendrocytes will help us understand the mechanism behind early disease pathology and develop more effective treatments.

The current dissertation will describe and examine a transgenic mouse model (PLP-150Q) that expresses an N-terminal fragment of mutant htt containing 150Q polyglutamines in oligodendrocytes. The PLP-150Q mice show obvious axonal degeneration and an early-onset polyglutamine disease phenotype that includes impaired rotarod performance, body weight loss and early death, providing strong evidence that mutant htt in oligodendrocytes contributes to the pathogenesis of Huntington's disease.

3.3 Results

Expression of mutant huntingtin in oligodendrocytes in HD knock-in mouse.

Although htt is ubiquitously expressed in neuronal and non-neuronal cells, strong evidence for the presence of mutant htt in oligodendrocytes is still lacking. To examine whether mutant htt is expressed in oligodendrocytes at the endogenous level, I crossed HD 140CAG knock-in (KI) mice with transgenic mice that selectively express GFP in oligodendrocytes under the control of the proteolipid protein *(PLP)* gene promoter (Mallon et al., 2002), which drives transgene expression specifically in oligodendrocytes in adult mouse brain (Michalski et al., 2011). The crossed mice would thus allow us to determine whether full-length mutant htt is expressed in GFP-positive oligodendrocytes. Immunofluorescent staining of PLP-GFP/KI mouse brains showed that GFP-positive oligodendrocytes (arrows in **Figure 3.1A**) indeed express mutant htt, although their htt staining is weaker than in neurons. Transgenic GFP expression in oligodendrocytes also allowed us to clearly visualize their processes. By comparing the GFP-positive processes in the cortex and striatum in wild-type and KI mice, we noted a reduction in the density of these processes reduced in KI brains (**Figure 3.1B, Figure 3.2**), as well as shorter process length compared to WT (**Fig 3.1C**). Since these GFP-positive processes represent myelinated axons and oligodendrocyte processes (Mallon et al., 2002), these results strongly suggest that mutant htt negatively affects the axon-myelinating function of oligodendrocytes.

Generation of PLP-150Q transgenic mice that selectively express mutant htt in oligodendrocytes.

To determine whether mutant htt in oligodendrocytes affects their function and contributes to HD neuropathology, we set out to establish transgenic mice that express

mutant htt under the control of the *PLP* promoter. We expressed N-terminal mutant htt (the first 212 amino acids), including 150 glutamines in the repeat region (htt-150Q). We chose this N-terminal fragment because proteolysis of mutant htt is crucial for HD pathogenesis and misfolded N-terminal mutant htt causes more severe pathology in animal models (Ehrnhoefer et al., 2011; Lee et al., 2013; Ross and Tabrizi, 2011). In control mice, we expressed the same N-terminal htt fragment containing 23 glutamines (htt-23Q) driven by the *PLP* promoter (**Figure 3.3A**). We obtained 9 positive htt-150Q founders and 7 positive htt-23Q founders. Western blot analysis with mEM48 showed that htt-150Q forms aggregated htt in the stacking gel, though its soluble level is lower than htt-23Q in the brains of transgenic mice (**Figure 3.3B**). Using the 1C2 antibody, which reacts selectively with expanded polyglutamine repeats, we found that PLP-150Q is more abundant in the brainstem, striatum and corpus callosum, which contain more oligodendrocytes than the cortex and cerebellum, in three lines of transgenic htt-150Q mice (150Q-1, 150Q-4a and 150Q-5). Also consistent with oligodendrocyte-selective expression driven by the *PLP* promoter, there was no htt-150Q detected in the peripheral tissues, including heart, kidney and muscle (**Figure 3.3C**). Immunohistochemical analysis of the brains of 150Q-4a mice at 1,2, and 3 months of age showed that mutant htt is accumulated in the corpus callosum and striatum in an age-dependent manner (**Figure 3.3D**). Because of the similar expression levels of transgenic htt in different mouse lines, we focused on the 150Q-4a (simply named PLP-150Q) and 23Q-4 (named PLP-23Q) lines for more detailed characterization.

Immunohistochemical studies showed that mutant htt is restricted to areas that are enriched in oligodendrocytes, such as the corpus callosum, and appears to be localized in the nuclei (**Figure 3.4A, B**). Compared with HD140Q KI mice, in which mutant htt is

ubiquitously expressed in neuronal and glial cells, PLP-150Q mice showed selective distribution of mutant htt in glial cells and less abundant aggregates (**Figure 3.4C**). Using primers specific for human htt, we performed quantitative RT-PCR to compare the mRNA expression levels of transgenic htt. Compared with mutant htt in HD140Q KI mice, which is expressed at the endogenous level, transgenic htt mRNA was slightly higher (**Figure 3.5A**). However, western blotting revealed that transgenic mutant htt in the striatum and brainstem is expressed at a lower protein level than mutant htt in HD140Q KI mouse brain (**Figure 3.5B**).

To verify that transgenic mutant htt is indeed localized in the nuclei of oligodendrocytes, we crossed PLP-150Q mice with PLP-GFP mice. As expected, transgenic mutant htt is abundantly distributed in the white matter region (corpus callosum) between the cortex and striatum and is localized in the nuclei of GFP-positive oligodendrocytes (**Figure 3.6A**). Using anti-Olig2 and anti-htt antibodies for immunofluorescent double labeling, we confirmed that mutant htt accumulates and forms aggregates in the nuclei of oligodendrocytes in adult PLP-150Q mouse brain (**Figure 3.6B**). Importantly, none of these GFP-positive cells could be labeled by antibodies to the astrocyte-specific protein, GFAP, or the neuronal protein, NeuN (**Figure 3.6C**). These results, taken together, show that we have established transgenic mice that express transgenic htt specifically in oligodendrocytes.

Progressive neurological phenotypes of PLP-150Q mice.

Transgenic mice (PLP-23Q and PLP-150Q) generated from F1 were born normally. They can be bred normally as wild type mice and do not show obvious behavioral abnormalities and motor deficits during postnatal developmental stage and at

young ages (<2 months). However, PLP-150Q mice develop age-dependent neurological symptoms. We found that old PLP-150Q mice at age of 5 months display a clasping phenotype and reduced body weight compared with PLP-23Q mice (**Figure 3.7A**). PLP-150Q mice at 5 months of age also have tremors and difficulty walking. The body weight of PLP-150Q mice began to decrease at the age of 4 months and continued to decrease progressively (**Figure 3.7B**). As a result, PLP-150Q mice started to die at 5 months of age and could not live longer than 10 months (**Figure 3.7C**). Consistent with their severe body weight loss and early death, PLP-150Q mice showed a significant deficit in their motor function as measured by rotarod performance, and this motor dysfunction became progressively worse with age (**Figure 3.7D**). We also compared different PLP-150Q mouse lines at a young age (2 months) and found that all of these mouse lines had poor rotarod performance (**Figure 3.7E**). The locomotor activity of PLP-150Q mice is also lower than PLP-23Q and wild-type mice during their active time zone (7 pm-11 pm) (**Figure 3.7F**). We noticed that older mice had frequent spontaneous seizures. Since mutant htt is expressed in oligodendrocytes, it may cause dysfunction of these cells and affect axonal conductivity, which may alter the susceptibility to seizures; thus, we next measured the latency of mice to generalized seizure induced by flurothyl and found that PLP-150Q mice were more sensitive to seizure induction (**Figure 3.7G**).

Axonal degeneration and reduced myelin gene expression in PLP-150Q mouse brain.

Next, we wanted to examine whether mutant htt in PLP-150Q mice causes any myelination defect or axonal degeneration. The PLP-150Q/PLP-GFP mice allowed us to

examine the integrity of oligodendrocyte processes. We found that there is indeed reduced density of oligodendrocyte processes, but no difference in the number of oligodendrocyte cell bodies, in PLP-150Q mice (**Figure 3.8A**). Electron microscopy revealed that myelinated axons in the striatum of PLP-150Q and PLP-23Q mice at the age of 1 and 2 months are not distinguishable. However, at 3 months, there was a reduced myelination of axons in PLP-150Q mice compared with PLP-23Q mice, and this reduction became more severe at 5 months (**Figure 3.8B**). Quantitative analysis of g-ratios (the inner axonal diameter to the total outer diameter) indicated a significant increase in this ratio in PLP-150Q mice, suggesting that mutant htt significantly increased this ratio in PLP-150Q mice in an age-dependent manner (**Figure 3.8C**). It is well known that demyelination can lead to axonal degeneration (Lee et al., 2014; Lee et al., 2012; Rodriguez and Scheithauer, 1994; Sathornsumetee et al., 2000). Consistently, electron microscopy also revealed a number of degenerated axons, which appear swollen and dark, in PLP-150Q mice at 5 months of age (**Figure 3.8D**). The obvious axonal degeneration was not seen in 3-month-old PLP-150Q mice, suggesting that this degeneration occurs after demyelination (**Figure 3.9A**). We also obtained an HD patient brain that contains around 50 CAG repeats in the HD gene (**Table 3.1**). Although the ultrastructure of postmortem brain tissue was not well preserved, we were able to identify demyelinated axons in this HD patient brain compared with the control individual that did not die of neurodegenerative diseases (**Figure 3.9B**).

Mutant htt reduces the expression of myelin proteins.

To understand how mutant htt affects myelination-related gene expression, we examined RNA levels using microarrays aiming to identify molecules likely to be involved in htt-mediated toxicity. Microarray analysis of gene expression in PLP-150Q mouse spinal cord at 3 months revealed 998 significantly upregulated and 152 significantly downregulated genes in PLP-150Q compared to WT mice (**Figure 3.10A,B**). Of these potentially altered genes, many are important for lipid metabolism, cell death and proliferation (**Figure 3.10C**); their altered expression could be secondary responses to demyelination and axonal degeneration. Myelin synthesis requires cholesterol (Saher et al., 2011) and lipid metabolism is mediated by the transcription factor PGC1a (Camacho et al., 2013). Previous studies showed that the expression of PGC1a and the homeostasis of cholesterol are affected in HD mouse models ((Valenza and Cattaneo, 2011; Xiang et al., 2011). Quantitative RT-PCR analysis of PGC1 a**,** cholesterol transport (StarD4) and sterol regulatory element binding transcription factor 2 (*SREBF2*) revealed no significant differences in their expression in the striatum of PLP-23Q and PLP-150Q mice (**Figure 3.10D**). Further, using GFP-positive oligodendrocytes that were isolated via fluorescence-activated cell sorting from double transgenic mice expressing GFP and transgenic htt in oligodendrocytes, we did not see significant differences in the expression levels of PGC1, StarD4, and SREBF2 between WT, PLP-23Q, and PLP-150Q mice (**Figure 3.11**). It has been reported that MCT1, the monocarboxylate transporter 1 that is responsible for releasing lactate and ketone bodies from oligodendrocytes to axons, is affected in ALS (Lee et al., 2012). We performed both RT-PCR and western blotting assays but could not see a significant defect in its

expression in PLP-150Q mouse brains (**Figure 3.12**). Taken together, these results suggest that when mutant htt is selectively expressed in oligodendrocytes, it may selectively affect the expression of various genes via different mechanisms.

Since there is a marked defect in myelination in PLP-150Q mice, we performed western blotting to detect the expression of myelin proteins, such as the oligodendrocyte-specific proteins 2',3' cyclic nucleotide 3'-phosphodiesterase *(*CNP*),* myelin basic protein *(*MBP*),* myelin-associated oligodendrocytic basic protein (MOBP) and myelin oligodendrocyte glycoprotein *(*MOG*),* in mouse brains at different ages and found that their expression is upregulated from postnatal day 14 (**Figure 3.13A**). Importantly, mutant htt does not affect the postnatal expression of myelin proteins at postnatal day 14. However, at 1 month, PLP-150Q mice showed decreases in the expression of these oligodendrocyte-specific proteins, in both the striatum and brainstem (**Figure 3.13B,C, Figure 3.14A, B**). Importantly, these decreases are age dependent and became more significant when PLP-150Q mice were 6 months old and were also seen in different PLP-150Q mouse lines (**Figure 3.13 and Figure 3.14C**). To further verify that the reduced expression of MBP is due to the effect of nuclear mutant htt on gene transcription, we performed quantitative PCR. Results confirmed the reduction in MBP mRNA in PLP-150Q mouse brains (**Figure 3.13D**). To test if reduced MBP also occurs in the brains of HD patients, we performed both RT-PCR (**Figure 3.13E**) and western blot analyses (**Figure 3.13F, G**). The results indicate that MBP is indeed decreased at both mRNA and protein levels in HD patient brains.

Because there were no significant decreases in these proteins at 1 month, mutant htt may not have an impact on them during development, but may affect mature

oligodendrocytes in adult mouse brains. In support of this idea, oligodendrocyte transcription factor (Olig2), which is also expressed in undifferentiated oligodendrocytes and their precursors (Ligon et al., 2006; Meijer et al., 2012), is not affected significantly by mutant htt. To further verify the selective effect of mutant htt in adult mouse brains, we examined the expression of neuronal and glial marker proteins in postnatal mouse brains. Western blot results revealed no alteration of these proteins in PLP-150Q mouse brains at P1, P7, and P14 (**Figure 3.15A**). Neither western blot nor immunocytochemical analyses detected caspase-3 activation and increased GFAP (**Figure 3.15A, B**). Immunocytochemical analyses of NeuN and Olig2 staining also support the western blot results, which demonstrate the unaltered expression of these neuronal and oligodendrocyte specific proteins in PLP-150Q mouse brains (**Figure 3.15C**). In addition, we did not find that mutant htt affects proliferation of glial cells in the corpus callosum of PLP-150Q mice and differentiation of cultured oligodendrocytes from PLP-150Q mice (**Figure 3.16**). All these results support the idea that mutant htt affects the expression of myelin genes in an age-dependent manner, which is consistent with the aging-related and progressive symptoms of HD mice.

3.4 Discussion

By establishing transgenic mice that express mutant htt selectively in oligodendrocytes, we provide strong evidence for the important contribution of mutant htt in oligodendrocytes to HD neuropathology. PLP-150Q mice displayed progressive, neurological symptoms such as locomotor impairment, body weight loss, reduced survival, hypoactivity, and increased seizure susceptibility. We show that mutant htt can affect cell

type-specific gene expression by reducing myelin gene expression, leading to reduced myelination and axonal degeneration. We examined mRNA and protein levels of MCT1, a lactate transporter that is highly expressed in oligodendrocytes, provides lactate to axons, and is essential for axon function and neuronal survival (Lee et al., 2012). We did not see significant changes in MCT1 levels in PLP-150Q mice compared to WT and PLP-23Q, suggesting that mutant htt specifically impairs the myelinating function of oligodendrocytes. However, the mechanism by which mutant htt alters myelin gene expression remains to be investigated.

Although transgenic mice expressing N-terminal mutant htt are valuable models for exploring the pathogenesis of HD, whether their pathological characteristics can be replicated in HD mouse models that express full-length mutant htt merits discussion here. All full-length htt HD mouse models, transgenic or knock-in, show milder disease progression than transgenic mice expressing N-terminal mutant htt (Heng et al., 2008; Menalled and Chesselet, 2002). Because only N-terminal mutant htt is able to misfold and form aggregates, proteolysis of full-length mutant htt has been widely held to be an important step toward HD pathogenesis (Ehrnhoefer et al., 2011; Lee et al., 2013; Ross et al., 2014). In this regard, the expression of N-terminal mutant htt can facilitate disease progression and yield robust phenotypes in mice, allowing us to identify pathogenic pathways and evaluate therapeutic targets (Menalled & Chesselet, 2002; Heng et al., 2008). One good example is that young R6/2 mice at 3-4 months of age, which express exon1 mutant htt, recapitulate many pathological changes seen in the end stage of HD KI mice at 2 years of age (Woodman et al., 2007).

Since HD pathogenesis involves cell-autonomous and non-cell-autonomous toxicity of mutant htt (Gu et al., 2005), generating animal models with cell type-specific pathology is important to dissect HD pathogenesis. In our PLP-150Q transgenic mice, we saw that mutant htt in oligodendrocytes forms aggregates in their nuclei, and reduces myelin MBP gene expression. These important pathogenic events were also seen in HD KI mouse brains, and similar pathological changes are also found in HD patients' brains. Moreover, the effect of mutant htt on axons in PLP-150Q mice is consistent with our early findings that axonal degeneration is seen in the brains of a HD KI mouse model (Li et al., 2001) and transgenic monkey brains (Wang et al., 2008). Our PLP-150Q mouse model supports the idea that axonal degeneration can also be caused by the non-cell-autonomous toxicity of mutant htt in oligodendrocytes.

That said, however, PLP-150Q mice develop much more progressive and severe phenotypes, even when mutant htt is selectively expressed in oligodendrocytes. Such severe phenotypes are unlikely to be due to the overexpression of N-terminal mutant htt since the level of htt-150Q is lower than the control transgenic htt-23Q, which did not elicit any neurological phenotypes. Also, other transgenic HD mouse models expressing N-terminal mutant htt at levels lower than endogenous mouse htt in either astrocytes or axonal terminals show early death and progressive phenotypes (Bradford et al., 2009; Xu et al., 2013). All these findings suggest that, once N-terminal mutant htt accumulates in oligodendrocytes, it can greatly facilitate disease progression.

A new insight from our study is that the transcription dysfunction in oligodendrocytes is both cell type-specific and protein context-dependent. Our findings also suggest that mutant htt affects the function of mature oligodendrocytes. The

accumulation of N-terminal mutant htt in the nuclei of mature oligodendrocytes in adult mice is age-dependent, as evidenced by the following facts: (1) PLP-150Q mice show increased accumulation of mutant htt in the adult brain with aging; (2) PLP-150Q mice display demyelination and reduced myelin gene expression in an age-dependent manner; (3) PLP-150Q mice develop age-dependent and progressive neurological symptoms. Perhaps in mature oligodendrocytes, mutant htt is prone to accumulating in their nuclei, thereby affecting gene expression. Consistent with these facts, we also found that mutant htt did not affect the survival of neuronal cells and oligodendrocyte proliferation during early postnatal development. Although the PLP promoter was found to drive gene expression in different types of cells during embryonic and early developmental stages, transgenic gene expression under this promoter becomes restricted to oligodendrocytes in adult mouse brain (Michalski et al., 2011). Mutant htt-mediated toxicity in oligodendrocytes requires an age-dependent accumulation of misfolded htt in cells. It is likely that mature oligodendrocytes are less capable of clearing misfolded N-terminal htt than undifferentiated precursor cells. Thus, the expression of N-terminal mutant htt, which is prone to misfolding, even at a low level could greatly facilitate the accumulation of the toxic form of mutant htt in oligodendrocytes, whereas in HD KI mice, it takes a much longer time to accumulate N-terminal mutant htt after being generated by the proteolysis of full-length mutant htt.

It is well known that N-terminal mutant htt interacts with transcription factors to inhibit their association with target gene promoters (Harjes and Wanker, 2003; Li and Li, 2004). Therefore, it is likely that mutant htt in oligodendrocytes interacts with a transcription factor to affect myelin gene expression. A recently identified transcription

factor, myelin regulatory factor (MYRF or MRF), which is expressed only in mature, postmitotic oligodendrocytes, was shown to be necessary for the expression of myelin genes (Emery et al., 2009). Knocking out MYRF in adult mice results in reduced myelin gene expression, demyelination, axonal damage, and neurological phenotypes such as tremors and seizures (Koenning et al., 2012). The similarities between MYRF knockout mice and PLP-150Q mice suggest that mutant htt might interact with MYRF to cause oligodendrocyte dysfunction in HD. Understanding the mechanism by which mutant htt causes oligodendrocyte dysfunction will allow us to identify potential targets for therapeutic intervention.

Figure 3.1

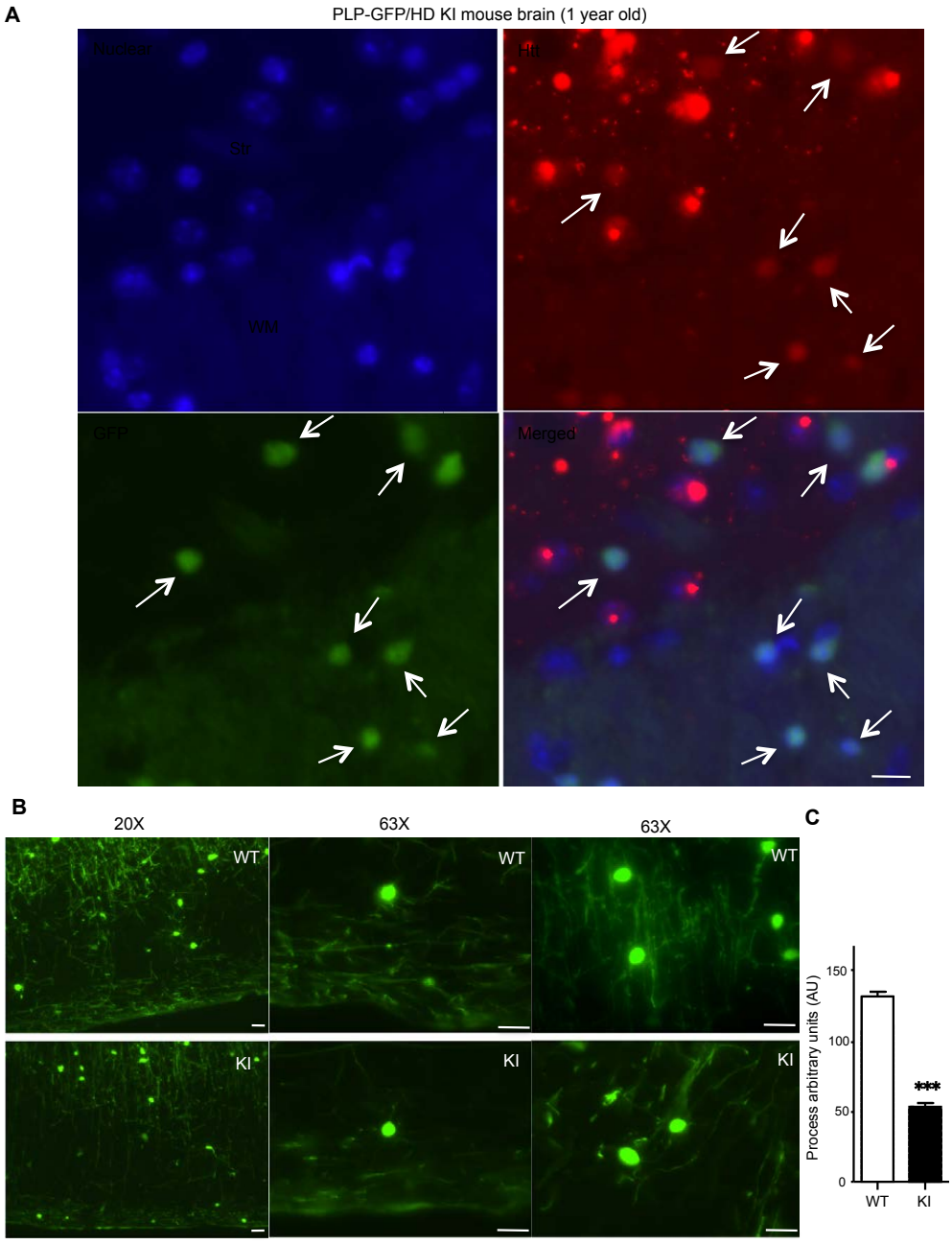
A
PLP-GFP/HD KI mouse brain (1 year old)
Nuclear
Str
WM
Htt
GFP
Merged
B
20X
63X
63X
WT
KI
C
Process arbitrary units (AU)
150
100
50
0
***
WT
KI

Figure 3.1

Expression of mutant htt in oligodendrocytes of HD 140Q knock-in mouse brain. **(A)** PLP-GFP mice were crossed with HD 140Q KI mice, and the brains of the crossed mice (PLP-GFP/KI) at one year of age were examined via immunofluorescent staining with anti-htt (red). Arrows: GFP-positive oligodendrocytes (green) also express mutant htt (red), though neuronal cells show more abundant htt staining. **(B)** In the brain cortex sections that reveal processes of GFP-positive oligodendrocytes, GFP-positive processes are shorter in KI mouse brains. Length is reported in arbitrary units (AU). (**C**) Quantitative analysis of processes of GFP-positive oligodendrocytes in WT and KI mouse brain cortex. *** $p<0.001$. (3= mice per group). Scale bars: (A), 10 mm; (B), 5 mm.

Figure 3.2

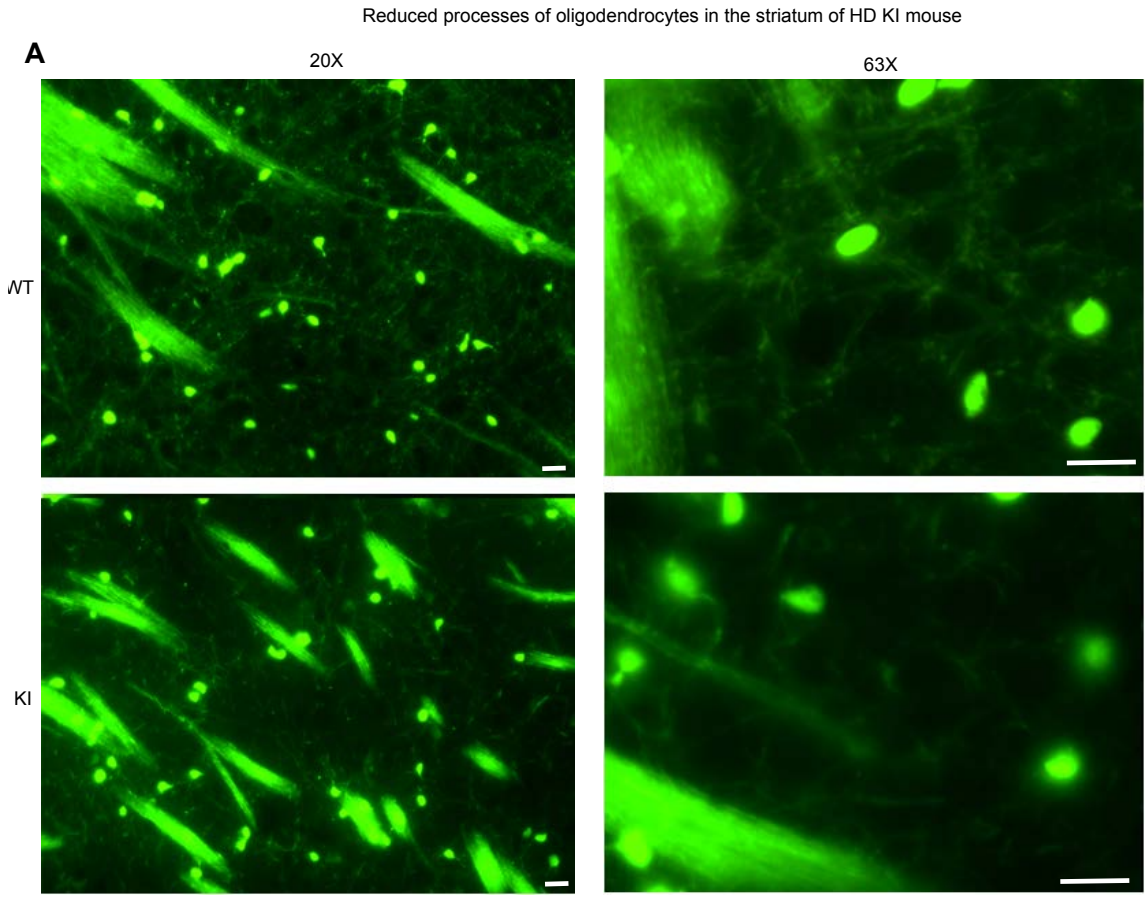
Reduced processes of oligodendrocytes in the striatum of HD KI mouse
A
20X
63X
WT
KI

Figure 3.2

Reduced processes of oligodendrocytes in HD KI mouse brain. PLP-GFP/KI mouse brain sections showing reduced processes of oligodendrocytes in KI mouse brain compared to PLP-GFP mouse brain. Scale bars: 10 μm.

Figure 3.3

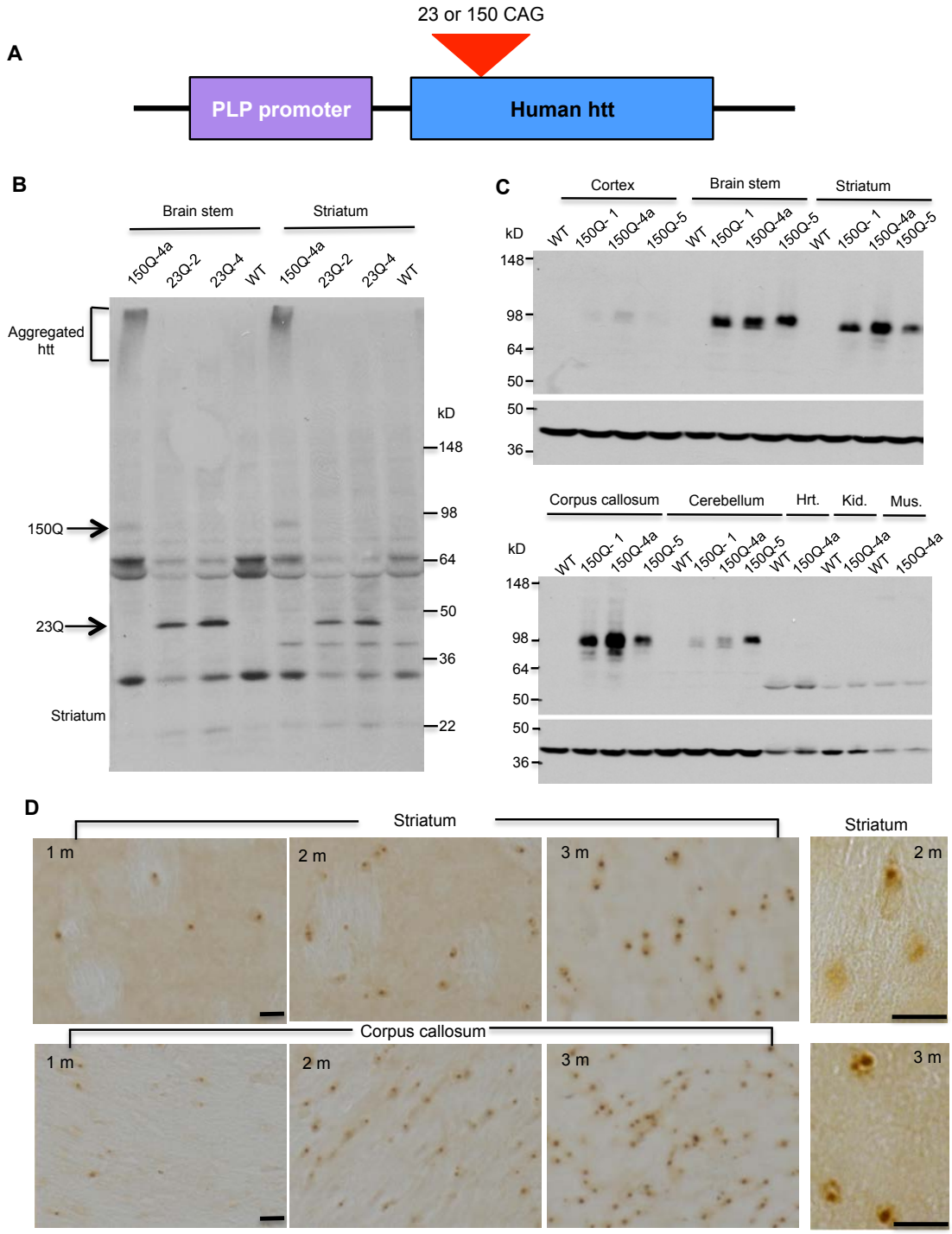
A
23 or 150 CAG
PLP promoter
Human htt
B
Brain stem
Striatum
150Q-4a
23Q-2
23Q-4
WT
Aggregated htt
150Q
23Q
Striatum
kD
148
98
64
50
36
22
C
Cortex
Brain stem
Striatum
Corpus callosum
Cerebellum
Hrt.
Kid.
Mus.
150Q- 1
150Q-5
D
1 m
2 m
3 m

Figure 3.3

Generation of PLP-htt transgenic mice. (A) DNA construct of the vector used to generate transgenic mice expressing N-terminal htt (1-212 amino acids) with 23Q or 150Q under the control of the PLP promoter. **(B)** EM48 western blot analysis of transgenic mouse brain regions (brainstem and striatum) expressing transgenic mutant htt (150Q4a line) and normal htt (23Q-2 and 23Q-4). Aggregated htt in the stacking gel is indicated. (**C**) 1C2 western blot analysis of multiple PLP-150Q lines showing mhtt expression in different brain tissues, but not in peripheral tissues. (**D**) mEM48 immunohistochemical staining of the striatum of PLP-150Q mice at 1, 2, and 3 months of age showing an increased accumulation of mutant htt in the older mice. Right panels show high magnification micrographs. Scale bars: 10 mm.

Figure 3.4

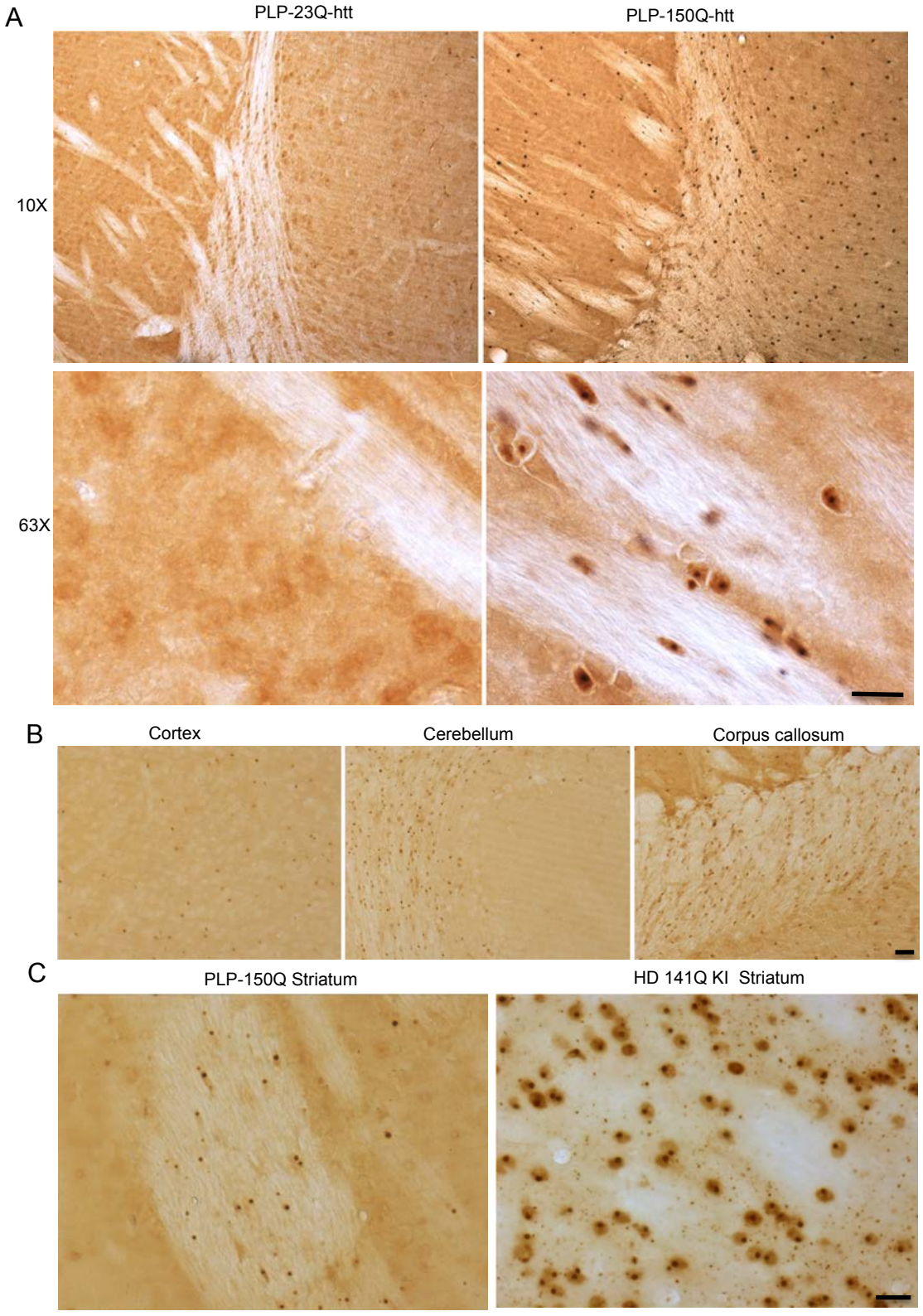
A
PLP-23Q-htt
PLP-150Q-htt
10X
63X
B
Cortex
Cerebellum
Corpus callosum
C
PLP-150Q Striatum
HD 141Q KI Striatum

Figure 3.4

Distribution of transgenic mutant htt in the brains of PLP-150Q mice. (A) Immunostaining with mEM48 showing specific labeling of mutant htt in PLP-150Q mouse brain compared with PLP-23Q mouse brain. **(B)** Immunostaining with mEM48 showing the expression of mutant htt in different regions of the PLP-150Q mouse brain. (C) Comparison of the distribution of mutant htt in the striatum of PLP-150Q mouse (5 months) and HD141Q KI mouse (10 months). Scale bars: 10 μm.

Figure 3.5

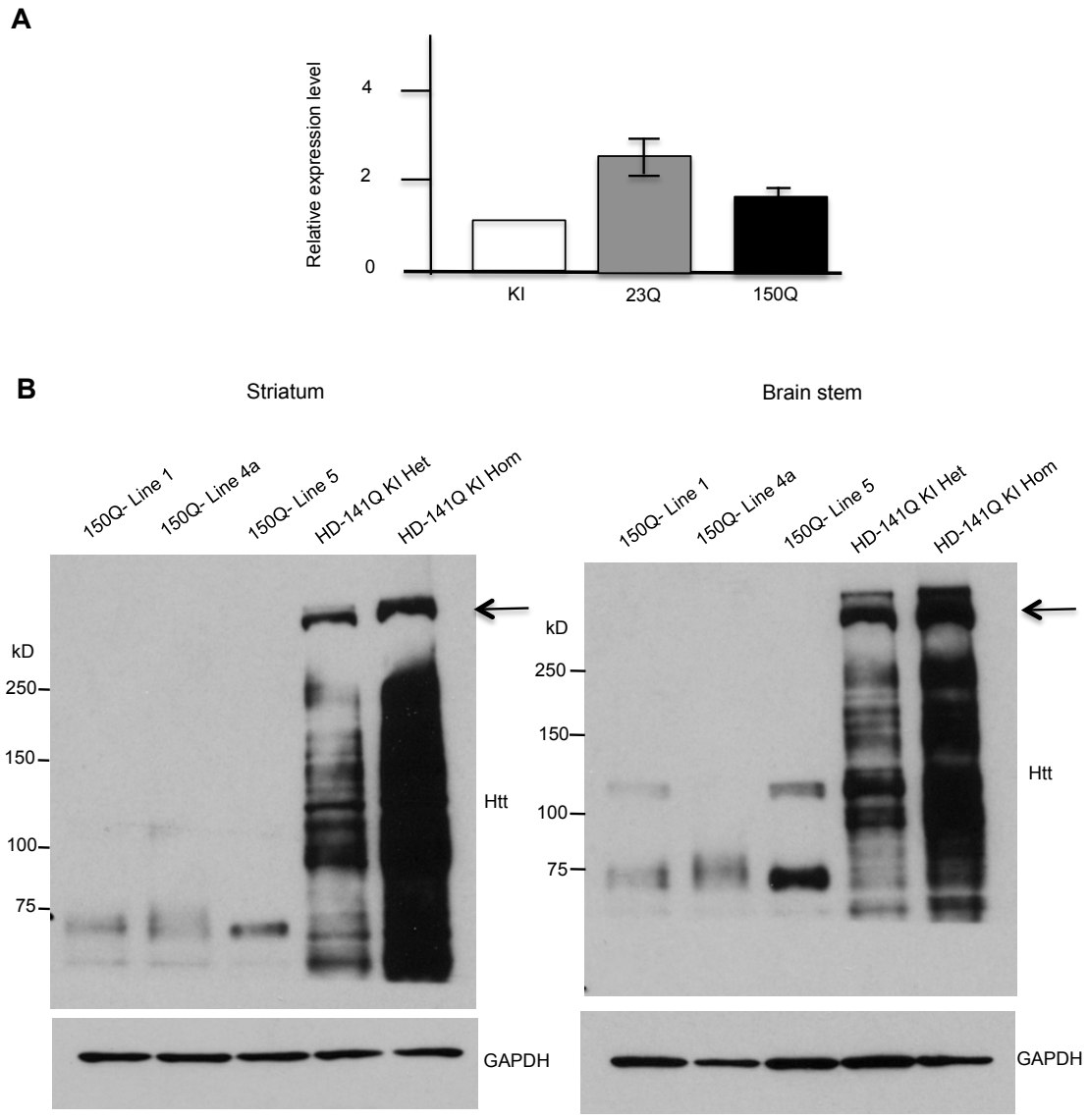
A
Relative expression level
4
2
0
KI
23Q
150Q
B
Striatum
Brain stem
150Q- Line 1
150Q- Line 4a
150Q- Line 5
HD-141Q KI Het
HD-141Q KI Hom
kD
250
150
100
75
Htt
GAPDH

Figure 3.5

Comparison of the expression levels of mutant htt in PLP-150Q and HD141Q KI mouse brains at the age of 6 months. (**A**) Quantitative RT-PCR analysis of mutant human htt mRNAs in the striatum of PLP-150Q and heterozygous HD140Q KI mice. n=3 mice per genotype. (**B**) Western blot analysis of the expression of mutant htt in the brainstem and striatum in PLP-150Q lines and HD140Q KI mouse. 1C2 antibody was used to probe the blots.

Figure 3.6

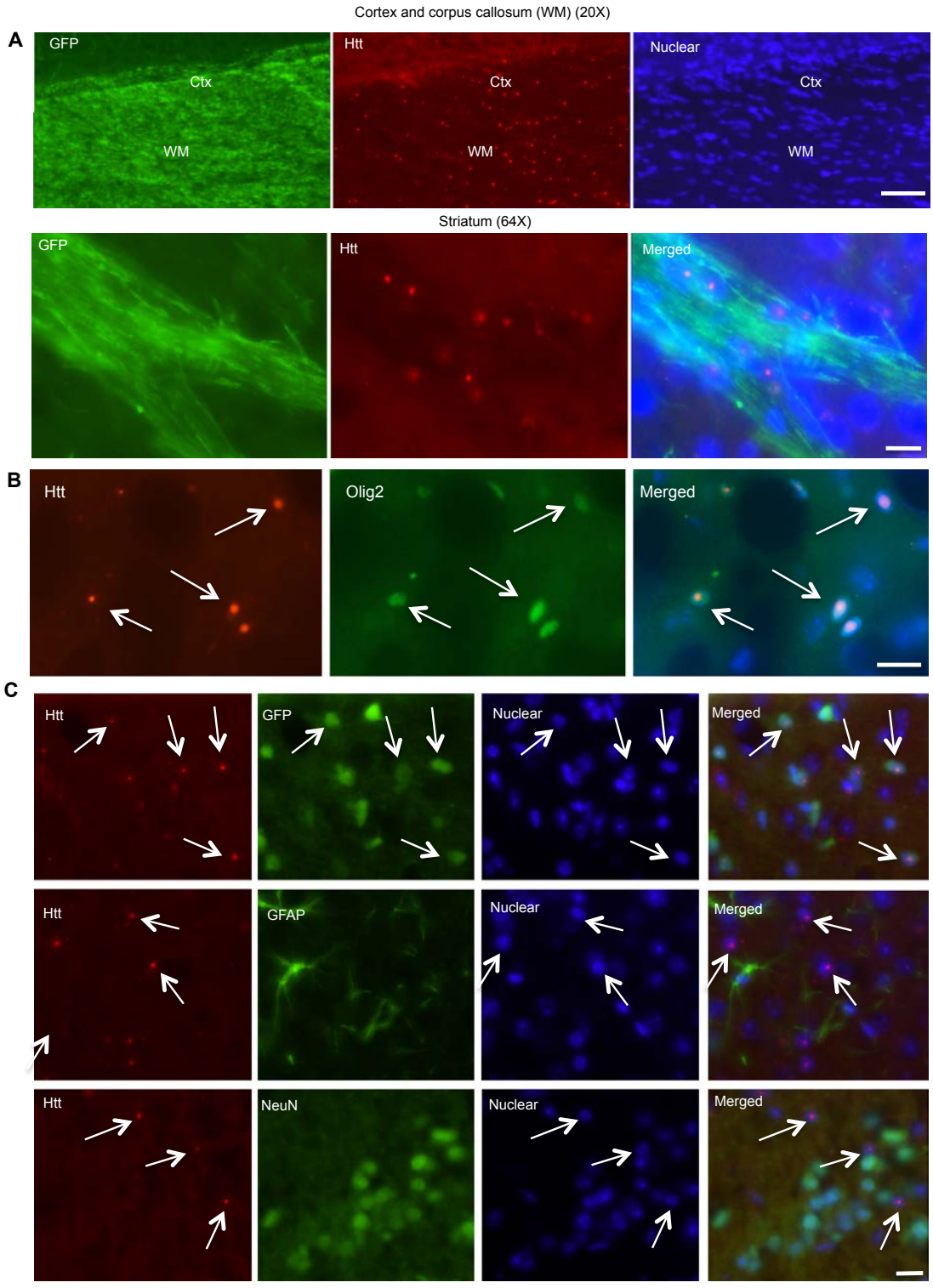
Cortex and corpus callosum (WM) (20X)
A
GFP
Ctx
WM
Htt
Ctx
WM
Nuclear
Ctx
WM
Striatum (64X)
GFP
Htt
Merged
B
Htt
Olig2
Merged
C
Htt
GFP
Nuclear
Merged
Htt
GFAP
Nuclear
Merged
Htt
NeuN
Nuclear
Merged

Figure 3.6

Selective expression of mutant htt in oligodendrocytes of adult PLP-150Q mice. (**A**) PLP-150Q mice were crossed with PLP-GFP mice, resulting in PLP-150Q/GFP mice in which GFP-positive oligodendrocytes (arrows) express mutant htt. Immunostaining with mEM48 (red) showing that mutant htt is enriched in the GFP-positive cells in the white matter (corpus callasum) and also localized in the nucleus. (**B**) Double immunocytochemical staining with antibodies to htt (mEM48) and Olig2 showing the selective expression of mutant htt in oligodendrocytes in in the striatum of 3-month-old PLP-150Q mouse. (**C**) Double staining with antibodies to GFAP and NeuN revealed that mutant Htt is expressed in GFP-positive oligodendrocytes, but not in GFAP-positive astrocytes or NeuN-positive neuronal cells. Scale bars: (A), 40 mm; (B, C): 10 mm.

Figure 3.7

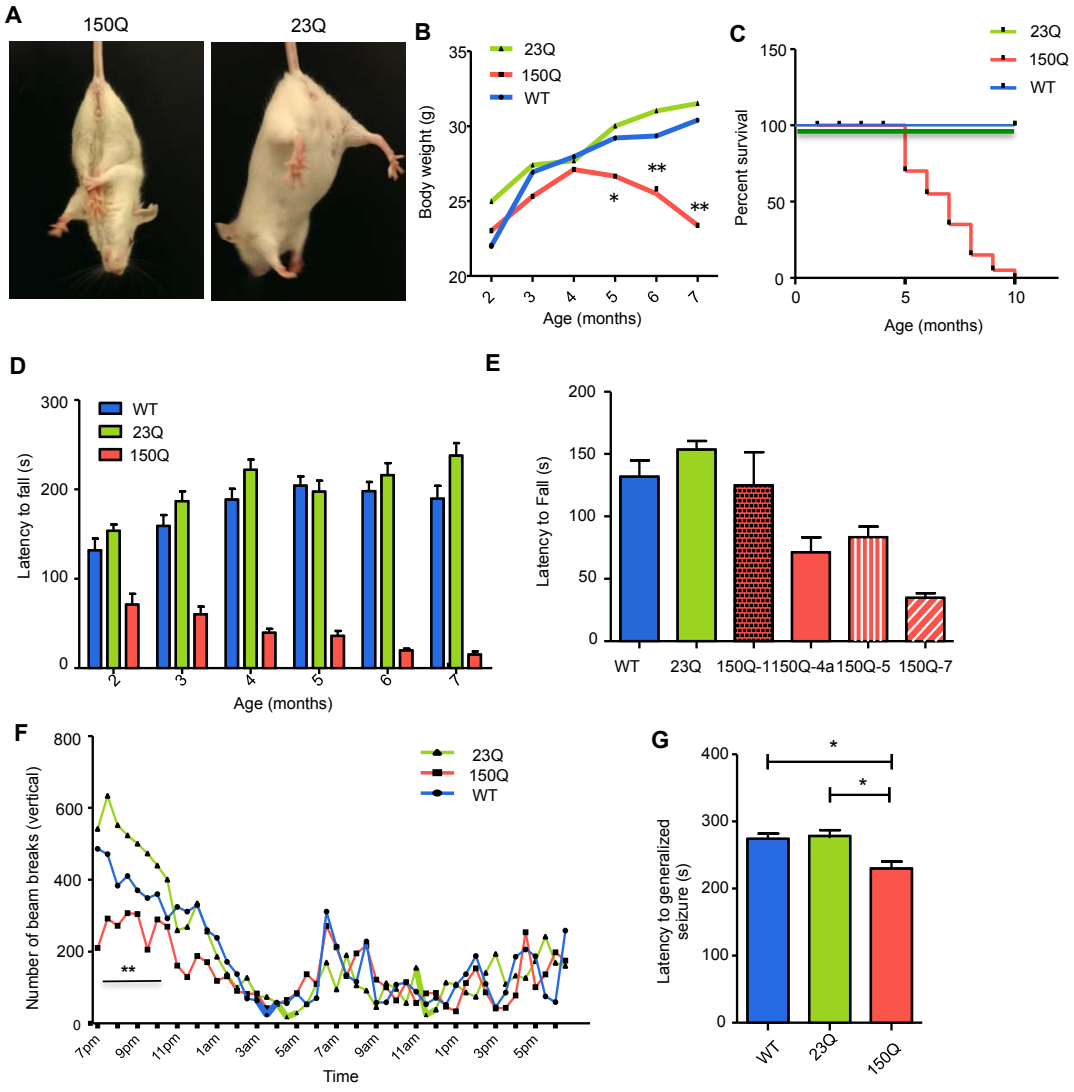
A
150Q
23Q
B
23Q
150Q
WT
Body weight (g)
Age (months)
C
23Q
150Q
WT
Percent survival
Age (months)
D
WT
23Q
150Q
Latency to fall (s)
Age (months)
E
Latency to Fall (s)
WT
23Q
150Q-1
150Q-4a
150Q-5
150Q-7
F
23Q
150Q
WT
Number of beam breaks (vertical)
Time
G
Latency to generalized seizure (s)
WT
23Q
150Q

Figure 3.7

Progressive neurological symptoms of PLP-150Q mice. (**A**) Representative photos of PLP-23Q and PLP-150Q mice, 6 months old. (**B**) Age-dependent loss of body weight in PLP-150Q mice; at least 15 animals per group. (**C**) Early death of PLP-150Q mice. The survival plot shows that PLP-150Q mice die at the age of 5-10 months, n=15. (**D**) Age-dependent worsening of rotarod performance of PLP-150Q mice compared with wild-type and PLP-23Q control mouse lines. At least 15 animals per genotype were examined. (**E**) Motor deficits in different PLP-150Q mouse lines compared with the PLP-23Q mouse line, n=5. (**F**) Locomotor activity was recorded for 24 hours. Statistical analysis shows reduced activity of PLP-150Q mice during the dark cycle, n=8-9, 2-3 months of age. (**G**) Increased susceptibility of PLP-150Q mice to flurothyl-induced seizures. At least 10 animals per genotype, 3-6 months of age. In (A, D-G), data are mean ± SEM. (E) and (G), one-way ANOVA, $p<0.05$. (B) and (F), two-way ANOVA, $p<0.05$. In (B), * significant compared to PLP-23Q; ** significant compared to PLP-23Q and WT.

Figure 3.8

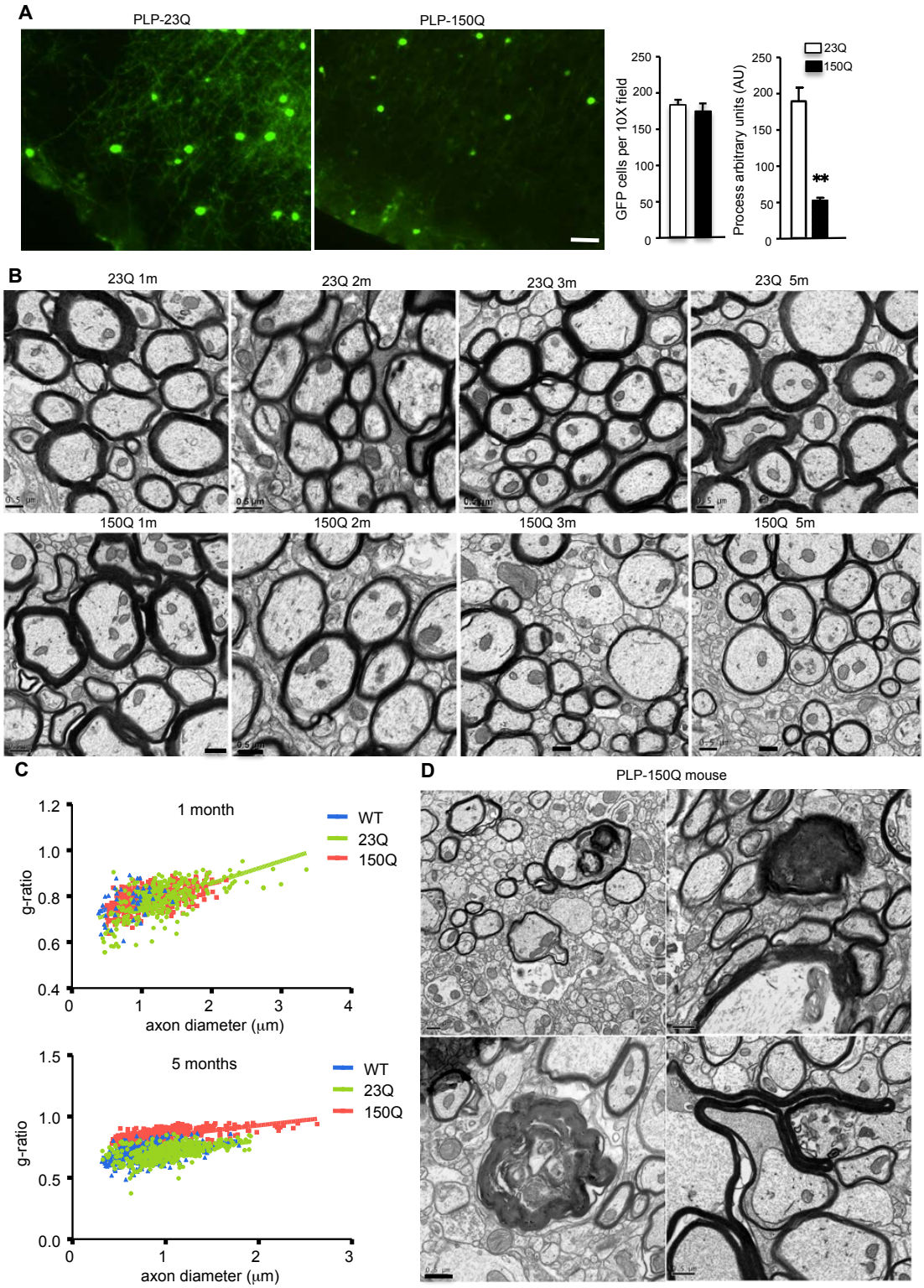
A
PLP-23Q
PLP-150Q
GFP cells per 10X field
Process arbitrary units (AU)
23Q
150Q
**
B
23Q 1m
23Q 2m
23Q 3m
23Q 5m
150Q 1m
150Q 2m
150Q 3m
150Q 5m
C
1 month
WT
23Q
150Q
g-ratio
axon diameter (μm)
5 months
D
PLP-150Q mouse

Figure 3.8

Demyelination and axonal degeneration in PLP-150Q mice. (**A**) Loss of oligodendrocyte processes in the brain cortex in PLP-150Q mouse. Quantitative analysis of the number of GFP-positive oligodendrocytes and process length is shown in the right panel. Oligodendrocytes in PLP-150Q mouse brain have significantly shorter processes than PLP-23Q. Process length is reported in arbitrary units (AU). Data are mean ± SEM. ** $P<0.01$. (**B**) Electron microscopic graphs of the striatum of PLP-23Q and PLP-150Q mice at 1, 2, 3, and 5 months of age. When PLP-150Q mice become old (3 and 5 months), they show demyelination compared with one-month-old PLP-150Q mice and the age-matched PLP-23Q mice. Scale bars: 0.5 μm. (**C**) G-ratios were calculated and plotted against axon diameter with linear regression. G-ratio is significantly increased in PLP-150Q striatum ($g=0.7568\pm0.0068$) compared to age-matched WT and PLP-23Q ($g=0.6315\pm0.0099$ and $g=0.6083\pm.0095$, respectively). One-way ANOVA, $p<0.05$. At least 327 axons per genotype were examined. (**D**) Axonal degeneration and demyelination were also seen in PLP-150Q mice at the age of 5 months. Scale bar: 0.5 μm.

Figure 3.9

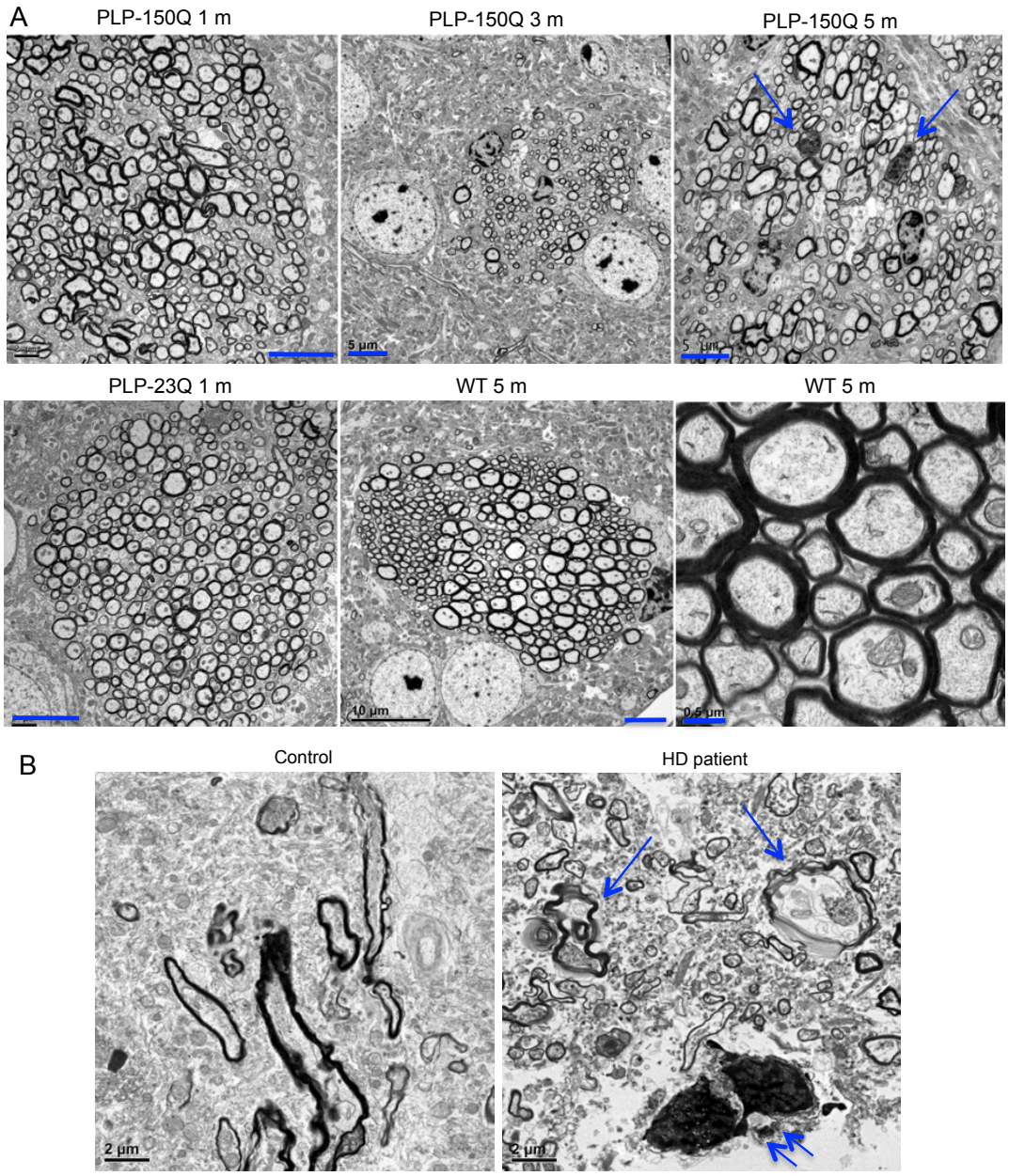
A
PLP-150Q 1 m
PLP-150Q 3 m
PLP-150Q 5 m
5 µm
5 µm
PLP-23Q 1 m
WT 5 m
WT 5 m
10 µm
0.5 µm
B
Control
HD patient
2 µm
2 µm

Figure 3.9

Demyelination and axonal degeneration in PLP-150Q mouse brains and HD patient brains. (A) Electron microscopy revealing age-dependent demyelination and axonal degeneration in PLP-150Q mice at 1, 3, and 5 months of age. Scale bars 2 mm. High magnification (scale bar: 0.5 mm) of the brainstem in WT mouse at 5 months of age is also present. **(B)** Electron microscopic examination of the striatum of the control human and HD patient brains also revealing demyelinated axons (arrows) and dark neurons (double arrows). Scale bar: 2 mm.

Figure 3.10

A

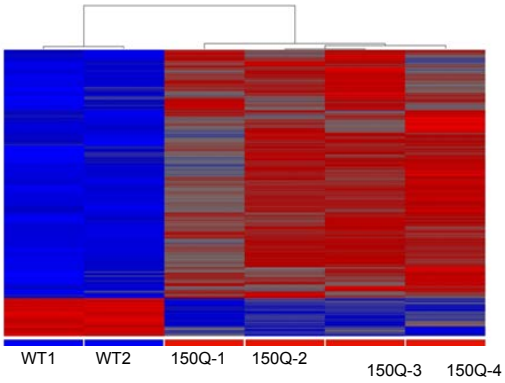

B

Gene	Gene Title	Anova P	Fold-Change	TG vs WT	Description
Zfp488	zinc finger protein 488	8.92E-05	3.44205	TG up vs WT	oligodendrocyte differentiation
Afap1l2	actin filament associated protein 1-like 2	0.00013	2.34299	TG up vs WT	inflammatory response
Tyrobp	TYRO protein tyrosine kinase binding protein	0.00029	4.56297	TG up vs WT	microglia function
Msr1	macrophage scavenger receptor 1	0.00029	6.26569	TG up vs WT	macropgagy scaverge receptor
Myt1	myelin transcription factor 1	0.00036	1.76258	TG up vs WT	role in remyelination
Plau	plasminogen activator, urokinase	0.00039	6.99216	TG up vs WT	serine protease
Lilrb4	leukocyte immunoglobulin-like receptor, subfamily B, member 4	0.00042	5.72042	TG up vs WT	immune response
Ccl3	chemokine (C-C motif) ligand 3	0.00049	9.62351	TG up vs WT	immune response
Mpa2l	macrophage activation 2 like	0.0006	1.9381	TG up vs WT	immune response
Glipr1	GLI pathogenesis-related 1 (glioma)	0.0006	3.14615	TG up vs WT	proapoptotic gene
Itga4	integrin alpha 4	0.00065	1.78102	TG up vs WT	immune response
Bcl2a1d	B-cell leukemia/lymphoma 2 related protein A1d	0.00066	3.29994	TG up vs WT	immune response
Lgals3	lectin, galactose binding, soluble 3	0.00067	4.02685	TG up vs WT	immune response
Cd52	CD52 antigen	0.00069	3.75626	TG up vs WT	immune response
Pten	phosphatase and tensin homolog	0.00073	1.86454	TG up vs WT	apoptosis
Qdpr	Quinoid dihydropteridine reductase	6.36E-06	-1.50285	TG down vs WT	quinoid dihydropteridine reductase
Sc4mol	sterol-C4-methyl oxidase-like	1.05E-05	-2.82109	TG down vs WT	cholestrol biogenesis
Sc5d	sterol-C5-desaturase (fungal ERG3, delta-5-desaturase)	1.53E-05	-1.9392	TG down vs WT	cholestrol biogenesis
Aspa	aspartoacylase	7.77E-05	-3.70398	TG down vs WT	Help maintain whitematter
Serpinb1a	serine (or cysteine) peptidase inhibitor, clade B	7.79E-05	-5.92953	TG down vs WT	proteinase inhibitor
Fa2h	fatty acid 2-hydroxylase	0.00025	-2.33402	TG down vs WT	myelin maintenance
Nsdhl	NAD(P) dependent steroid dehydrogenase-like	0.00027	-2.2123	TG down vs WT	cholesterol biosynthesis
Fdft1	farnesyl diphosphate farnesyl transferase	0.00061	-2.75984	TG down vs WT	cholesterol synthesis
Insig1	insulin induced gene 1	0.00063	-2.80084	TG down vs WT	sterol homeostasis
Mal	myelin and lymphocyte protein, T-cell differentiation protein	0.00068	-1.84538	TG down vs WT	myelination
Hapln2	hyaluronan and proteoglycan link protein 2	0.00112	-2.85075	TG down vs WT	cell adhesion
Mobp	myelin-associated oligodendrocytic basic protein	0.00145	-2.00095	TG down vs WT	myelination
Cyp51	cytochrome P450, family 51	0.00161	-2.36649	TG down vs WT	cholesterol biosynthesis

C

Rank	Functions involved in network	# of genes
1	Lipid Metabolism, Molecular Transport, Small Molecule Biochemistry	29
2	Lipid Metabolism, Small Molecule Biochemistry, Vitamin and Mineral Metabolism	27
3	Cell-To-Cell Signaling and Interaction, Hematological System Development and Function, Immune Cell Trafficking	25
4	Cell Morphology, Cellular Function and Maintenance, Hematological System Development and Function	24
5	Cellular Movement, Skeletal and Muscular System Development and Function, Lipid Metabolism	24
6	Cellular Movement, Hematological System Development and Function, Immune Cell Trafficking	22
7	Cell Death, DNA Replication, Recombination, and Repair, Embryonic Development	22
8	Cellular Growth and Proliferation, Hematological System Development and Function, Cell Death	22

D

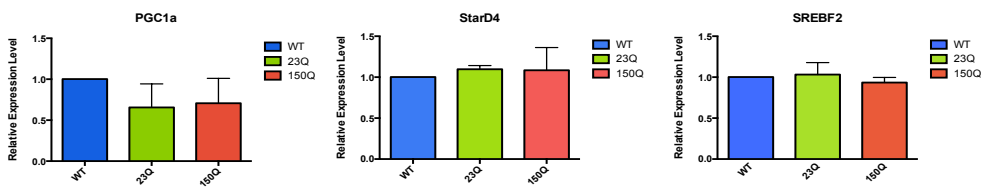

Figure 3.10

Transcript expression in PLP-150Q mouse brain. (A) Microarray analysis of gene expression in PLP-150Q-htt mouse spinal cord at 3 months revealed 998 significantly upregulated and 152 significantly downregulated genes in PLP-150Q compared to WT. **(B)** Most significantly upregulated and downregulated genes. **(C)** Most significant gene networks of differentially expressed genes. **(D)** qPCR analysis of transcripts of several candidate genes (PGC1a, StarD4, SREBF2) in oligodendrocytes in the striatum of PLP-150Q, PLP-23Q and WT mouse brains.

Figure 3.11

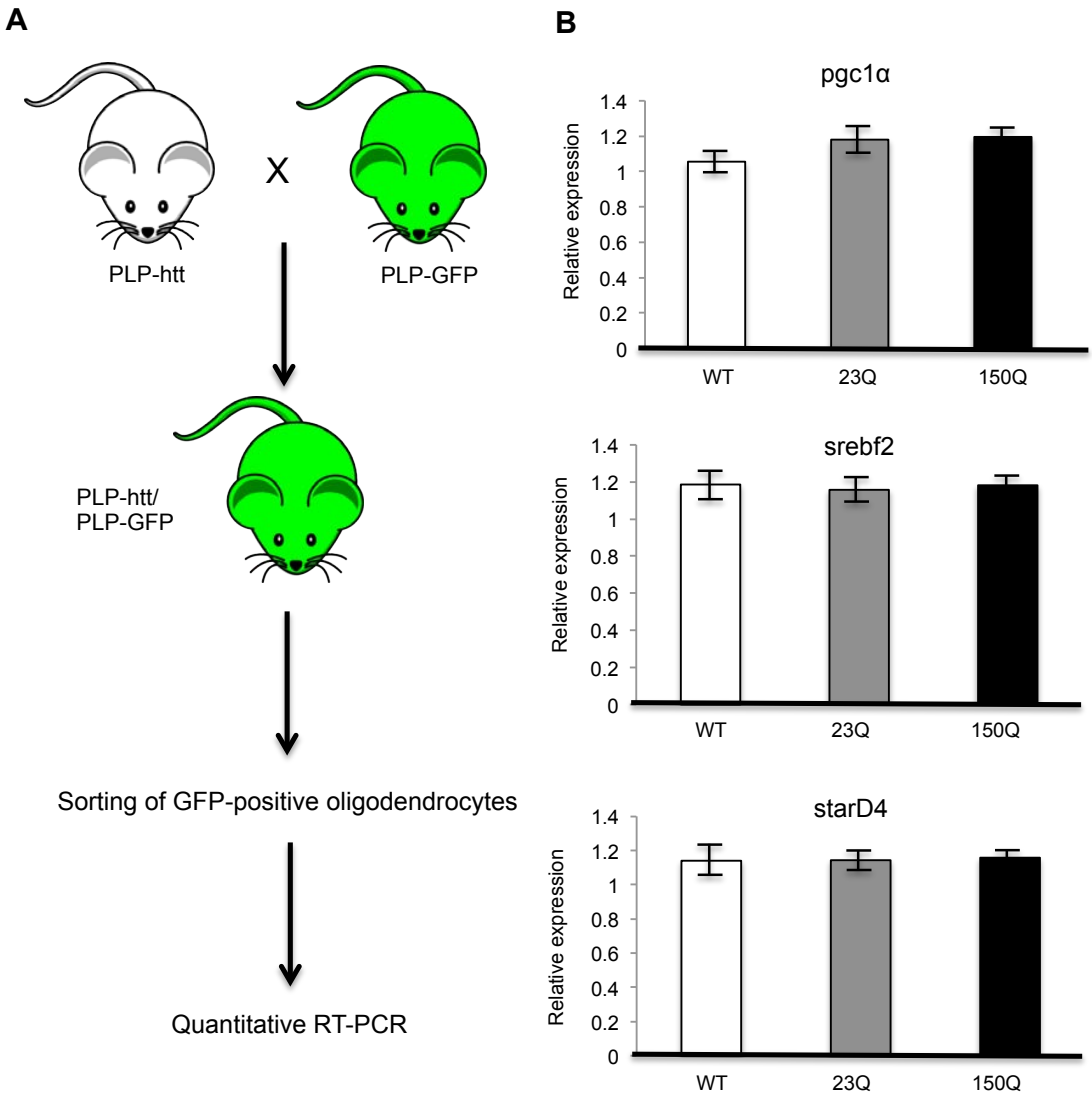
A
PLP-htt
X
PLP-GFP
PLP-htt/
PLP-GFP
Sorting of GFP-positive oligodendrocytes
Quantitative RT-PCR
B
pgc1α
Relative expression
1.4
1.2
1
0.8
0.6
0.4
0.2
0
WT
23Q
150Q
srebf2
Relative expression
1.4
1.2
1
0.8
0.6
0.4
0.2
0
WT
23Q
150Q
starD4
Relative expression
1.4
1.2
1
0.8
0.6
0.4
0.2
0
WT
23Q
150Q

Figure 3.11

Quantitative RT-PCR analysis of the expression of PGC1a, StarD4, SREBF2 in isolated oligodendrocytes. (**A**) PLP-GFP mice were crossed with PLP-23Q or PLP-150Q mice, resulting in WT and double transgenic mice expressing PLP-GFP with PLP-23Q or PLP-150Q. (**B**) GFP-positive oligodendorcytes were isolated by fluorescence sorting and subjected to quantitative PCR analysis of the expression PGC1a, StarD4, SREBF2. The data are shown as mean ± SEM (n= 3 mice per group).

Figure 3.12

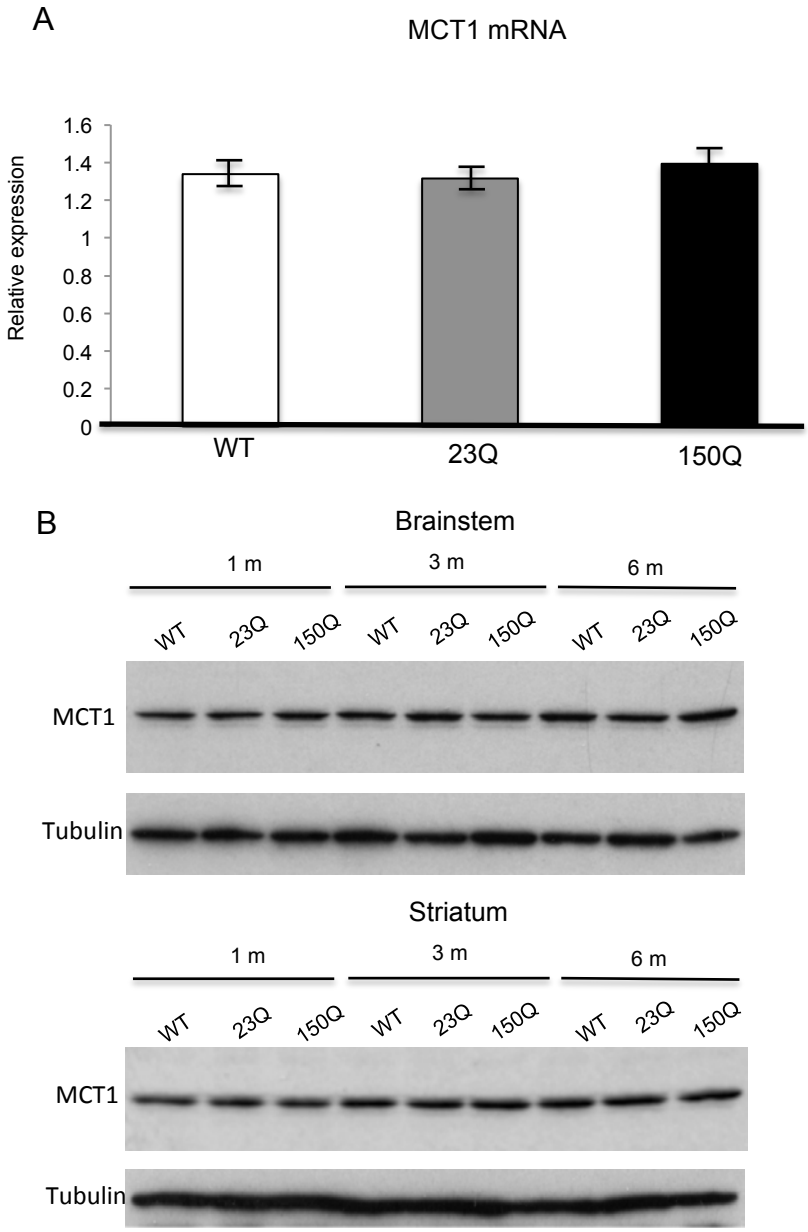
A
MCT1 mRNA
Relative expression
1.6
1.4
1.2
1
0.8
0.6
0.4
0.2
0
WT
23Q
150Q
B
Brainstem
1 m
3 m
6 m
WT
23Q
150Q
MCT1
Tubulin
Striatum
1 m
3 m
6 m
WT
23Q
150Q
MCT1
Tubulin

Figure 3.12

MCT1 expression in control and PLP-150Q mouse brainstem and striatum. **(A)** Quantitative RT-PCR (n=3 mice per genotype) and western blot (B) analyses of mRNA and protein expression levels of MCT1 in wild type, PLP-23Q, and PLP-150Q mice at the age of 3-5 months.

Figure 3.13

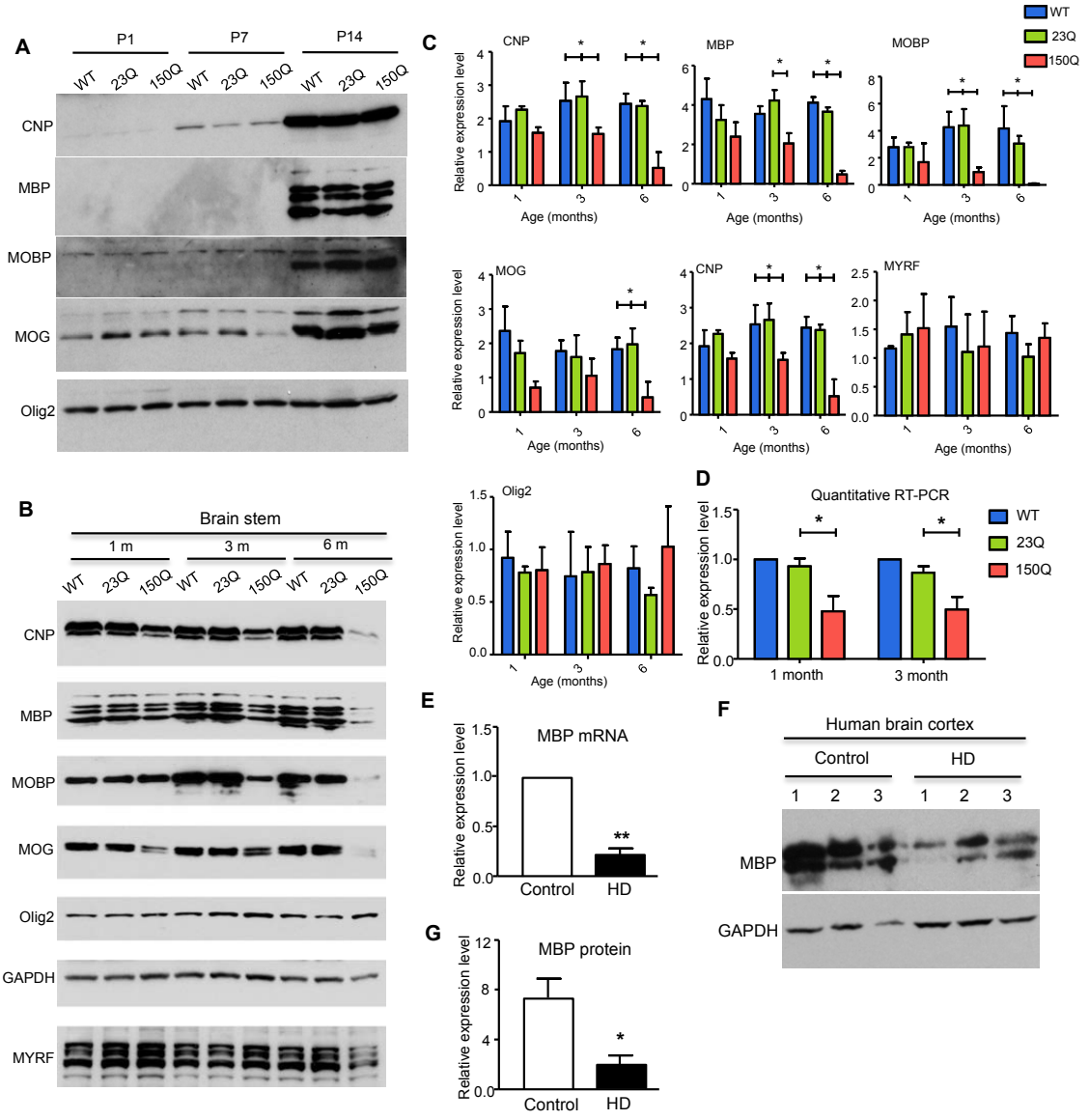
A
P1
P7
P14
WT
23Q
150Q
CNP
MBP
MOBP
MOG
Olig2
B
Brain stem
1 m
3 m
6 m
GAPDH
MYRF
C
WT
23Q
150Q
Relative expression level
Age (months)
MOG
Olig2
D
Quantitative RT-PCR
1 month
3 month
E
MBP mRNA
Control
HD
F
Human brain cortex
G
MBP protein

Figure 3.13

Reduced expression of myelin genes in PLP-150Q mice. (A) Western blotting showing up-regulation of multiple myelin proteins (MBP, CNP, MOBP and MOG) in the mouse brains during postnatal days, which is not affected by mutant htt. **(B)** Western blotting showing the age-dependent decrease of myelin proteins (MBP, CNP, MOBP and MOG) in the brainstem of adult PLP-150Q, but not PLP-23Q and WT, mice. Transcription factor MYRF for the myelin genes and oligodendroglial lineage marker olig-2 remain unchanged in PLP-150Q mouse brain. **(C)** Densitometric analysis of the relative levels of myelin proteins (ratio of myelin protein to GAPDH) in (B). **(D)** qPCR of MBP transcripts verified that MBP mRNA levels are reduced in PLP-150Q mouse brain (n=3/genotype). (A-D): n=3 per genotype and age. Data are mean ± SEM. Two-way ANOVA, $p<0.05$. (**E, F**) qPCR (E) and Western blot (F) analysis of the expression of MBP in the brain cortex of HD patients and control individuals (n=3 each group). (**G**) The relative levels of MBP were quantified by measuring the ratios of MBP to GAPDH on the western blots in (F). * $p< 0.05$; ** $p<0.01$.

Figure 3.14

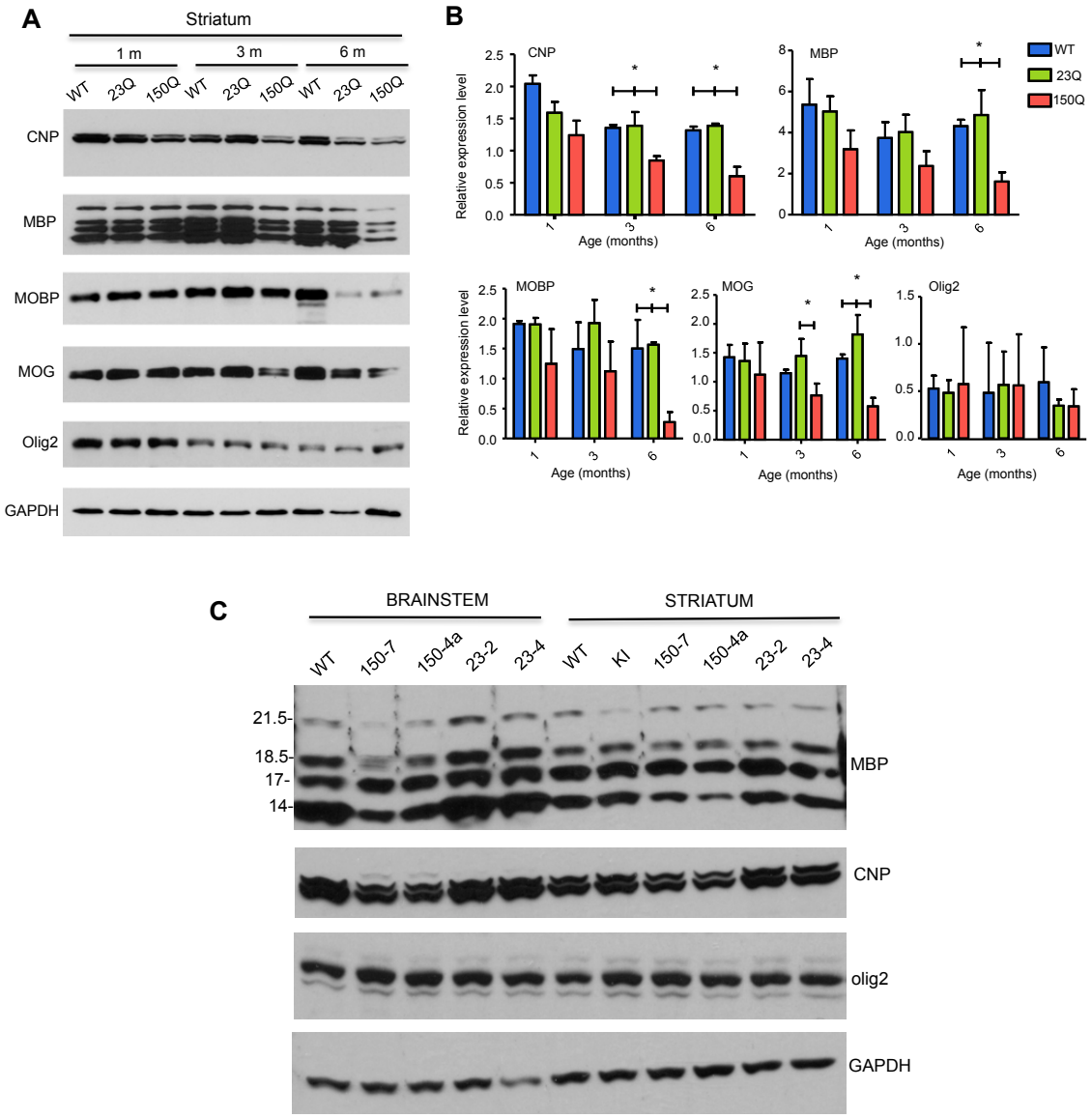
A
Striatum
1 m
3 m
6 m
WT
23Q
150Q
CNP
MBP
MOBP
MOG
Olig2
GAPDH
B
CNP
MBP
MOBP
MOG
Olig2
Relative expression level
Age (months)
WT
23Q
150Q
C
BRAINSTEM
STRIATUM
WT
150-7
150-4a
23-2
23-4
KI
21.5-
18.5-
17-
14-
MBP
CNP
olig2
GAPDH

Figure 3.14

Reduced myelin proteins in HD mouse brains. (A) Age-dependent decrease of myelin proteins in the striatum of PLP-150Q mice. **(B)** The relative levels of myelin proteins (ratio to GAPDH) were obtained from the western blots in (A). *** p<0.05. (C)** Western blotting analysis of the brainstem and striatum showing that expression of MBP is reduced in multiple PLP-150Q mouse lines and the striatum of HD KI mouse.

Figure 3.15

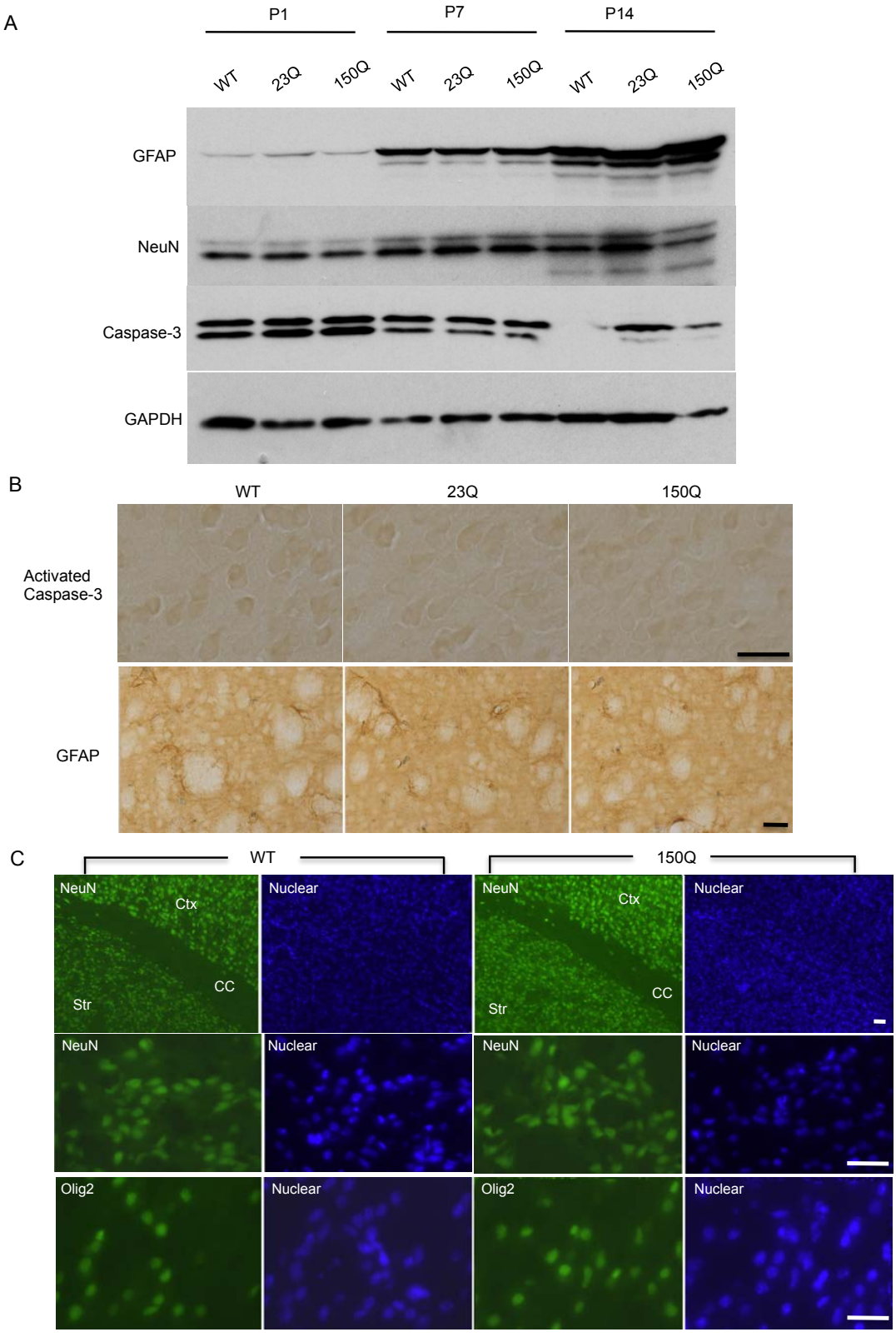
A
P1
P7
P14
WT
23Q
150Q
GFAP
NeuN
Caspase-3
GAPDH
B
WT
23Q
150Q
Activated Caspase-3
GFAP
C
WT
150Q
NeuN
Ctx
CC
Str
Nuclear
Olig2

Figure 3.15

Mutant htt does not affect postnatal expression of myelin proteins as well as neuronal and glial proteins. (A) Western blot analysis of GFAP, NeuN, and caspase-3 in PLP-150Q and control mice at P1, P7, and P14. **(B)** Immunostaining showing no difference in the expression of activated caspase-3 and GFAP in the striatum between WT, PLP-23Q, and PLP-150Q mice. **(C)** Immunofluorescent staining did not reveal altered expression of NeuN and Olig2 in the striatum of PLP-150Q and the WT littermate control mice at P14. Scale bars: 20 mm.

Figure 3.16

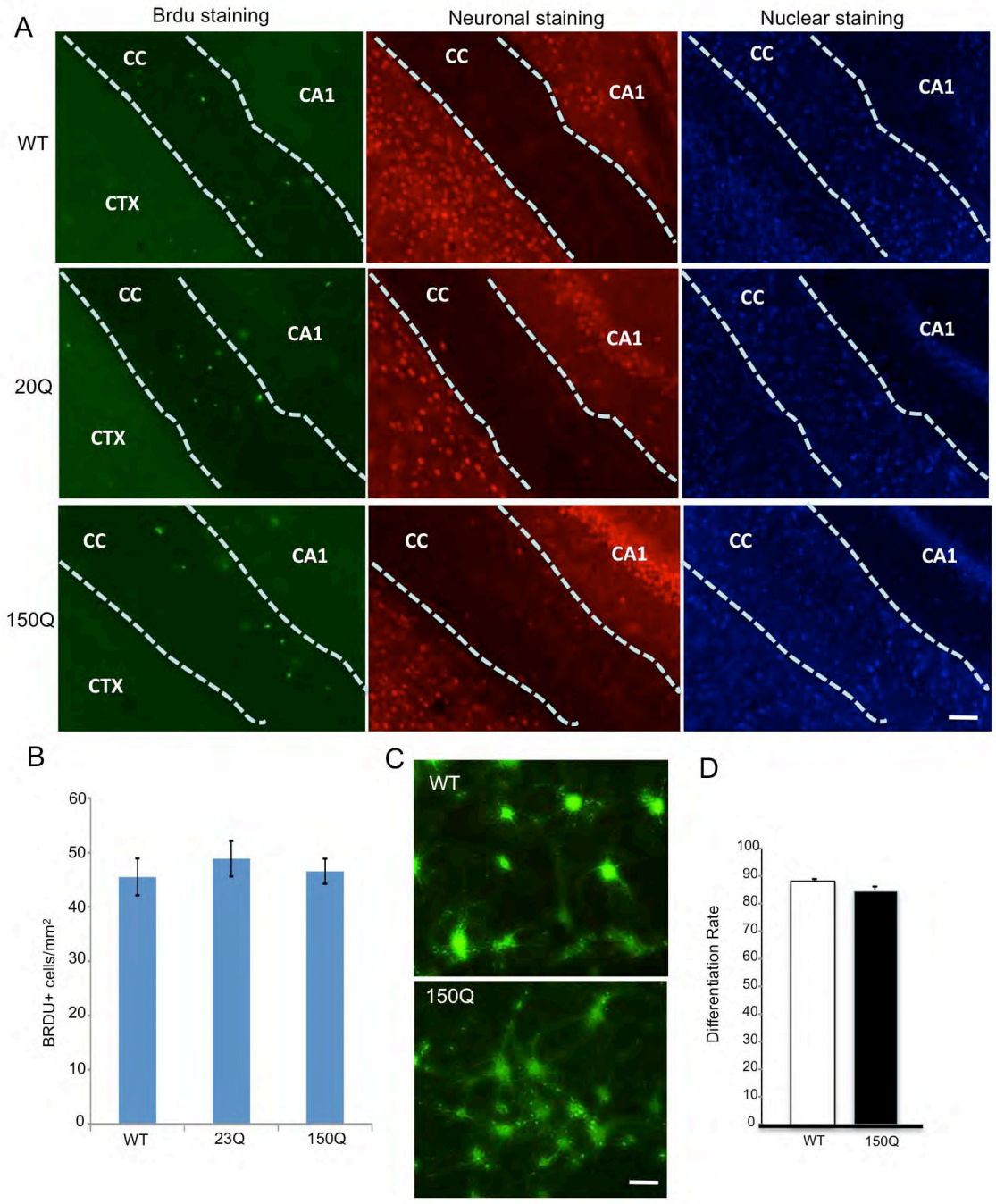
A
Brdu staining
Neuronal staining
Nuclear staining
WT
20Q
150Q
CC
CA1
CTX
B
BRDU+ cells/mm²
60
50
40
30
20
10
0
WT
23Q
150Q
C
WT
150Q
D
Differentiation Rate
100
90
80
70
60
50
40
30
20
10
0
WT
150Q

Figure 3.16

Mutant htt does not affect the glial proliferation and differentiation of oligodendrocytes. (A) Brdu was injected into 2-week-old mice and 3 days later, the Brdu-positive glial cells in the corpus callosum, which was defined by the lack of neuronal staining (red) and the presence of nuclear staining (blue), were counted. **(B)** The numbers (mean+/-SE) of Brdu-positive glial cells per mm^2 in the corpus callosum**. (C)** Cultured oligodendrocytes from PLP-150Q and wild type littermate controls were stained with the antibody to mature oligodendrocyte marker CNP to examine their differentiation**. (D)** The differentiation rates (%) were obtained by counting cells (282 cells in WT and 314 cells in PLP-150Q) with long processes.

Table 3.1 Information for control and HD human samples used in this study

qPCR	Age at death	repeats	tissue	Sample #
Control	57		cortex	6-45
Control	53		cortex	6-114
Control	78		cortex	8-101
HD	57	≈45	cortex	HD5295
HD	65	≈47	cortex	HD5297
HD	39	≈53	cortex	HD5299

Western Blot	Age at death	repeats	tissue	Sample #
Control	78		cortex	8-101
Control	92		cortex	8-137
Control	94		cortex	10-142
HD	57	≈45	cortex	HD5295
HD	65	≈47	cortex	HD5297
HD	39	≈53	cortex	HD5299

EM	Age at death	repeats	tissue	Sample #
control	57		Basal ganglia	6-41
HD	46/56	≈47	Basal ganglia	5-119

CHAPTER 4:

MUTANT HUNTINGTIN DOWNREGULATES MYELIN REGULATOR FACTOR-MEDIATED MYELIN GENE EXPRESSION IN MATURE OLIGODENDROCYTES

This chapter was submitted in part as: Brenda Huang, Wenjie Wei, Guohao Wang, Marta A. Gaertig, Yue Feng, Wei Wang, Xiao-Jiang Li, and Shihua Li. Mutant huntingtin downregulates myelin regulatory factor-mediated myelin gene expression and affects mature oligodendrocytes. *Neuron*. In Press. 2015. Brenda Huang generated the majority of the constructs used for the experiments described in this chapter. Wenjie Wei performed subsequent experiments. Guohao Wang performed experiments described in Figures 4.1C and D. Xiao-Jiang Li, Shihua Li, and Wenjie Wei helped in writing and editing the manuscript.

4.1 Abstract

PLP-150Q transgenic mice, which express N-terminal mutant htt selectively in oligodendrocytes, exhibit progressive, neurological symptoms that include locomotor impairment, body weight loss, reduced lifespan, and increased seizure susceptibility compared to WT and PLP-23Q mice. Electron microscopy revealed age-dependent demyelination (indicated by reduced myelin sheath thickness) as well as axon degeneration in the striatum of PLP-150Q brains. Additionally, we found that the expression of essential myelin-specific genes, such as myelin basic protein (MBP) and 2',3' cyclic nucleotide 3'-phosphodiesterase (CNP) was reduced in an age-dependent manner in PLP-150Q brainstem and striatum, as well as in human HD samples. These findings suggest that the dysfunction of oligodendrocytes is involved in HD pathogenesis. However, the exact mechanism by which mutant htt affects oligodendrocyte function to reduce myelin gene expression and cause demyelination, remains unclear. We examined a recently identified transcription factor, MYRF, which specifically activates and maintains the expression of myelin genes in mature oligodendrocytes. We found that mutant huntingtin binds abnormally to MYRF and affects its transcriptional activity. Our findings suggest that dysfunction of mature oligodendrocytes is involved in HD pathogenesis and may also make a good therapeutic target.

4.2 Introduction

Recent studies have shown that mutant huntingtin affects the function of glial cells, in particular astrocytes and microglia, to cause neuronal degeneration in a non-cell-autonomous manner (Bradford et al., 2009; Crotti et al., 2014; Xu et al., 2013). However,

the role of oligodendrocyte dysfunction in Huntington's disease is not well understood. PLP-150Q mice express mutant htt selectively in oligodendrocytes, and exhibited progressive neurological symptoms including clasping, reduced body weight, reduced survival, locomotor impairment as measured by rotarod performance, and increased seizure susceptibility, all of which are apparent by 2-3 months of age. These mice also show age-dependent demyelination and reduced expression of essential myelin proteins. Our findings indicate that the expression of mutant htt in oligodendrocyte contributes to HD. However, the mechanisms by which mutant htt affects oligodendrocyte function is unknown.

Mutant htt is known to interact with transcription factors to affect gene expression. For example, in neurons, mutant htt binds to Sp1 to inhibit the expression of Sp1 target genes, which include genes that are essential for neuronal survival (Chen-Plotkin et al., 2006; Li et al., 2002). In astrocytes, the increased interaction between mutant htt and Sp1 prevents Sp1 from associating with the promoter of GLT-1, resulting in reduced GLT-1 expression, reduced glutamate uptake from synapses, and neuronal excitotoxicity (Bradford et al., 2009). A recently identified transcription factor, myelin regulatory factor (MYRF or MRF) was found to be critical for myelin gene expression (Emery et al., 2009). MYRF is expressed only by mature, postmitotic oligodendrocytes and localizes to the endoplasmic reticulum, where it is self-cleaved to generate an N-terminal fragment that translocates to the nucleus to act as a transcriptional activator. ((Bujalka et al., 2013; Li et al., 2013). Emery et al. found that knocking down MYRF in cultured oligodendrocytes and mice inhibit the expression of myelin genes, which include those that had reduced expression in PLP-150Q mice. Additionally, knockout mice

displayed myelination defects as well as tremors and seizures (Emery et al., 2009). When MYRF is knocked out in adult mice, there is significant reduction of myelin gene expression and severe demyelination accompanied by axonal damage (Koenning et al., 2012). These results demonstrate that continuous MYRF expression is necessary for the maintenance of myelin in the adult brain. These findings, combined with our own regarding PLP-150Q mice, suggest that mutant htt might interact with MYRF to affect myelin gene expression in PLP-150Q mice.

In order to determine if mutant htt interacts with MYRF, we first used co-immunoprecipitation to show that mutant htt binds to N-terminal MYRF in PLP-150Q and HD140Q KI mice. We then generated MYRF constructs to show *in vitro* that mutant htt binds more strongly to MYRF compared to wild-type htt. We found that MYRF increases MBP promoter activity, and that this increase is inhibited by mutant htt. Lastly, we show that mutant htt reduces the association of MYRF with target gene promoter DNA. Our results demonstrate that mutant htt affects MYRF to reduce myelin gene expression in mature oligodendrocytes, offering new mechanistic insight into the neural dysfunction and axonal degeneration seen in HD.

4.3 Results

Mutant htt binds N-terminal MYRF in HD140Q KI and PLP-150Q mouse brain.

The decrease in several oligodendrocyte-specific proteins in the striatum and brainstem of PLP-150Q mice led us to focus on the transcription factors that mediate the expression of these proteins. Recently, myelin regulatory factor (MYRF) was found to regulate the expression of myelin-specific proteins (Emery et al., 2009; Hornig et al.,

2013). MYRF is not expressed in oligodendrocyte precursors (McKenzie et al., 2014) but expressed only in postmitotic oligodendrocytes (Cahoy et al., 2008), and its depletion in oligodendrocytes causes failures in myelin gene expression and myelin formation (Emery, 2010). However, western blotting showed that MYRF is not decreased in the brains of PLP-150Q mice (**Figure 3.13B**). Because mutant N-terminal htt is able to interact with a number of transcription factors in neuronal cells (Harjes and Wanker, 2003; Li and Li, 2004), we wanted to know whether mutant htt interacts with MYRF and affects myelin gene expression. To this end, we first generated the plasmid encoding mouse MYRF and expressed it in transfected HEK293 cells. We found that MYRF is unstable and cleaved to a smaller N-terminal fragment, which is labeled by an antibody against the N-terminal region of MYRF (**Figure 4.1A**). This finding is consistent with the recent report that MYRF can be self-cleaved (Bujalka et al., 2013; Li et al., 2013). Treatment of cells with the proteasome inhibitor MG132 significantly increased the expression levels of full-length MYRF and its cleaved products (**Figure 4.1B**). Using brain tissues of HD KI mice that express full-length mutant htt at the endogenous level, we performed htt immunoprecipitation and found that more N-terminal MYRF was also co-precipitated with mutant htt (**Figure 4.1C**). To verify that this *in vivo* interaction also occurs in our transgenic htt mouse brain tissues, we performed htt immunoprecipitation and found that mutant htt could co-precipitate more N-terminal MYRF (nMYRF) than full-length MYRF (**Figure 4.1D**).

Mutant htt binds more N-terminal MYRF than normal htt *in vitro* and interacts directly with MRYF.

Although the above immunoprecipitations demonstrate the *in vivo* interaction of MYRF with mutant htt, it remains unclear whether mutant htt binds more N-terminal MYRF than normal htt, as the antibodies (mEM48 and 1C2) we used for immunoprecipitation and western blotting preferentially react with mutant htt and precipitate more mutant htt. To examine whether mutant htt binds abnormally to MYRF, we used transfected cells to express N-terminal htt and MYRF for studying their interactions. We generated N-terminal MYRF (nMYRF) tagged with the Myc epitope and C-terminal MYRF (cMYRF) tagged with the flag epitope (**Figure 4.1E**). Transfection of these two proteins in HEK293 cells confirmed that nMYRF is localized in the nucleus, and cMYRF is in the cytoplasm (**Figure 4.1F**). These results are in agreement with recent findings that nMYRF, once generated from the self-cleavage of full-length MYRF, is able to translocate into the nucleus to execute its transcription function (Bujalka et al., 2013; Li et al., 2013).

By co-expressing nMYRF or cMYRF with NLS-tagged N-terminal htt (1-212 amino acids) containing 23Q or 150Q in HEK293 cells and performing immunoprecipitation of transfected MYRF, we found that more htt-150Q was precipitated by nMYRF when the same levels of htt-23Q and htt-150Q were present in the input (**Figure 4.2A**). In contrast, immunoprecipitation of cMYRF failed to precipitate transfected htt (**Figure 4.2B**). These results support the *in vivo* interaction of mutant htt with N-terminal MYRF in HD mouse brains (**Figure 4.1C,D**). To further verify that mutant htt can interact with MYRF directly, we performed an *in vitro* binding assay using

in vitro synthesized htt incubated with GST-nMYRF fusion proteins. The result also showed that more mutant htt bound to GST-nMYRF than normal htt (**Figure 4.2C**).

Mutant htt interacts with proline-rich domain of MYRF.

Expression of fragments of MYRF with mutant htt in transfected cells followed by co-immunoprecipitation, showed that N-terminal MYRF containing the proline-rich domain interacts with htt and that polyQ expansion could increase this interaction (**Figure 4.3**). Since N-terminal MYRF has transcriptional activity, the binding of mutant htt to the N-terminal region of MYRF suggests this interaction affects the transcription activity of MYRF. Also, the interaction between mutant htt and MYRF suggests that soluble mutant htt binds MYRF, which is supported by immunofluorescent staining of transfected cells in which soluble MYRF is diffuse with mutant htt in the nucleus, but is not colocalized with htt aggregates (**Figure 4.4**).

Mutant htt inhibits transcriptional activity of MYRF.

Based on the above findings, we went on to test whether mutant htt affects the transcription activity of MYRF. For this assay, we isolated the promoter region of the mouse MBP gene based on an earlier report (Mack et al., 2007) and linked this promoter with the luciferase reporter. An assay of luciferase reporter activity showed that MYRF significantly increased MBP promoter activity, which was inhibited by mutant htt (**Figure 4.5A**). Importantly, nMYRF, but not cMYRF, could also stimulate the MBP promoter activity and reverse the inhibition caused by mutant htt (**Figure 4.5B**). Via chromatin immunoprecipitation (ChIP) assay, we immunoprecipitated nMYRF

associated-DNAs in the presence of normal and mutant htt and measured the associated MBP promoter DNAs using quantitative PCR. We found that mutant htt significantly inhibited the association of nMYRF with the MBP promoter (**Figure 4.5C**). These results support the idea that mutant htt binds nMYRF to affect its transcription activity by altering its association with target gene promoter DNA. Based on the fact that MYRF is self-cleaved to nMYRF, which is then translocated into the nucleus to activate myelin gene expression (Bujalka et al., 2013; Li et al., 2013), we propose a model in which N-terminal mutant htt accumulates in the nuclei of oligodendrocytes in an age-dependent manner. This age-related accumulation leads mutant htt to bind nMYRF in mature oligodendrocytes and affects its transcription activity, resulting in decreased expression of myelin genes and an associated myelination deficiency and axonal degeneration in HD (**Figure 4.5D**).

4.4 Discussion

Previously, we established transgenic mice that express mutant htt selectively in oligodendrocytes, and provided strong evidence for the important contribution of mutant htt in oligodendrocytes to HD neuropathology. We also showed that mutant htt can affect cell type-specific gene expression to reduce myelin protein expression, leading to loss of myelination and axonal degeneration. Now, we show that mutant htt affects MYRF transcriptional activity via its abnormal association with MYRF, providing mechanistic insight into the specific effect of mutant htt on a particular type of non-neuronal cell.

The current observation of the effect of mutant htt on MYRF-mediated myelin gene expression is consistent with the findings that N-terminal mutant htt can interact

with a number of transcription factors and affect gene transcription (Harjes and Wanker, 2003; Li and Li, 2004). The age-dependent accumulation of mutant htt, demyelination and reduction of myelin gene expression, and progressive neurological symptoms in PLP-150Q mice suggest that mutant htt affects MYRF-mediated gene expression in mature oligodendrocytes of the adult brain. The idea that mutant htt affects the expression of selective genes in mature oligodendrocytes is also supported by the fact that mutant htt does not reduce the expression of Olig2, which is predominantly expressed in oligodendrocyte precursor cells and undifferentiated oligodendrocytes. Since Olig2 is also present in mature oligodendrocytes and MYRF is restricted to mature oligodendrocytes (Cahoy et al., 2008; Emery et al., 2009), the lack of effect of mutant htt on Olig2 is consistent with the finding that Olig2 expression is not mediated by MYRF (Emery et al., 2009) and indicates a specific effect of mutant htt on MYRF.

Because oligodendrocytes are critical for axonal function and are also a desirable transplant population for remyelination strategies, the findings from our study provide a new therapeutic target for treating HD. Oligodendrocytes are generated mostly during the postnatal periods (P7-P14) in rodents. These cells differentiate from proliferative, migratory oligodendrocyte precursors (OPCs) and produce myelin proteins required for myelination. Although most myelination occurs early in life, myelination processes may exhibit substantial plasticity in adult brains and have evolved to combat a range of infectious, metabolic and immune insults, which can cause demyelination and lead to multiple sclerosis (Emery, 2010; Franklin and Ffrench-Constant, 2008; Paus et al., 1999). A recent study demonstrates that depletion of MYRF prevents adult myelination, reduces the production of new oligodendrocytes during adulthood, and affects motor skill

learning in mice (McKenzie et al., 2014). Newly differentiated oligodendrocytes are widely thought to generate additional myelin (Emery, 2010; Franklin and Ffrench-Constant, 2008), and based on this idea, approaches to promote differentiation of OPCs into myelinating oligodendrocytes have been hotly pursued for the treatment of demyelination-related pathology (Boulanger and Messier, 2014; Rivers et al., 2008). Our studies indicate that mutant htt affects mature oligodendrocytes to cause a decrease in myelin proteins and subsequent loss of myelin, suggesting that the production of myelin proteins in mature oligodendrocytes is important for the maintenance of myelin in adult brains, as well. This idea is also supported by the finding that mutant htt does not reduce Olig2, but rather affects the function of MYRF, which is expressed only in postmitotic oligodendrocytes, and that continuous expression of MYRF in the adult CNS is essential for maintaining mature oligodendrocyte identity and myelin (Cahoy et al., 2008; Emery et al., 2009; Koenning et al., 2012; McKenzie et al., 2014). The findings from our study therefore suggest that improving the function of mature oligodendrocytes could be beneficial in HD, and perhaps other age-dependent neurodegenerative diseases that involve the dysfunction of mature oligodendrocytes and associated axonal dysfunction, as well.

Figure 4.1

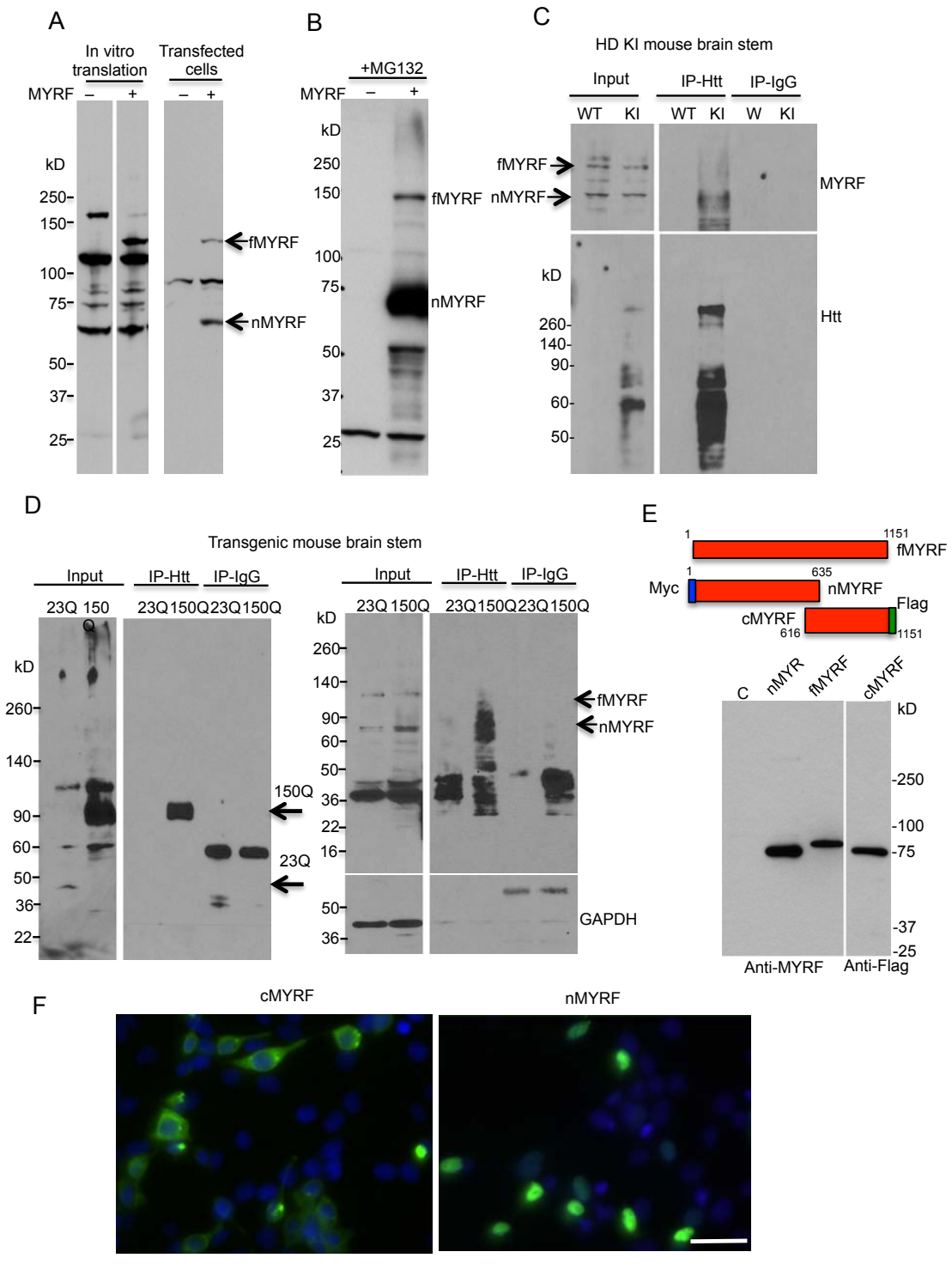
A
In vitro translation
Transfected cells
MYRF
kD
250
150
100
75
50
37
25
fMYRF
nMYRF
B
+MG132
MYRF
kD
250
150
100
75
50
37
25
fMYRF
nMYRF
C
HD KI mouse brain stem
Input
IP-Htt
IP-IgG
WT KI WT KI W KI
fMYRF
nMYRF
MYRF
kD
260
140
90
60
50
Htt
D
Transgenic mouse brain stem
Input
IP-Htt
IP-IgG
23Q 150Q
23Q150Q23Q150Q
kD
260
140
90
60
50
36
22
150Q
23Q
fMYRF
nMYRF
16
GAPDH
E
1
1151
fMYRF
Myc
635
nMYRF
Flag
cMYRF
616
C
nMYR
fMYRF
cMYRF
kD
250
100
75
37
25
Anti-MYRF
Anti-Flag
F
cMYRF
nMYRF

Figure 4.1

Interaction of mutant htt with MYRF in HD140Q KI and PLP-150Q mouse brain. **(A)** Comparison of *in vitro* synthesized and transfected MYRF showing that transfected full-length MYRF is cleaved to N-terminal MYRF (nMYRF) in cells. (**B**) Inhibition of MG132 markedly increased the levels of transfected full-length MYRF and nMYRF, suggesting that the ubiquitin-proteasome system degrades them. **(C)** Immunoprecipitation of mutant htt from HD KI mouse brain selectively co-precipitates N-terminal MYRF (nMYRF). WT and IgG IP served as controls. **(D)** Immunoprecipitation of mutant htt via mEM48 from PLP-150Q transgenic mouse brain also selectively co-precipitates N-terminal MYRF (nMYRF). Htt-150Q was preferentially labeled by 1C2 antibody on western blot (left panel). More nMYRF than full-length MYRF was precipitated with mutant htt (right upper panel). Anti-GAPDH was also used to probe the immunoprecipitates (right low panel). **(E)** Expression of MYRF, nMYRF (1-635 aa) and cMYRF (616-1151 aa) in HEK293 cells. MYRF and nMYRF were detected with anti-myc, whereas cMYRF was detected by anti-flag. **(F)** Transfection of nMYRF and cMYRF into HEK293 cells revealed that only nMYRF is localized in the nucleus, supporting its role in gene transcription. Scale bars: 20 μm.

Figure 4.2

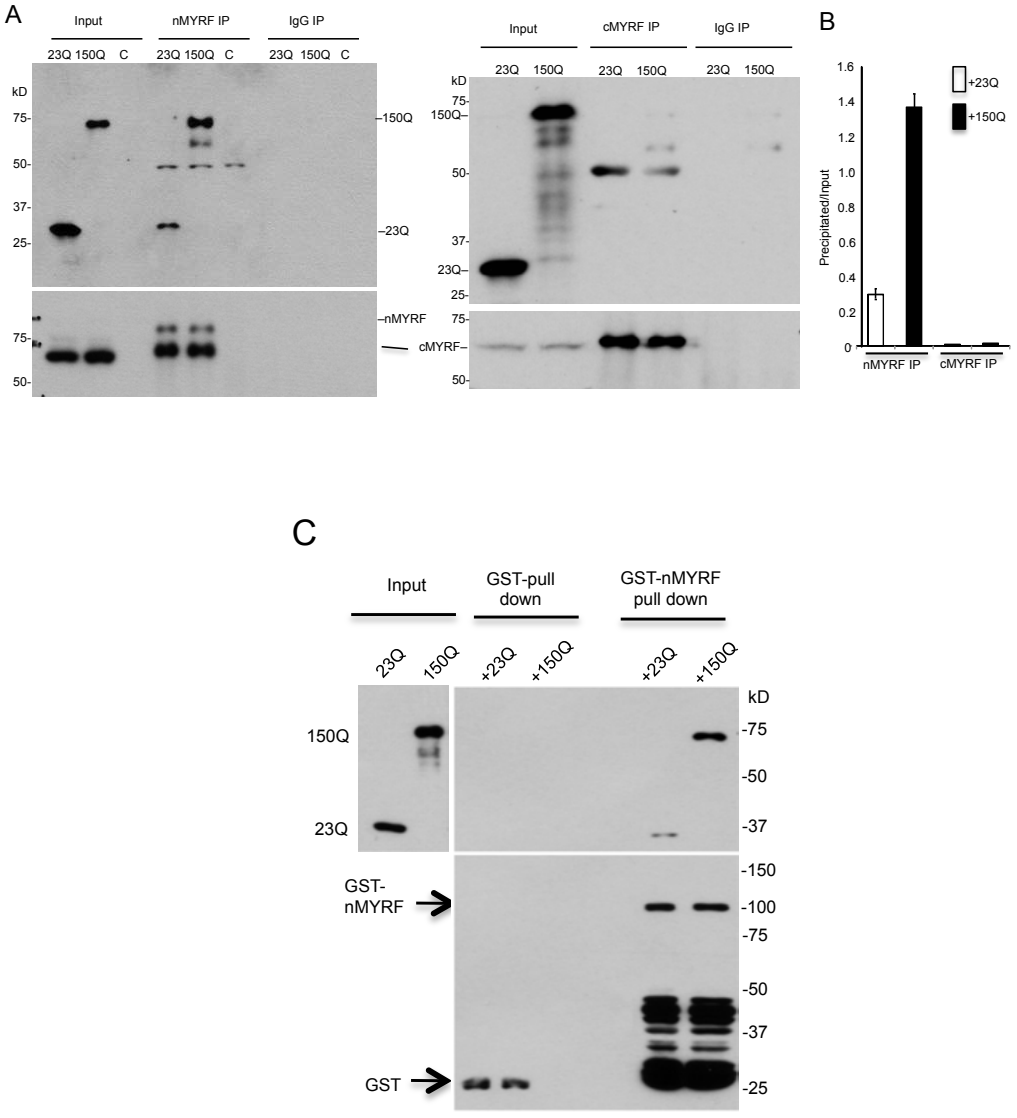
A
Input
nMYRF IP
IgG IP
23Q 150Q C 23Q 150Q C 23Q 150Q C
kD
75-
50-
37-
25-
150Q
23Q
nMYRF
cMYRF
Input
cMYRF IP
IgG IP
23Q 150Q 23Q 150Q 23Q 150Q
B
Precipitated/Input
+23Q
+150Q
nMYRF IP
cMYRF IP
C
Input
GST-pull down
GST-nMYRF pull down
23Q
150Q
+23Q
+150Q
GST-nMYRF
GST
-150
-100
-75
-50
-37
-25

Figure 4.2

Mutant htt binds more N-terminal MYRF than normal htt *in vitro* and interacts directly with MRYF.

(A) Co-transfection of nMYRF (left panel) with N-terminal htt containing 23Q or 150Q into HEK293 cells and immunoprecipitation of nMYRF. More htt-150Q binds nMYRF than htt-23Q. Co-transfection of cMYRF (right panel) with N-terminal htt containing 23Q or 150Q into HEK293 cells showing no interaction between cMYRF and htt. **(B)** The ratio of precipitated to input in (a) is shown. **(C)** GST-nMYRF and GST were expressed and purified to incubate with *in vitro* synthesized N-terminal htt containing 23Q and 150Q also demonstrating that mutant htt directly binds more MYRF.

Figure 4.3

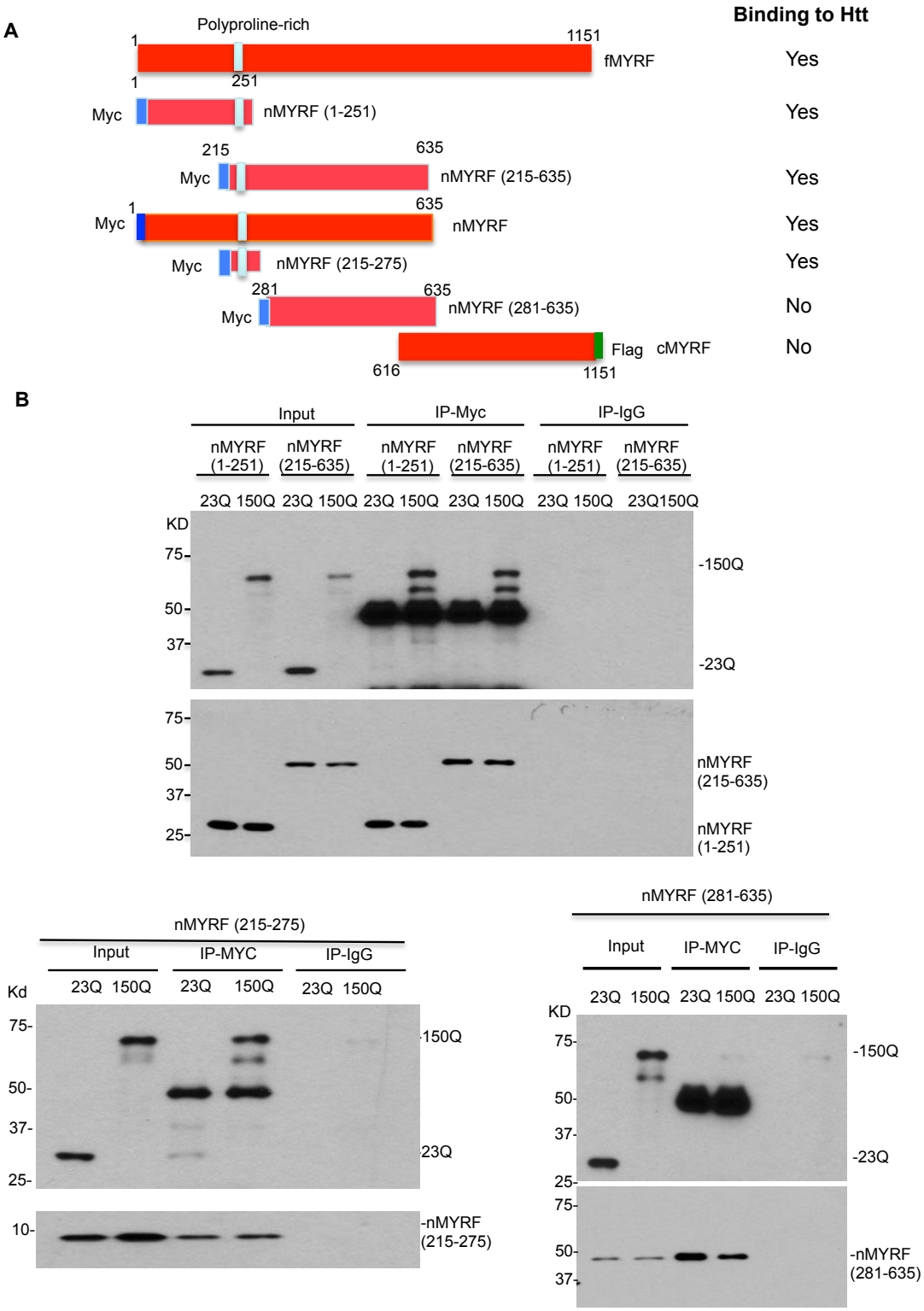
A
Binding to Htt
Polyproline-rich
1
1151
fMYRF
Yes
1
251
Myc
nMYRF (1-251)
Yes
215
635
Myc
nMYRF (215-635)
Yes
1
635
Myc
nMYRF
Yes
Myc
nMYRF (215-275)
Yes
281
635
Myc
nMYRF (281-635)
No
Flag
cMYRF
No
616
1151
B
Input
IP-Myc
IP-IgG
nMYRF (1-251)
nMYRF (215-635)
23Q 150Q 23Q 150Q 23Q 150Q 23Q 150Q 23Q 150Q 23Q150Q
KD
75-
50-
37-
-150Q
-23Q
75-
50-
37-
25-
nMYRF (215-635)
nMYRF (1-251)
nMYRF (215-275)
Input
IP-MYC
IP-IgG
Kd
23Q 150Q 23Q 150Q 23Q 150Q
75-
50-
37-
25-
-150Q
23Q
10-
-nMYRF (215-275)
nMYRF (281-635)
Input
IP-MYC
IP-IgG
23Q 150Q 23Q 150Q 23Q 150Q
KD
75-
50-
37-
25-
-150Q
-23Q
75-
50-
37-
-nMYRF (281-635)

Figure 4.3

Huntingtin-interacting domain of MYRF.

(**A**) Generation of MYRF fragments containing different regions. MYRF containing N-terminal, but not C-terminal, region binds htt. (**B, C**) Western blot analysis of the immunoprecipitated htt and MYRF fragments in transfected HEK 293 cells. Amino acids of each MYRF fragment have been indicated.

Figure 4.4

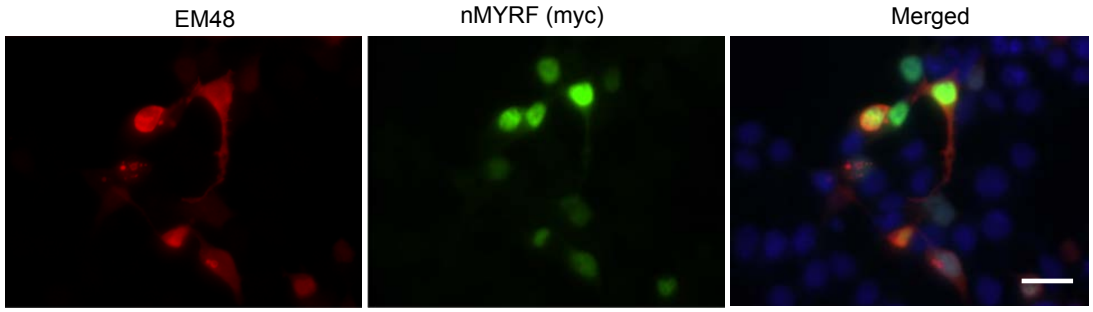

Figure 4.4

Soluble MYRF is not localized in htt aggregates.

Co-expression of NLS-htt in the nucleus with nMYRF reveals no co-localization of MYRF with aggregated htt. Scale bar: 10 μm.

Figure 4.5

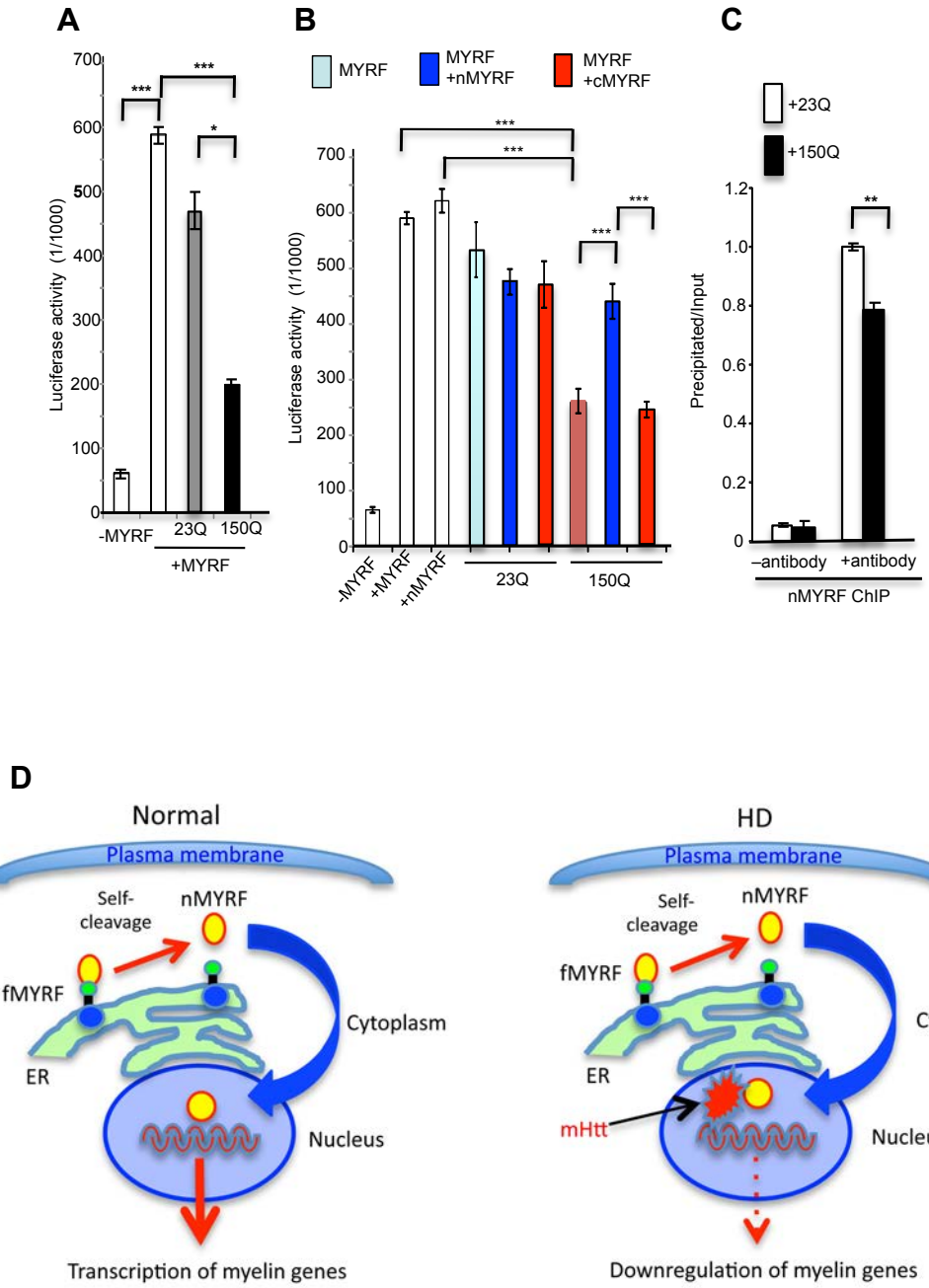
A
B
C
Luciferase activity (1/1000)
-MYRF
23Q
150Q
+MYRF
MYRF
MYRF +nMYRF
MYRF +cMYRF
+nMYRF
Precipitated/Input
+23Q
+150Q
–antibody
+antibody
nMYRF ChIP
D
Normal
HD
Plasma membrane
Self-cleavage
nMYRF
fMYRF
ER
Cytoplasm
Nucleus
mHtt
Transcription of myelin genes
Downregulation of myelin genes

Figure 4.5

Mutant htt inhibits transcriptional activity of MYRF.

(A) MBP promoter was co-expressed with MYRF and htt to assess its transcription activity via luciferase assay. MYRF markedly promotes MBP promoter activity. Co-expression of N-terminal htt with 23Q did not significantly ($p>0.05$) affect the MBP promoter activity, whereas htt-150Q significantly ($p<0.001$) reduces the MBP promoter activity. * $p<0.05$; *** $p<0.001$. **(B)** Expression of nMYRF, but not cMYRF, could rescue the inhibitory effect of mutant htt on the MBP promoter activity. * $p<0.05$; ** $p<0.01$, *** $p<0.001$. (**C**) qPCR quantification of the MBP promoter DNAs associated with Myc-nMYRF that was immunoprecipitated by anti-Myc in ChIP assay. The results were obtained from three independent experiments. ** $p=0.019$. **(D)** A proposed model for the effect of mutant htt in oligodendrocytes. According to recent studies (Bujalka et al., 2013; Li et al., 2013), full-length MYRF is self-cleaved to N-terminal MYRF (nMYRF), which is dissociated from ER and translocalized to the nucleus to activate the expression of myelin genes. In HD, the accumulation of N-terminal mutant htt in the nucleus can lead to the abnormal binding of nMYRF and affects its transcription activity, leading to reduced expression of myelin genes and oligodendrocyte dysfunction.

CHAPTER 5:

CONCLUSIONS AND FUTURE DIRECTIONS

5.1 Summary

Previous studies demonstrated that there are white matter abnormalities (Bartzokis et al., 2007; Fennema-Notestine et al., 2004; Tabrizi et al., 2009), myelination defects (Wade et al., 2008; Xiang et al., 2011), and axonal degeneration (Li et al., 2001; Sapp et al., 1999; Wang et al., 2008) in the brains of HD human patients and animals models. These findings suggest that oligodendrocyte dysfunction plays a role in HD. However, in human tissue and the animal models used in these studies, mutant htt is expressed ubiquitously, making it impossible to determine exactly how mutant htt affects oligodendrocytes. Myelination is regulated by extrinsic factors, such as electrical activity of axons, and proteins secreted by astocytes and neurons (Demerens et al., 1996; Emery et al., 2009; Giulian et al., 1991; Ishibashi et al., 2006). Intrinsic control of myelination, such as transcriptional regulation of genes that are required for myelin formation, is also essential for proper myelination. Therefore, abnormalities in myelination may be a result of neuronal or astrocyte dysfunction, impaired oligodendrocyte function, or a combination of both. The lack of knowledge regarding if and how mutant htt affects oligodendrycte function to cause neuronal degeneration necessitated the development of a new mouse model of HD in which mutant htt is selectively expressed in oligodendrocytes.

In this study, we generated the PLP-150Q model to examine the specific effects of mutant htt on oligodendrocyte function. These mice display robust neurological phenotypes that include clasping, reduced body weight, early death at around 6 months, increased seizure susceptibility, and impaired rotarod performance. A comparison of PLP-150Q and HD140Q KI mice, which expresses mutant htt at the endogenous level,

have a much milder disease progression, revealed that PLP-150Q mice have a lower mutant htt protein level than HD140Q KI. Similarly, a comparison of PLP-150Q and PLP-23Q mice, which lack neurological symptoms, revealed that PLP-150Q mice have a lower level of N-terminal htt than PLP-23Q mice. This suggests that the pronounced phenotypes of PLP-150Q mice are not due to the overexpression of mutant htt, but rather the specific effects of mutant htt on oligodendrocyte function.

In addition to neurological symptoms, PLP-150Q mice had morphological abnormalities, such as reduced oligodendrocyte process length and demyelination of striatal axons that was apparent by 3 months of age. Interestingly, axonal degeneration was present at 5 months but not at 3 months, suggesting that axonal degeneration occurs after, and possibly as a result of, demyelination. Due to the demyelination phenotype of PLP-150Q mice, we next looked at the expression of myelin genes and proteins and found that PLP-150Q mice have reduced myelin protein expression that is noticeable at 1 month of age and becomes significant with age. When we looked at the expression of myelin basic protein, MBP, the major protein component of myelin, we found a significant decrease in MBP mRNA by 1 month of age, indicating that dysregulation of MBP expression occurs early, although MBP protein level is not dramatically reduced until 3 months of age.

We then sought to determine how mutant htt causes axon degeneration and myelin defects. One possible explanation for axon degeneration is that mutant htt affects the expression of MCT1, a lactate transporter that is highly expressed in oligodendrocytes and was previously demonstrated to be essential for axon function and neuronal survival. Lee at al. showed that disruption of MCT1 results in axonal degeneration and neuronal

apoptosis. However, we found that there is no difference in MCT1 mRNA and protein levels, suggesting that mutant htt does not affect MCT1 to cause axonal degeneration in PLP-150Q mice. Reduced myelination and expression of myelin proteins could be due to a reduced number of oligodendrocytes. However, quantification of oligodendrocytes numbers showed there was no difference between PLP-150Q and control mice at 1 month and 3 months of age. We also considered the possibility that oligodendrocyte proliferation and differentiation were affected, but we found no difference in the number of BrdU+ cells or percentage of differentiated oligodendrocytes. These findings suggest that reduced myelin protein expression is not due to impaired oligodendrocyte differentiation, proliferation, or survival. Microarray analysis revealed a significant number of downregulated genes in PLP-150Q that are involved cholesterol synthesis. Therefore, another possibility to consider is that mutant htt affects the synthesis of cholesterol, the major lipid component of myelin. Our qRT-PCR results indicate that there is no difference in the expression of candidate genes that are involved in cholesterol synthesis when comparing PLP-150Q to control mice, suggesting that cholesterol synthesis is not impaired in PLP-150Q mice. Therefore, we believe that mutant htt specifically affects the ability of oligodendrocytes to express myelin genes.

Next, we focused our attention on MYRF, a recently identified transcription factor that has been shown to be necessary for expression of the myelin proteins that were affected in PLP-150Q mice, and is required for the maintenance of myelin. Due to the fact that PLP-150Q mice form myelin normally and display demyelination at 3 months of age, we believed that mutant htt might affect MYRF to impair myelin maintenance. Indeed, we identified a novel interaction between mutant htt and MYRF. We observed

that full-length MYRF is cleaved, and the N-terminal fragment localizes to the nucleus, while the C-terminal fragment remains in the cytoplasm, which is in agreement with previous studies (Bujalka et al., 2013). We determined that htt directly binds to MYRF via a proline-rich domain of N-terminal MYRF, and that this interaction is increased by the polyglutamine expansion. Further, we found that N-terminal MYRF activates MBP promoter activity by directly binding to the promoter, and that mutant htt inhibits the association of MYRF with target gene promoter DNA. We believe that, as mutant htt accumulates in the nucleus, it binds to N-terminal MYRF and inhibits it from binding to myelin gene promoters, thereby reducing myelin gene expression. Our findings demonstrate the important contribution of mutant htt in oligodendrocytes to HD pathology.

5.2 Remaining Questions and Future Directions

As with all animal models of HD, it is important to consider how relevant our findings in PLP-150Q mice are to human HD. Our analysis of human HD tissue revealed a similar decrease in MBP mRNA and protein, as well as demyelinated axons and degenerating neurons. While these results suggest that our findings in PLP-150Q mice may translate to HD patients, we have yet to demonstrate the interaction between mutant htt and MYRF in human tissue. However, our attempts to study MYRF *in vivo* have been hindered by the lack of good antibodies against human MYRF, and until better antibodies are developed, it will be very difficult to determine how mutant htt affects MYRF in human tissue.

We show that mutant htt affects myelination by interacting with MYRF. An interesting study would be to determine what other genes are regulated by MRYF. Bujalka et al. performed ChIP-Seq using N-terminal MYRF to identify a defined consensus motif for MYRF as well as its associated DNAs (Bujalka et al., 2013). It would be worthwhile to determine what the functions of these DNAs are, and if MYRF binding activates the transcription of these DNA-containing genes. It is possible that MYRF-targeted genes include those that are not involved in myelination, and therefore mutant htt may affect additional functions of oligodendrocytes. Similarly, are there other functions of oligodendrocytes that are affected by mutant htt in a MYRF-independent manner? While we demonstrated that mutant htt does not affect MCT1 expression, it is still possible that mutant htt impairs oligodendroglial trophic support of axons through other mechanisms, as oligodendrocytes also release neurotrophic factors to support neuronal survival. We observed increased seizure susceptibility in PLP-150-Q mice, which suggests that mutant htt may affect the insulating properties of the myelin sheath and cause altered electrical activity of neurons. As a future experiment, we can use electrophysiology to determine if there are changes in neuronal activity in symptomatic mice, and if these changes precede demyelination and axonal degeneration.

There are a number of additional experiments that can be done to strengthen the findings of our study. We have shown that the selective expression of mutant htt in oligodendrocytes is sufficient to generate severe neurological phenotypes in PLP-150Q mice. We can perform the inverse experiment using the BACHD mouse model, a conditional transgenic line with two LoxP sites flanking mutant htt-exon 1, which allow Cre-mediated excision of mutant htt-exon 1 and inactivation of mutant htt expression

(Gray et al., 2008). By crossing these mice to an oligodendrocyte-specific Cre-line, such as PLP-Cre (Fuss et al., 2000), we can inactivate mutant htt expression in oligodendrocytes so that all cell types other than oligodendrocytes express mutant htt. Based on our PLP-150Q findings, we would expect inactivation of mutant htt in oligodendrocytes to ameliorate neurological symptoms of the BACHD mouse. This would strongly support our idea that mutant htt-mediated dysfunction of oligodendrocytes plays a critical role in HD. We have also shown in vitro that mutant htt affects oligodendrocyte function by inhibiting the transcriptional activity of MYRF, and that the addition of N-terminal MYRF can relieve the inhibition caused by mutant htt. We would like to use an adeno-associated virus (AAV) vector containing the MYRF gene to determine if overexpression of MYRF in oligodendrocytes *in vivo* can rescue the demyelination and axonal degeneration of PLP-150Q mice. Such an experiment can be done by comparing the brain region injected with AAV-MYRF and the control viral vector that express GFP.

Our study sheds light on the non-cell-autonomous mechanisms involved in Huntington's disease pathogenesis. We provide strong evidence for mutant htt-induced oligodendrocyte dysfunction and subsequent demyelination and axon degeneration. Previous studies in the lab have similarly demonstrated the importance of glial cells in HD. Bradford et al. generated GFAP-160Q mice, which express N-terminal mutant htt specifically in astrocytes. These mice exhibited progressive, late-onset neurological symptoms, including body weight loss, reduced lifespan, and impaired rotarod performance. However, compared to PLP-150Q mice, GFAP-160Q mice have a mild phenotype, with no evidence of neuronal degeneration. It is well studied that astrocytes

are important for oligodendrocyte precursor cell proliferation, migration, and differentiation, and that astrocytes promote myelination (Clemente et al., 2013; Ishibashi et al., 2006). Therefore, we would like to determine if there is a synergistic effect when mutant htt is expressed in both oligodendrocytes and astrocytes. We crossed PLP-150Q mice to GFAP-160Q mice to generate double transgenic mice (PLPxGFAP) expressing mutant htt in both oligodendrocytes and astrocytes. Analysis of body weight loss, survival, and rotarod performance indicate PLPxGFAP mice do not have more severe phenotypes than PLP-150Q (**Figure 5.1**). While we did not observe an exacerbation of neurological symptoms in PLPxGFAP mice, it is likely that PLP-150Q symptoms are too severe to notice a synergistic effect of mutant htt expression in astrocytes. Instead of the PLP-150Q-4a line, which was used in this study, another line with a lower transgene expression level should allow us to see if there is any enhancement of phenotype when mutant htt is expressed in both astrocytes and oligodendrocytes. Also, by crossing HD knock-in mice with transgenic mice expressing GFP in astrocytes or oligodendrocytes selectively and fluorescence activated cell sorting, we can sort out astrocytes and oligodndrocytes expressing full-length mutant htt at the endogenous level. These cells can be subjected to RNAseq analysis to see whether mutant htt affects gene expression to different extents or impairs the expression of specific genes in different types of glial cells. Such studies will reveal cell-type specific effects of mutant htt and their relative contributions to the neurological symptoms of HD. The findings will further guide us to develop effective therapeutics to treat HD.

5.3 Conclusions

Our study demonstrates the important role of oligodendrocyte dysfunction in HD, and suggests that oligodendrocytes could be a potential therapeutic target in treating Huntington's disease. Our findings indicate that reduced myelin gene expression and demyelination occur prior to, and perhaps cause, axonal and neuronal degeneration in PLP-150Q mice. Therefore, remyelination strategies such as implantation of oligodendrocyte precursor cells (Wang et al., 2013) or perhaps induction of MYRF expression may be effective at counteracting mutant htt-induced oligodendrocyte dysfunction. Our findings may provide insight into mechanisms that are involved in other neurodegenerative diseases. Oligodendrocyte dysfunction has been observed in other neurodegenerative diseases, but it remains unclear if impaired oligodendrocyte function is a primary event leading to neuronal degeneration, or a secondary event in response to neuronal or glial dysfunction. Perhaps, there are common mechanisms underlying oligodendrocyte dysfunction in HD and other forms of neurodegeneration. By understanding if and how oligodendrocyte function is affected in other diseases, we will be able to develop therapeutics that can be used for not just Huntington's disease, but possibly many other neurodegenerative diseases.

Figure 5.1

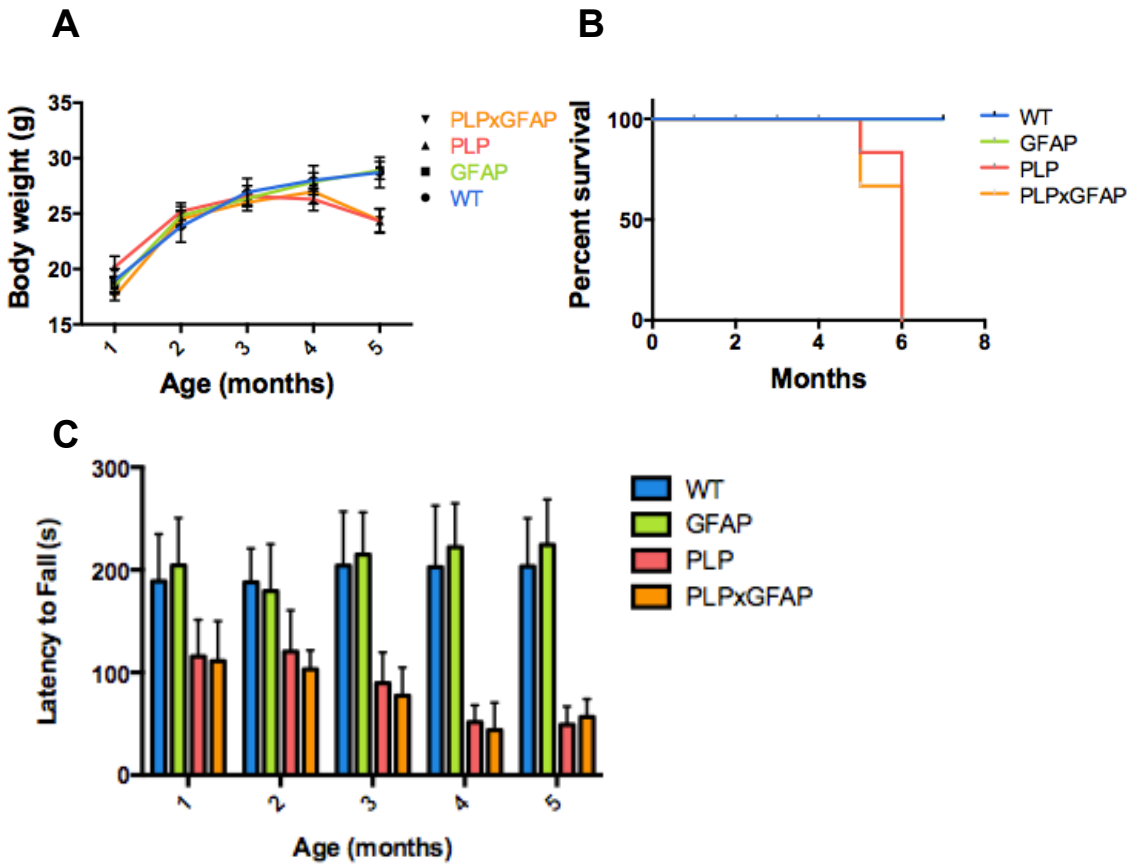
A
Body weight (g)
35
30
25
20
15
1
2
3
4
5
Age (months)
PLPxGFAP
PLP
GFAP
WT
B
Percent survival
100
50
0
0
2
4
6
8
Months
WT
GFAP
PLP
PLPxGFAP
C
Latency to Fall (s)
300
200
100
0
1
2
3
4
5
Age (months)
WT
GFAP
PLP
PLPxGFAP

Figure 5.1

Mice expressing mutant htt in both astrocytes and oligodendrocytes do not display more severe phenotypes than PLP-150Q mice. (A) Age-dependent body weight loss in PLP-150Q (PLP) and double transgenic PLP-150Q x GFAP-160Q (PLPxGFAP). No significant different between PLP and PLPxGFAP; at least 8 animals per group. (**B**) Early death of PLP and PLPxGFAP mice, with mice in both groups dying between 5 and 6 months of age. No significant difference between PLP and PLPxGFAP; at least 6 animals per group. (**C**) Age-dependent worsening of rotarod performance of PLP and PLPxGFAP. No significant difference between PLP and PLPxGFAP performance; at least 7 animals per group. Data are mean ± SEM. Two-way ANOVA, $p<0.05$ when comparing WT or GFAP to PLP or PLPxGFAP, p.>0.05 when comparing PLP to PLPxGFAP.

LITERATURE CITED

Andrade, M.A., and Bork, P. (1995). HEAT repeats in the Huntington's disease protein. Nature genetics *11*, 115-116.

Bankston, A.N., Mandler, M.D., and Feng, Y. (2013). Oligodendroglia and neurotrophic factors in neurodegeneration. Neuroscience bulletin *29*, 216-228.

Barnes, T.D., Kubota, Y., Hu, D., Jin, D.Z., and Graybiel, A.M. (2005). Activity of striatal neurons reflects dynamic encoding and recoding of procedural memories. Nature *437*, 1158-1161.

Bartzokis, G., Lu, P.H., Tishler, T.A., Fong, S.M., Oluwadara, B., Finn, J.P., Huang, D., Bordelon, Y., Mintz, J., and Perlman, S. (2007). Myelin breakdown and iron changes in Huntington's disease: pathogenesis and treatment implications. Neurochemical research *32*, 1655-1664.

Bence, N.F., Sampat, R.M., and Kopito, R.R. (2001). Impairment of the ubiquitin-proteasome system by protein aggregation. Science *292*, 1552-1555.

Bennett, E.J., Bence, N.F., Jayakumar, R., and Kopito, R.R. (2005). Global impairment of the ubiquitin-proteasome system by nuclear or cytoplasmic protein aggregates precedes inclusion body formation. Molecular cell *17*, 351-365.

Bessert, D.A., Gutridge, K.L., Dunbar, J.C., and Carlock, L.R. (1995). The identification of a functional nuclear localization signal in the Huntington disease protein. Brain research Molecular brain research *33*, 165-173.

Boulanger, J.J., and Messier, C. (2014). From precursors to myelinating oligodendrocytes: contribution of intrinsic and extrinsic factors to white matter plasticity in the adult brain. Neuroscience *269*, 343-366.

Bradford, J., Shin, J.Y., Roberts, M., Wang, C.E., Li, X.J., and Li, S. (2009). Expression of mutant huntingtin in mouse brain astrocytes causes age-dependent neurological symptoms. Proceedings of the National Academy of Sciences of the United States of America *106*, 22480-22485.

Bujalka, H., Koenning, M., Jackson, S., Perreau, V.M., Pope, B., Hay, C.M., Mitew, S., Hill, A.F., Lu, Q.R., Wegner, M.*, et al.* (2013). MYRF is a membrane-associated transcription factor that autoproteolytically cleaves to directly activate myelin genes. PLoS biology *11*, e1001625.

Cahoy, J.D., Emery, B., Kaushal, A., Foo, L.C., Zamanian, J.L., Christopherson, K.S., Xing, Y., Lubischer, J.L., Krieg, P.A., Krupenko, S.A.*, et al.* (2008). A transcriptome database for astrocytes, neurons, and oligodendrocytes: a new resource for understanding

brain development and function. The Journal of neuroscience : the official journal of the Society for Neuroscience *28*, 264-278.

Camacho, A., Huang, J.K., Delint-Ramirez, I., Yew Tan, C., Fuller, M., Lelliott, C.J., Vidal-Puig, A., and Franklin, R.J. (2013). Peroxisome proliferator-activated receptor gamma-coactivator-1 alpha coordinates sphingolipid metabolism, lipid raft composition and myelin protein synthesis. The European journal of neuroscience *38*, 2672-2683.

Chen, Y., and Swanson, R.A. (2003). Astrocytes and brain injury. Journal of cerebral blood flow and metabolism : official journal of the International Society of Cerebral Blood Flow and Metabolism *23*, 137-149.

Chen-Plotkin, A.S., Sadri-Vakili, G., Yohrling, G.J., Braveman, M.W., Benn, C.L., Glajch, K.E., DiRocco, D.P., Farrell, L.A., Krainc, D., Gines, S.*, et al.* (2006). Decreased association of the transcription factor Sp1 with genes downregulated in Huntington's disease. Neurobiology of disease *22*, 233-241.

Clemente, D., Ortega, M.C., Melero-Jerez, C., and de Castro, F. (2013). The effect of glia-glia interactions on oligodendrocyte precursor cell biology during development and in demyelinating diseases. Frontiers in cellular neuroscience *7*, 268.

Cornett, J., Cao, F., Wang, C.E., Ross, C.A., Bates, G.P., Li, S.H., and Li, X.J. (2005). Polyglutamine expansion of huntingtin impairs its nuclear export. Nature genetics *37*, 198-204.

Crotti, A., Benner, C., Kerman, B.E., Gosselin, D., Lagier-Tourenne, C., Zuccato, C., Cattaneo, E., Gage, F.H., Cleveland, D.W., and Glass, C.K. (2014). Mutant Huntingtin promotes autonomous microglia activation via myeloid lineage-determining factors. Nature neuroscience *17*, 513-521.

Dai, X., Lercher, L.D., Clinton, P.M., Du, Y., Livingston, D.L., Vieira, C., Yang, L., Shen, M.M., and Dreyfus, C.F. (2003). The trophic role of oligodendrocytes in the basal forebrain. The Journal of neuroscience : the official journal of the Society for Neuroscience *23*, 5846-5853.

Damrath, E., Heck, M.V., Gispert, S., Azizov, M., Nowock, J., Seifried, C., Rub, U., Walter, M., and Auburger, G. (2012). ATXN2-CAG42 sequesters PABPC1 into insolubility and induces FBXW8 in cerebellum of old ataxic knock-in mice. PLoS genetics *8*, e1002920.

Davies, J.E., Sarkar, S., and Rubinsztein, D.C. (2007). The ubiquitin proteasome system in Huntington's disease and the spinocerebellar ataxias. BMC biochemistry *8 Suppl 1*, S2.

Demerens, C., Stankoff, B., Logak, M., Anglade, P., Allinquant, B., Couraud, F., Zalc, B., and Lubetzki, C. (1996). Induction of myelination in the central nervous system by

electrical activity. Proceedings of the National Academy of Sciences of the United States of America *93*, 9887-9892.

Desai, M.K., Mastrangelo, M.A., Ryan, D.A., Sudol, K.L., Narrow, W.C., and Bowers, W.J. (2010). Early oligodendrocyte/myelin pathology in Alzheimer's disease mice constitutes a novel therapeutic target. The American journal of pathology *177*, 1422-1435.

Desmond, C.R., Atwal, R.S., Xia, J., and Truant, R. (2012). Identification of a karyopherin beta1/beta2 proline-tyrosine nuclear localization signal in huntingtin protein. The Journal of biological chemistry *287*, 39626-39633.

Diaz-Hernandez, M., Valera, A.G., Moran, M.A., Gomez-Ramos, P., Alvarez-Castelao, B., Castano, J.G., Hernandez, F., and Lucas, J.J. (2006). Inhibition of 26S proteasome activity by huntingtin filaments but not inclusion bodies isolated from mouse and human brain. Journal of neurochemistry *98*, 1585-1596.

DiFiglia, M., Sapp, E., Chase, K., Schwarz, C., Meloni, A., Young, C., Martin, E., Vonsattel, J.P., Carraway, R., Reeves, S.A.*, et al.* (1995). Huntingtin is a cytoplasmic protein associated with vesicles in human and rat brain neurons. Neuron *14*, 1075-1081.

Dutta, R., and Trapp, B.D. (2011). Mechanisms of neuronal dysfunction and degeneration in multiple sclerosis. Progress in neurobiology *93*, 1-12.

Duyao, M., Ambrose, C., Myers, R., Novelletto, A., Persichetti, F., Frontali, M., Folstein, S., Ross, C., Franz, M., Abbott, M.*, et al.* (1993). Trinucleotide repeat length instability and age of onset in Huntington's disease. Nature genetics *4*, 387-392.

Ehrnhoefer, D.E., Sutton, L., and Hayden, M.R. (2011). Small changes, big impact: posttranslational modifications and function of huntingtin in Huntington disease. The Neuroscientist : a review journal bringing neurobiology, neurology and psychiatry *17*, 475-492.

Eidelberg, D., and Surmeier, D.J. (2011). Brain networks in Huntington disease. The Journal of clinical investigation *121*, 484-492.

Emery, B. (2010). Regulation of oligodendrocyte differentiation and myelination. Science *330*, 779-782.

Emery, B., Agalliu, D., Cahoy, J.D., Watkins, T.A., Dugas, J.C., Mulinyawe, S.B., Ibrahim, A., Ligon, K.L., Rowitch, D.H., and Barres, B.A. (2009). Myelin gene regulatory factor is a critical transcriptional regulator required for CNS myelination. Cell *138*, 172-185.

Faideau, M., Kim, J., Cormier, K., Gilmore, R., Welch, M., Auregan, G., Dufour, N., Guillermier, M., Brouillet, E., Hantraye, P.*, et al.* (2010). In vivo expression of polyglutamine-expanded huntingtin by mouse striatal astrocytes impairs glutamate

transport: a correlation with Huntington's disease subjects. Human molecular genetics *19*, 3053-3067.

Fennema-Notestine, C., Archibald, S.L., Jacobson, M.W., Corey-Bloom, J., Paulsen, J.S., Peavy, G.M., Gamst, A.C., Hamilton, J.M., Salmon, D.P., and Jernigan, T.L. (2004). In vivo evidence of cerebellar atrophy and cerebral white matter loss in Huntington disease. Neurology *63*, 989-995.

Franciosi, S., Ryu, J.K., Shim, Y., Hill, A., Connolly, C., Hayden, M.R., McLarnon, J.G., and Leavitt, B.R. (2012). Age-dependent neurovascular abnormalities and altered microglial morphology in the YAC128 mouse model of Huntington disease. Neurobiology of disease *45*, 438-449.

Franklin, R.J., and Ffrench-Constant, C. (2008). Remyelination in the CNS: from biology to therapy. Nature reviews Neuroscience *9*, 839-855.

Friedman, M.J., Shah, A.G., Fang, Z.H., Ward, E.G., Warren, S.T., Li, S., and Li, X.J. (2007). Polyglutamine domain modulates the TBP-TFIIB interaction: implications for its normal function and neurodegeneration. Nature neuroscience *10*, 1519-1528.

Funfschilling, U., Supplie, L.M., Mahad, D., Boretius, S., Saab, A.S., Edgar, J., Brinkmann, B.G., Kassmann, C.M., Tzvetanova, I.D., Mobius, W.*, et al.* (2012). Glycolytic oligodendrocytes maintain myelin and long-term axonal integrity. Nature *485*, 517-521.

Fuss, B., Mallon, B., Phan, T., Ohlemeyer, C., Kirchhoff, F., Nishiyama, A., and Macklin, W.B. (2000). Purification and analysis of in vivo-differentiated oligodendrocytes expressing the green fluorescent protein. Developmental biology *218*, 259-274.

Gauthier, L.R., Charrin, B.C., Borrell-Pages, M., Dompierre, J.P., Rangone, H., Cordelieres, F.P., De Mey, J., MacDonald, M.E., Lessmann, V., Humbert, S.*, et al.* (2004). Huntingtin controls neurotrophic support and survival of neurons by enhancing BDNF vesicular transport along microtubules. Cell *118*, 127-138.

Ghosh, A., Manrique-Hoyos, N., Voigt, A., Schulz, J.B., Kreutzfeldt, M., Merkler, D., and Simons, M. (2011). Targeted ablation of oligodendrocytes triggers axonal damage. PloS one *6*, e22735.

Giulian, D., Johnson, B., Krebs, J.F., Tapscott, M.J., and Honda, S. (1991). A growth factor from neuronal cell lines stimulates myelin protein synthesis in mammalian brain. The Journal of neuroscience : the official journal of the Society for Neuroscience *11*, 327-336.

Godin, J.D., Poizat, G., Hickey, M.A., Maschat, F., and Humbert, S. (2010). Mutant huntingtin-impaired degradation of beta-catenin causes neurotoxicity in Huntington's disease. The EMBO journal *29*, 2433-2445.

Graham, R.K., Deng, Y., Slow, E.J., Haigh, B., Bissada, N., Lu, G., Pearson, J., Shehadeh, J., Bertram, L., Murphy, Z.*, et al.* (2006). Cleavage at the caspase-6 site is required for neuronal dysfunction and degeneration due to mutant huntingtin. Cell *125*, 1179-1191.

Gray, M., Shirasaki, D.I., Cepeda, C., Andre, V.M., Wilburn, B., Lu, X.H., Tao, J., Yamazaki, I., Li, S.H., Sun, Y.E.*, et al.* (2008). Full-length human mutant huntingtin with a stable polyglutamine repeat can elicit progressive and selective neuropathogenesis in BACHD mice. The Journal of neuroscience : the official journal of the Society for Neuroscience *28*, 6182-6195.

Gu, X., Li, C., Wei, W., Lo, V., Gong, S., Li, S.H., Iwasato, T., Itohara, S., Li, X.J., Mody, I.*, et al.* (2005). Pathological cell-cell interactions elicited by a neuropathogenic form of mutant Huntingtin contribute to cortical pathogenesis in HD mice. Neuron *46*, 433-444.

Harjes, P., and Wanker, E.E. (2003). The hunt for huntingtin function: interaction partners tell many different stories. Trends in biochemical sciences *28*, 425-433.

Havel, L.S., Wang, C.E., Wade, B., Huang, B., Li, S., and Li, X.J. (2011). Preferential accumulation of N-terminal mutant huntingtin in the nuclei of striatal neurons is regulated by phosphorylation. Human molecular genetics *20*, 1424-1437.

Heng, M.Y., Detloff, P.J., and Albin, R.L. (2008). Rodent genetic models of Huntington disease. Neurobiology of disease *32*, 1-9.

Herculano-Houzel, S. (2009). The human brain in numbers: a linearly scaled-up primate brain. Frontiers in human neuroscience *3*, 31.

Hickey, M.A., Kosmalska, A., Enayati, J., Cohen, R., Zeitlin, S., Levine, M.S., and Chesselet, M.F. (2008). Extensive early motor and non-motor behavioral deficits are followed by striatal neuronal loss in knock-in Huntington's disease mice. Neuroscience *157*, 280-295.

Hodgson, J.G., Agopyan, N., Gutekunst, C.A., Leavitt, B.R., LePiane, F., Singaraja, R., Smith, D.J., Bissada, N., McCutcheon, K., Nasir, J.*, et al.* (1999). A YAC mouse model for Huntington's disease with full-length mutant huntingtin, cytoplasmic toxicity, and selective striatal neurodegeneration. Neuron *23*, 181-192.

Hornig, J., Frob, F., Vogl, M.R., Hermans-Borgmeyer, I., Tamm, E.R., and Wegner, M. (2013). The transcription factors Sox10 and Myrf define an essential regulatory network module in differentiating oligodendrocytes. PLoS genetics *9*, e1003907.

Ishibashi, T., Dakin, K.A., Stevens, B., Lee, P.R., Kozlov, S.V., Stewart, C.L., and Fields, R.D. (2006). Astrocytes promote myelination in response to electrical impulses. Neuron *49*, 823-832.

Kalchman, M.A., Koide, H.B., McCutcheon, K., Graham, R.K., Nichol, K., Nishiyama, K., Kazemi-Esfarjani, P., Lynn, F.C., Wellington, C., Metzler, M.*, et al.* (1997). HIP1, a human homologue of S. cerevisiae Sla2p, interacts with membrane-associated huntingtin in the brain. Nature genetics *16*, 44-53.

Kang, S.H., Li, Y., Fukaya, M., Lorenzini, I., Cleveland, D.W., Ostrow, L.W., Rothstein, J.D., and Bergles, D.E. (2013). Degeneration and impaired regeneration of gray matter oligodendrocytes in amyotrophic lateral sclerosis. Nature neuroscience *16*, 571-579.

Kim, Y.J., Yi, Y., Sapp, E., Wang, Y., Cuiffo, B., Kegel, K.B., Qin, Z.H., Aronin, N., and DiFiglia, M. (2001). Caspase 3-cleaved N-terminal fragments of wild-type and mutant huntingtin are present in normal and Huntington's disease brains, associate with membranes, and undergo calpain-dependent proteolysis. Proceedings of the National Academy of Sciences of the United States of America *98*, 12784-12789.

Koenning, M., Jackson, S., Hay, C.M., Faux, C., Kilpatrick, T.J., Willingham, M., and Emery, B. (2012). Myelin gene regulatory factor is required for maintenance of myelin and mature oligodendrocyte identity in the adult CNS. The Journal of neuroscience : the official journal of the Society for Neuroscience *32*, 12528-12542.

Kreitzer, A.C., and Malenka, R.C. (2008). Striatal plasticity and basal ganglia circuit function. Neuron *60*, 543-554.

Lam, Y.C., Bowman, A.B., Jafar-Nejad, P., Lim, J., Richman, R., Fryer, J.D., Hyun, E.D., Duvick, L.A., Orr, H.T., Botas, J.*, et al.* (2006). ATAXIN-1 interacts with the repressor Capicua in its native complex to cause SCA1 neuropathology. Cell *127*, 1335-1347.

Landles, C., Sathasivam, K., Weiss, A., Woodman, B., Moffitt, H., Finkbeiner, S., Sun, B., Gafni, J., Ellerby, L.M., Trottier, Y.*, et al.* (2010). Proteolysis of mutant huntingtin produces an exon 1 fragment that accumulates as an aggregated protein in neuronal nuclei in Huntington disease. The Journal of biological chemistry *285*, 8808-8823.

Lee, C.Y., Cantle, J.P., and Yang, X.W. (2013). Genetic manipulations of mutant huntingtin in mice: new insights into Huntington's disease pathogenesis. The FEBS journal *280*, 4382-4394.

Lee, J., Taghian, K., and Petratos, S. (2014). Axonal degeneration in multiple sclerosis: can we predict and prevent permanent disability? Acta neuropathologica communications *2*, 97.

Lee, Y., Morrison, B.M., Li, Y., Lengacher, S., Farah, M.H., Hoffman, P.N., Liu, Y., Tsingalia, A., Jin, L., Zhang, P.W.*, et al.* (2012). Oligodendroglia metabolically support axons and contribute to neurodegeneration. Nature *487*, 443-448.

Lerner, R.P., Trejo Martinez Ldel, C., Zhu, C., Chesselet, M.F., and Hickey, M.A. (2012). Striatal atrophy and dendritic alterations in a knock-in mouse model of Huntington's disease. Brain research bulletin *87*, 571-578.

Li, H., Li, S.H., Yu, Z.X., Shelbourne, P., and Li, X.J. (2001). Huntingtin aggregate-associated axonal degeneration is an early pathological event in Huntington's disease mice. The Journal of neuroscience : the official journal of the Society for Neuroscience *21*, 8473-8481.

Li, S., and Li, X.J. (2006). Multiple pathways contribute to the pathogenesis of Huntington disease. Molecular neurodegeneration *1*, 19.

Li, S.H., Cheng, A.L., Zhou, H., Lam, S., Rao, M., Li, H., and Li, X.J. (2002). Interaction of Huntington disease protein with transcriptional activator Sp1. Molecular and cellular biology *22*, 1277-1287.

Li, S.H., Gutekunst, C.A., Hersch, S.M., and Li, X.J. (1998). Interaction of huntingtin-associated protein with dynactin P150Glued. The Journal of neuroscience : the official journal of the Society for Neuroscience *18*, 1261-1269.

Li, S.H., and Li, X.J. (2004). Huntingtin-protein interactions and the pathogenesis of Huntington's disease. Trends in genetics : TIG *20*, 146-154.

Li, Z., Park, Y., and Marcotte, E.M. (2013). A Bacteriophage tailspike domain promotes self-cleavage of a human membrane-bound transcription factor, the myelin regulatory factor MYRF. PLoS biology *11*, e1001624.

Ligon, K.L., Fancy, S.P., Franklin, R.J., and Rowitch, D.H. (2006). Olig gene function in CNS development and disease. Glia *54*, 1-10.

Lim, J., Crespo-Barreto, J., Jafar-Nejad, P., Bowman, A.B., Richman, R., Hill, D.E., Orr, H.T., and Zoghbi, H.Y. (2008). Opposing effects of polyglutamine expansion on native protein complexes contribute to SCA1. Nature *452*, 713-718.

Lin, C.H., Tallaksen-Greene, S., Chien, W.M., Cearley, J.A., Jackson, W.S., Crouse, A.B., Ren, S., Li, X.J., Albin, R.L., and Detloff, P.J. (2001). Neurological abnormalities in a knock-in mouse model of Huntington's disease. Human molecular genetics *10*, 137-144.

Lobsiger, C.S., and Cleveland, D.W. (2007). Glial cells as intrinsic components of non-cell-autonomous neurodegenerative disease. Nature neuroscience *10*, 1355-1360.

Longair, M.H., Baker, D.A., and Armstrong, J.D. (2011). Simple Neurite Tracer: open source software for reconstruction, visualization and analysis of neuronal processes. Bioinformatics *27*, 2453-2454.

Lonze, B.E., and Ginty, D.D. (2002). Function and regulation of CREB family transcription factors in the nervous system. Neuron *35*, 605-623.

Mack, J.T., Beljanski, V., Soulika, A.M., Townsend, D.M., Brown, C.B., Davis, W., and Tew, K.D. (2007). "Skittish" Abca2 knockout mice display tremor, hyperactivity, and abnormal myelin ultrastructure in the central nervous system. Molecular and cellular biology *27*, 44-53.

Makinson, C.D., Tanaka, B.S., Lamar, T., Goldin, A.L., and Escayg, A. (2014). Role of the hippocampus in Nav1.6 (Scn8a) mediated seizure resistance. Neurobiology of disease *68*, 16-25.

Mallon, B.S., Shick, H.E., Kidd, G.J., and Macklin, W.B. (2002). Proteolipid promoter activity distinguishes two populations of NG2-positive cells throughout neonatal cortical development. The Journal of neuroscience : the official journal of the Society for Neuroscience *22*, 876-885.

Mangiarini, L., Sathasivam, K., Seller, M., Cozens, B., Harper, A., Hetherington, C., Lawton, M., Trottier, Y., Lehrach, H., Davies, S.W.*, et al.* (1996). Exon 1 of the HD gene with an expanded CAG repeat is sufficient to cause a progressive neurological phenotype in transgenic mice. Cell *87*, 493-506.

Martinez-Vicente, M., Talloczy, Z., Wong, E., Tang, G., Koga, H., Kaushik, S., de Vries, R., Arias, E., Harris, S., Sulzer, D.*, et al.* (2010). Cargo recognition failure is responsible for inefficient autophagy in Huntington's disease. Nature neuroscience *13*, 567-576.

Matamales, M., Bertran-Gonzalez, J., Salomon, L., Degos, B., Deniau, J.M., Valjent, E., Herve, D., and Girault, J.A. (2009). Striatal medium-sized spiny neurons: identification by nuclear staining and study of neuronal subpopulations in BAC transgenic mice. PloS one *4*, e4770.

McKenzie, I.A., Ohayon, D., Li, H., de Faria, J.P., Emery, B., Tohyama, K., and Richardson, W.D. (2014). Motor skill learning requires active central myelination. Science *346*, 318-322.

Meijer, D.H., Kane, M.F., Mehta, S., Liu, H., Harrington, E., Taylor, C.M., Stiles, C.D., and Rowitch, D.H. (2012). Separated at birth? The functional and molecular divergence of OLIG1 and OLIG2. Nature reviews Neuroscience *13*, 819-831.

Menalled, L.B., and Chesselet, M.F. (2002). Mouse models of Huntington's disease. Trends in pharmacological sciences *23*, 32-39.

Menalled, L.B., Sison, J.D., Dragatsis, I., Zeitlin, S., and Chesselet, M.F. (2003). Time course of early motor and neuropathological anomalies in a knock-in mouse model of Huntington's disease with 140 CAG repeats. The Journal of comparative neurology *465*, 11-26.

Menalled, L.B., Sison, J.D., Wu, Y., Olivieri, M., Li, X.J., Li, H., Zeitlin, S., and Chesselet, M.F. (2002). Early motor dysfunction and striosomal distribution of huntingtin microaggregates in Huntington's disease knock-in mice. The Journal of neuroscience : the official journal of the Society for Neuroscience *22*, 8266-8276.

Michalski, J.P., Anderson, C., Beauvais, A., De Repentigny, Y., and Kothary, R. (2011). The proteolipid protein promoter drives expression outside of the oligodendrocyte lineage during embryonic and early postnatal development. PloS one *6*, e19772.

Miller, J.P., Holcomb, J., Al-Ramahi, I., de Haro, M., Gafni, J., Zhang, N., Kim, E., Sanhueza, M., Torcassi, C., Kwak, S.*, et al.* (2010). Matrix metalloproteinases are modifiers of huntingtin proteolysis and toxicity in Huntington's disease. Neuron *67*, 199-212.

Munoz-Sanjuan, I., and Bates, G.P. (2011). The importance of integrating basic and clinical research toward the development of new therapies for Huntington disease. The Journal of clinical investigation *121*, 476-483.

Orr, A.L., Li, S., Wang, C.E., Li, H., Wang, J., Rong, J., Xu, X., Mastroberardino, P.G., Greenamyre, J.T., and Li, X.J. (2008). N-terminal mutant huntingtin associates with mitochondria and impairs mitochondrial trafficking. The Journal of neuroscience : the official journal of the Society for Neuroscience *28*, 2783-2792.

Pang, Y., Fan, L.W., Tien, L.T., Dai, X., Zheng, B., Cai, Z., Lin, R.C., and Bhatt, A. (2013). Differential roles of astrocyte and microglia in supporting oligodendrocyte development and myelination in vitro. Brain and behavior *3*, 503-514.

Paulson, H.L., Bonini, N.M., and Roth, K.A. (2000). Polyglutamine disease and neuronal cell death. Proceedings of the National Academy of Sciences of the United States of America *97*, 12957-12958.

Paus, T., Zijdenbos, A., Worsley, K., Collins, D.L., Blumenthal, J., Giedd, J.N., Rapoport, J.L., and Evans, A.C. (1999). Structural maturation of neural pathways in children and adolescents: in vivo study. Science *283*, 1908-1911.

Pavese, N., Gerhard, A., Tai, Y.F., Ho, A.K., Turkheimer, F., Barker, R.A., Brooks, D.J., and Piccini, P. (2006). Microglial activation correlates with severity in Huntington disease: a clinical and PET study. Neurology *66*, 1638-1643.

Pekny, M., and Nilsson, M. (2005). Astrocyte activation and reactive gliosis. Glia *50*, 427-434.

Philips, T., Bento-Abreu, A., Nonneman, A., Haeck, W., Staats, K., Geelen, V., Hersmus, N., Kusters, B., Van Den Bosch, L., Van Damme, P.*, et al.* (2013). Oligodendrocyte dysfunction in the pathogenesis of amyotrophic lateral sclerosis. Brain : a journal of neurology *136*, 471-482.

Pitt, D., Gonzales, E., Cross, A.H., and Goldberg, M.P. (2010). Dysmyelinated axons in shiverer mice are highly vulnerable to alpha-amino-3-hydroxy-5-methylisoxazole-4-propionic acid (AMPA) receptor-mediated toxicity. Brain research *1309*, 146-154.

Rivers, L.E., Young, K.M., Rizzi, M., Jamen, F., Psachoulia, K., Wade, A., Kessaris, N., and Richardson, W.D. (2008). PDGFRA/NG2 glia generate myelinating oligodendrocytes and piriform projection neurons in adult mice. Nature neuroscience *11*, 1392-1401.

Rodriguez, M., and Scheithauer, B. (1994). Ultrastructure of multiple sclerosis. Ultrastructural pathology *18*, 3-13.

Rosas, H.D., Koroshetz, W.J., Chen, Y.I., Skeuse, C., Vangel, M., Cudkowicz, M.E., Caplan, K., Marek, K., Seidman, L.J., Makris, N.*, et al.* (2003). Evidence for more widespread cerebral pathology in early HD: an MRI-based morphometric analysis. Neurology *60*, 1615-1620.

Ross, C.A., Aylward, E.H., Wild, E.J., Langbehn, D.R., Long, J.D., Warner, J.H., Scahill, R.I., Leavitt, B.R., Stout, J.C., Paulsen, J.S.*, et al.* (2014). Huntington disease: natural history, biomarkers and prospects for therapeutics. Nature reviews Neurology *10*, 204-216.

Ross, C.A., and Tabrizi, S.J. (2011). Huntington's disease: from molecular pathogenesis to clinical treatment. The Lancet Neurology *10*, 83-98.

Saher, G., Quintes, S., and Nave, K.A. (2011). Cholesterol: a novel regulatory role in myelin formation. The Neuroscientist : a review journal bringing neurobiology, neurology and psychiatry *17*, 79-93.

Sapp, E., Kegel, K.B., Aronin, N., Hashikawa, T., Uchiyama, Y., Tohyama, K., Bhide, P.G., Vonsattel, J.P., and DiFiglia, M. (2001). Early and progressive accumulation of reactive microglia in the Huntington disease brain. Journal of neuropathology and experimental neurology *60*, 161-172.

Sapp, E., Penney, J., Young, A., Aronin, N., Vonsattel, J.P., and DiFiglia, M. (1999). Axonal transport of N-terminal huntingtin suggests early pathology of corticostriatal projections in Huntington disease. Journal of neuropathology and experimental neurology *58*, 165-173.

Sathasivam, K., Neueder, A., Gipson, T.A., Landles, C., Benjamin, A.C., Bondulich, M.K., Smith, D.L., Faull, R.L., Roos, R.A., Howland, D.*, et al.* (2013). Aberrant splicing of HTT generates the pathogenic exon 1 protein in Huntington disease. Proceedings of the National Academy of Sciences of the United States of America *110*, 2366-2370.

Sathornsumetee, S., McGavern, D.B., Ure, D.R., and Rodriguez, M. (2000). Quantitative ultrastructural analysis of a single spinal cord demyelinated lesion predicts total lesion

load, axonal loss, and neurological dysfunction in a murine model of multiple sclerosis. The American journal of pathology *157*, 1365-1376.

Scimeca, J.M., and Badre, D. (2012). Striatal contributions to declarative memory retrieval. Neuron *75*, 380-392.

Shin, J.Y., Fang, Z.H., Yu, Z.X., Wang, C.E., Li, S.H., and Li, X.J. (2005). Expression of mutant huntingtin in glial cells contributes to neuronal excitotoxicity. The Journal of cell biology *171*, 1001-1012.

Simons, M., and Trajkovic, K. (2006). Neuron-glia communication in the control of oligodendrocyte function and myelin biogenesis. Journal of cell science *119*, 4381-4389.

Slow, E.J., van Raamsdonk, J., Rogers, D., Coleman, S.H., Graham, R.K., Deng, Y., Oh, R., Bissada, N., Hossain, S.M., Yang, Y.Z*., et al.* (2003). Selective striatal neuronal loss in a YAC128 mouse model of Huntington disease. Human molecular genetics *12*, 1555-1567.

Song, W., Chen, J., Petrilli, A., Liot, G., Klinglmayr, E., Zhou, Y., Poquiz, P., Tjong, J., Pouladi, M.A., Hayden, M.R*., et al.* (2011). Mutant huntingtin binds the mitochondrial fission GTPase dynamin-related protein-1 and increases its enzymatic activity. Nature medicine *17*, 377-382.

Stadelmann, C., Wegner, C., and Bruck, W. (2011). Inflammation, demyelination, and degeneration - recent insights from MS pathology. Biochimica et biophysica acta *1812*, 275-282.

Sugars, K.L., and Rubinsztein, D.C. (2003). Transcriptional abnormalities in Huntington disease. Trends in genetics : TIG *19*, 233-238.

Suzuki, E., Zhao, Y., Ito, S., Sawatsubashi, S., Murata, T., Furutani, T., Shirode, Y., Yamagata, K., Tanabe, M., Kimura, S*., et al.* (2009). Aberrant E2F activation by polyglutamine expansion of androgen receptor in SBMA neurotoxicity. Proceedings of the National Academy of Sciences of the United States of America *106*, 3818-3822.

Tabrizi, S.J., Langbehn, D.R., Leavitt, B.R., Roos, R.A., Durr, A., Craufurd, D., Kennard, C., Hicks, S.L., Fox, N.C., Scahill, R.I*., et al.* (2009). Biological and clinical manifestations of Huntington's disease in the longitudinal TRACK-HD study: cross-sectional analysis of baseline data. The Lancet Neurology *8*, 791-801.
Tai, Y.F., Pavese, N., Gerhard, A., Tabrizi, S.J., Barker, R.A., Brooks, D.J., and Piccini, P. (2007). Microglial activation in presymptomatic Huntington's disease gene carriers. Brain : a journal of neurology *130*, 1759-1766.

Takano, H., and Gusella, J.F. (2002). The predominantly HEAT-like motif structure of huntingtin and its association and coincident nuclear entry with dorsal, an NF-kB/Rel/dorsal family transcription factor. BMC neuroscience *3*, 15.

Temburni, M.K., and Jacob, M.H. (2001). New functions for glia in the brain. Proceedings of the National Academy of Sciences of the United States of America *98*, 3631-3632.

Tong, X., Ao, Y., Faas, G.C., Nwaobi, S.E., Xu, J., Haustein, M.D., Anderson, M.A., Mody, I., Olsen, M.L., Sofroniew, M.V.*, et al.* (2014). Astrocyte Kir4.1 ion channel deficits contribute to neuronal dysfunction in Huntington's disease model mice. Nature neuroscience *17*, 694-703.

Valenza, M., and Cattaneo, E. (2011). Emerging roles for cholesterol in Huntington's disease. Trends in neurosciences *34*, 474-486.

van der Burg, J.M., Bjorkqvist, M., and Brundin, P. (2009). Beyond the brain: widespread pathology in Huntington's disease. The Lancet Neurology *8*, 765-774.

Vonsattel, J.P., and DiFiglia, M. (1998). Huntington disease. Journal of neuropathology and experimental neurology *57*, 369-384.

Wade, A., Jacobs, P., and Morton, A.J. (2008). Atrophy and degeneration in sciatic nerve of presymptomatic mice carrying the Huntington's disease mutation. Brain research *1188*, 61-68.

Wall, N.R., De La Parra, M., Callaway, E.M., and Kreitzer, A.C. (2013). Differential innervation of direct- and indirect-pathway striatal projection neurons. Neuron *79*, 347-360.

Wang, C.E., Tydlacka, S., Orr, A.L., Yang, S.H., Graham, R.K., Hayden, M.R., Li, S., Chan, A.W., and Li, X.J. (2008). Accumulation of N-terminal mutant huntingtin in mouse and monkey models implicated as a pathogenic mechanism in Huntington's disease. Human molecular genetics *17*, 2738-2751.

Wang, S., Bates, J., Li, X., Schanz, S., Chandler-Militello, D., Levine, C., Maherali, N., Studer, L., Hochedlinger, K., Windrem, M.*, et al.* (2013). Human iPSC-derived oligodendrocyte progenitor cells can myelinate and rescue a mouse model of congenital hypomyelination. Cell stem cell *12*, 252-264.

Wellington, C.L., Ellerby, L.M., Gutekunst, C.A., Rogers, D., Warby, S., Graham, R.K., Loubser, O., van Raamsdonk, J., Singaraja, R., Yang, Y.Z.*, et al.* (2002). Caspase cleavage of mutant huntingtin precedes neurodegeneration in Huntington's disease. The Journal of neuroscience : the official journal of the Society for Neuroscience *22*, 7862-7872.

White, J.K., Auerbach, W., Duyao, M.P., Vonsattel, J.P., Gusella, J.F., Joyner, A.L., and MacDonald, M.E. (1997). Huntingtin is required for neurogenesis and is not impaired by the Huntington's disease CAG expansion. Nature genetics *17*, 404-410.

Wilkins, A., Chandran, S., and Compston, A. (2001). A role for oligodendrocyte-derived IGF-1 in trophic support of cortical neurons. Glia *36*, 48-57.

Wilkins, A., Majed, H., Layfield, R., Compston, A., and Chandran, S. (2003). Oligodendrocytes promote neuronal survival and axonal length by distinct intracellular mechanisms: a novel role for oligodendrocyte-derived glial cell line-derived neurotrophic factor. The Journal of neuroscience : the official journal of the Society for Neuroscience *23*, 4967-4974.

Xiang, Z., Valenza, M., Cui, L., Leoni, V., Jeong, H.K., Brilli, E., Zhang, J., Peng, Q., Duan, W., Reeves, S.A.*, et al.* (2011). Peroxisome-proliferator-activated receptor gamma coactivator 1 alpha contributes to dysmyelination in experimental models of Huntington's disease. The Journal of neuroscience : the official journal of the Society for Neuroscience *31*, 9544-9553.

Xiao, H., Yu, Z., Wu, Y., Nan, J., Merry, D.E., Sekiguchi, J.M., Ferguson, D.O., Lieberman, A.P., and Dressler, G.R. (2012). A polyglutamine expansion disease protein sequesters PTIP to attenuate DNA repair and increase genomic instability. Human molecular genetics *21*, 4225-4236.

Xu, Q., Huang, S., Song, M., Wang, C.E., Yan, S., Liu, X., Gaertig, M.A., Yu, S.P., Li, H., Li, S.*, et al.* (2013). Synaptic mutant huntingtin inhibits synapsin-1 phosphorylation and causes neurological symptoms. The Journal of cell biology *202*, 1123-1138.

Yang, S., Huang, S., Gaertig, M.A., Li, X.J., and Li, S. (2014). Age-dependent decrease in chaperone activity impairs MANF expression, leading to Purkinje cell degeneration in inducible SCA17 mice. Neuron *81*, 349-365.

Yano, H., Baranov, S.V., Baranova, O.V., Kim, J., Pan, Y., Yablonska, S., Carlisle, D.L., Ferrante, R.J., Kim, A.H., and Friedlander, R.M. (2014). Inhibition of mitochondrial protein import by mutant huntingtin. Nature neuroscience *17*, 822-831.

Yu, Z.X., Li, S.H., Evans, J., Pillarisetti, A., Li, H., and Li, X.J. (2003). Mutant huntingtin causes context-dependent neurodegeneration in mice with Huntington's disease. The Journal of neuroscience : the official journal of the Society for Neuroscience *23*, 2193-2202.

Zoghbi, H.Y., and Orr, H.T. (2000). Glutamine repeats and neurodegeneration. Annual review of neuroscience *23*, 217-247